UNIVERSITY OF CENTRAL OKLAHOMA

Edmond, Oklahoma

Jackson College of Graduate Studies

Development of an Artificial Intelligence Method for the Analysis of Bloodstain Patterns

A THESIS

SUBMITTED TO

Dr. James Creecy

Mr. Craig Gravel

Dr. Jicheng Fu

In partial fulfilment of the requirements

For the degree of

MASTER OF SCIENCE IN FORENSIC SCIENCE

By

Niketha Ravivarma

Edmond, Oklahoma

2021

Development of an Artificial Intelligence Method for the Analysis of Bloodstain Patterns

By: Niketha Ravivarma

University of Central Oklahoma

May 2021

Jackson College of Graduate Studies at the University of Central Oklahoma

A THESIS APPROVED FOR

THE W. ROGER WEBB FORENSIC SCIENCE INSTITUTE

By ______________________

James Creecy, Ph.D., Committee Chairperson

By Jicheng Fu

Jicheng Fu, Ph.D., Committee member

By Craig Gravel

Craig Gravel, M.S., Committee member

Acknowledgments

First and foremost, I would like to thank the Forensic Science Institute Director, Dr. Dwight Adams, for his encouragement throughout my coursework at UCO. I want to express my very grateful appreciation to my academic advisor, Dr. James Creecy, for his valuable and constructive suggestions during this research work's planning and development. I am very thankful to him for his constant faith and support for me. I want to express my gratitude to Mr. Craig Gravel and Dr. Jicheng Fu, my research supervisors, for their patient guidance, encouragement, useful critiques for this research work. I want to thank Dr. Fu's research graduates for their generous contributions and assistance in keeping my progress on my research schedule. I am grateful to all of those I have had the pleasure to work with during this research. Each of my thesis committee members has provided me extensive personal and professional guidance and taught me a great deal about scientific research and life in general. Nobody has been more important to me in the pursuit of this project than my family members. I want to thank my parents; whose love and guidance are with me in whatever I pursue. Most importantly, I am grateful to my loving and supportive husband, Brockton Cameron, who provides eternal inspiration.

Thank you,

My father, for being my teacher, my guardian angel, for your unconditional love, faith, and support
My mother, for being my dear friend, my inspiration, my teacher, my love and for her guidance
My husband, for being my constant support, my accomplishments, and his unconditional love
My teachers for good Guidance, faith, inspiration, and support
My dear lord for this beautiful Life.

In India, there is a saying "Matha, Pitha, Guru, Deivam" (meaning Mother, Father, Teacher, and God). The slogan for my success.
Follow your heart, follow your mind, and follow your Dreams

"You build on failure. You use it as a steppingstone. You do not try to forget the mistakes, but you do not dwell on them. You don't let it have any of your energy, or any of your time, or any of your space."

THESIS ABSTRACT

NAME: Niketha Ravivarma

TITLE OF THESIS: Development of an Artificial Intelligence Method for the Analysis of Bloodstain Patterns

THESIS ADVISOR: Dr. James Creecy

ABSTRACT: Bloodstain Pattern Analysis (BPA) is a forensic discipline that plays a crucial role in reconstructing the events at a crime scene (Acampora, 2014). The shape, size, distribution, and location of bloodstains can help infer the potential murder weapon, the origin of the attack, and if the body has been moved or relocated from the original crime scene. Commonly, errors in identifying blood spatter evidence arise when the crime scene has large amounts of bloodstains which can yield less information during analysis. This study aims to utilize artificial intelligence (A.I.) algorithms to assist the analyst in the analysis of bloodstain patterns. To date, BPA relies on a manual analysis process; therefore, it is imperative to have forensic analysts who can accurately produce reliable results (Hoelz, 2009). However, human error is unavoidable, and analyst error can result in inaccurate conclusions that can jeopardize casework. The President's Council of Advisors on Science and Technology (PCAST) report on *Forensic Science in Criminal Courts: Ensuring Scientific Validity of Feature-Comparison Methods* brought to light the shortcomings of many forensic disciplines, including BPA. To improve the field of BPA, automated and computer-assisted methods of analysis are needed. In this study, we used A.I. to estimate the angle of impact from simulated crime scene samples. Our A.I.-assisted approach was determined to be accurate for 78.64% of all data analyzed. This study focused on the analysis of photos taken from a single impact angle as the primary input data. Bloodstain patterns were experimentally constructed using controlled conditions, and a single variable altered at a time.

KEYWORDS: *Artificial Intelligence (A.I.); Bloodstain Pattern Analysis; Forensic Science; PCAST, and Image-processing method*

Table of Contents

List of Figures

List of Tables

List of Appendices

Chapter I

Introduction to Bloodstain Pattern Analysis

Bloodstain Pattern Analysis (BPA) is the study of the interpretation of blood patterns at a crime scene. Bloodstain analysts process the crime scene by locating, observing, and documenting the bloodstain evidence patterns and then interpreting the evidence based on their training, experience, and education (Eckert, 1999). In forensic casework, BPA aids in determining the source of blood at the crime scene or the series of events that may have occurred during the criminal activity. Different objects with existing blood have been found to result in the formation of different types of bloodstain patterns, which are essential for demonstrating the analytical nature of BPA and its admissibility in court.

Types of Bloodstain pattern

Within BPA, bloodstain patterns are classified into three major categories: passive stains, transfer stains/ altered stains, and projected/impact stains (NFSTC, 2013). Passive stains are the result of bleeding or bloodstains formed due to the force of gravity. Transfer bloodstains result from a bloody object encountering a second surface with an existing bloodstain and include wipes, swipes, smears, and pattern transfer. A wipe pattern is a bloodstain pattern occurring due to an object encountering an existing bloodstain. A swipe pattern is a bloodstain pattern resulting from an existing blood surface pattern to a second surface with relative motion between the two surfaces (NFSTC, 2013, Patrick Laturnus,2014). A smear is a large volume of blood that has been distorted. A pattern transfer occurs when a wet bloody surface encounters a secondary surface. An example of a transfer bloodstain pattern a bloody shoe print. The focus of this thesis is on the analysis of projected/impact bloodstains. Projected stains result from projecting a blood source through the air at a greater force than gravity alone. Projected stains are more often referred to as spatter patterns (Gallagher, 2009). The different classes of projected stains are impact spatter, splashes, cast-off stains, arterial spurts, and gushes.

Impact Spatter Patterns

As mentioned above, impact spatter patterns are created by applying force to a bloodied object or source that results in a random dispersion of tiny blood droplets. Impact spatter patterns are classified into three types, Low Energy Spatter (LES), Medium Energy Spatter (MES), and High Energy Spatter (HES). LES caused by dripping blood at low energy (5 feet per second or less) to the ground level and has a large blood droplet diameter (4mm-8mm); an example for LES is the pattern associated with a nosebleed (Shanna Freeman, 2019). MES caused by a blunt object with a medium force (5 -25 ft per second) (Shanna Freeman, 2019); an example of MES are patterns associated with the use of a baseball bat in a physical assault. HES results from an exertion of higher force that travels in the energy of 100 ft per second, and the bloodstain pattern appears as a mist or a spray. The droplet diameter is minute, less than 1mm; spatter resulting from a gunshot wound is an example of HES (Shanna Freeman, 2019). Spatter pattern can be observed in cast-off, arterial spray, gunshot spatter, or expiratory blood patterns. Expiratory blood patterns occur due to having an injury in the mouth or nose resulting from breathing. The blood tends to expirate, and the blood droplets are tiny containing saliva representing bubbles in the blood droplet. Saturation bloodstain pattern occurs due to the accumulation of blood in an absorbent material where the blood is either dry or still wet; an example is a person’s clothing. A pool of blood is a large amount of blood deposited at a particular area with blood both in a liquid and solid (clotted blood) state. The pool stain helps in determining the time of the attack and when the injury has taken place. The pool stain results in a separation of liquid (serum) and solid-state of the blood during coagulation; this is called a serum stain.

Figure 1: Arterial spray (Blood Spatter Pattern, Cristabusheforensics.weebly.com, 2014)
A heart injury can cause such a pattern due to the pressure. The figure shows the illustration of an arterial spray which is in a zigzag motion on the wall.

Arterial spurting (or gushing) pattern refers to the escape of blood under pressure from any breach in an artery or heart (NFSTC, 2013). As seen in figure 1, the arterial spurting is caused when blood is released when a major artery is severed in the heart, that causes a pattern showing a zig zag motion (or arcing pattern) on the wall. The bloodstain pattern shows that the blood exiting the body under arterial pressure has large stains with the vertical surfaces' downward flow. The arterial spurting pattern is created by a severed artery and the physical characteristics of the pattern are influenced by location of the artery, volume of blood dispersed, blocking effect of skin, tissue, or clothing (Stuart, 2003).

Gunshot spatters or the bullet wounds can be from both forward spatter (F.S.), and a back spatter (B.S.) (Shanna Freeman, 2019). The blood spatter caused due to a gunshot can create a mist pattern or a gush pattern depending on various factors. The direction of the blood droplets helps to determine which side the shooter was. The back spatter is projected towards the force, and the forward spatter travels away from the force. From figure 2, the forward spatter patterns usually contain more blood and cover a larger surface than the backward spatter (NFSTC, 2013)

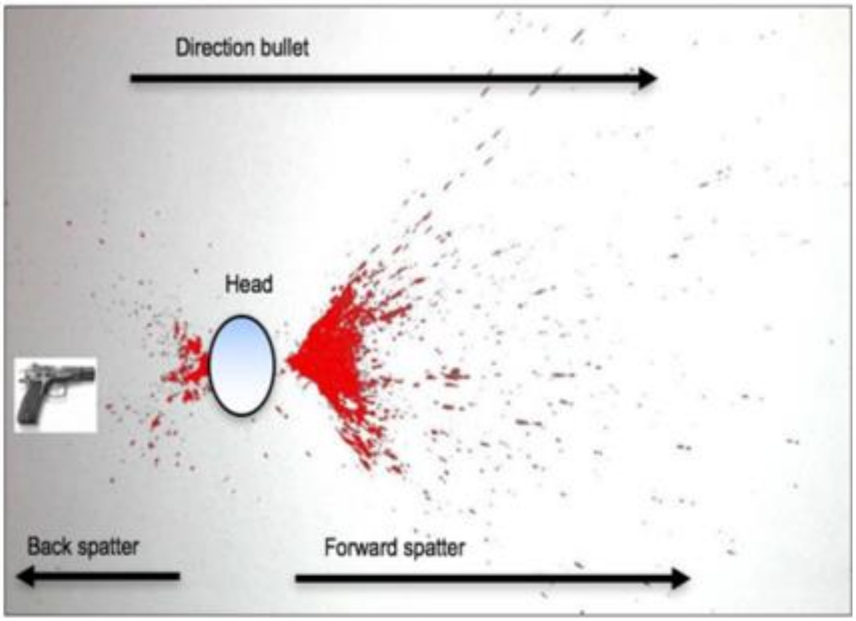

Figure 2: Forward and Backward spatter. (Independent Forensic Services, 2015.
When a gunshot fires from west to east, there are two different spatters, forward spatter, and backward spatter. The forward spatter has a high amount of blood spatter compared to the back spatter. The directionality of blood can determine the forward and backward spatter.

Cast off stains are lineal stains created by a moving object which encounters a blood surface. The cast-off is the centrifugal force created by the weapon in discharge, which is swung back and forth over the attacker's head. Often the hand that an attacker used in the assault can be identified by the cast-off pattern. The use of a weapon in a swinging motion results in the production of cast-off from the weapon, cast-off patterns are identified by the cessation patterns created due to the arrested motion of blood droplets, and the pattern is present behind the suspect's back or on the wall. As seen in figure 3, the bloodstains that are closer to the start of the swinging motion will be round, while those at the terminal end will have an oval pattern. This change in pattern results from the variation in direction that occurs in the act of swinging. The cast-off patterns may exhibit a slight curvature along the length of the pattern. Under some conditions, this curvature can indicate if the swing was left- or right-handed. Because cast-off patterns are easy to

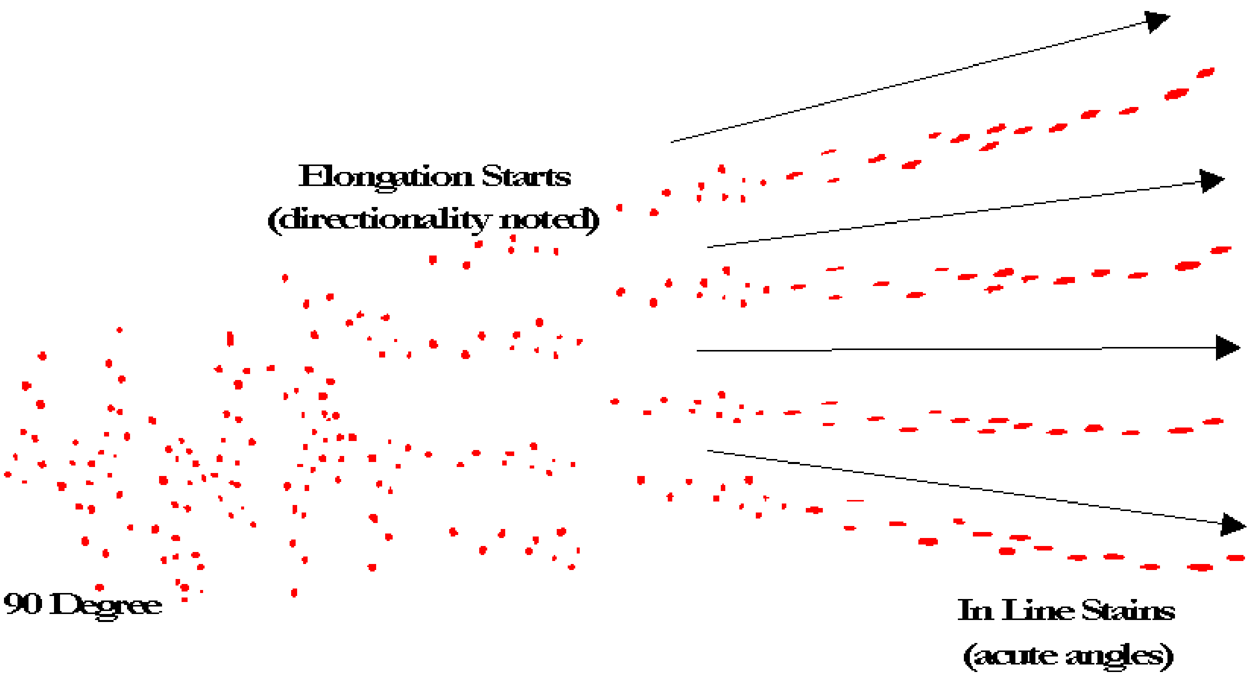

Figure 3: Cast-off stain (Blood Spatter Patterns, 2014).
The Directionality is elongated, and the In-Line stains are at acute angles. The bloodstains are oval-shaped due to the impact angle. The number of lines indicates the number of blows.

misinterpret, it is essential to be cautious when evaluating these patterns for the number of impacts or whether the swing was right- or left-handed (Tom Bevel, 2009).

Characteristics and Properties of Blood and Bloodstain Patterns

To interpret bloodstains, an analyst must understand the fundamental properties of blood. Blood consists of both liquid and solid components. The liquid component is called the serum. The serum is what remains after the blood has clotted. The solid component contains cells (red blood cells, white blood cells, and platelets). When the blood exits the body, it is in a liquid state, and after a several minutes, it turns into a solid-state called a clot, which looks like a gel substance.

Blood has cells that aid in clotting which can occur within a person or within a large pool of blood. The state of the blood at a crime scene provides an analyst with the information needed to estimate the nature of the attack and what kind of crime occurred. The bloodstain patterns help determine the type of injury, such as spurt (occurs due to arterial spray, refer figure 1), drip (bloodstain resulting from a falling drop formed due to gravity), or a flow (bloodstain resulting from the movement of the target). The principle of BPA focuses on the size and shape of the bloodstains. A bloodstain pattern's size and shape aid an analyst in determining how the pattern was formed. The size of the droplet can be influenced by the velocity. An example of this is low velocity spatter has a larger droplet diameter, whereas a high velocity has a smaller droplet diameter. The shape of the droplet can be influenced by various physical properties such as air resistance, surface tension, and gravity (Brodbeck, 2012). Initially, in-flight liquid forms a teardrop shape only when dropped from an object but then retains a spherical shape in flight due to surface tension, molecular bonding, and other forces that act upon. The viscosity (resistance of flow) and surface tension helps the blooddrop to control the oscillation.

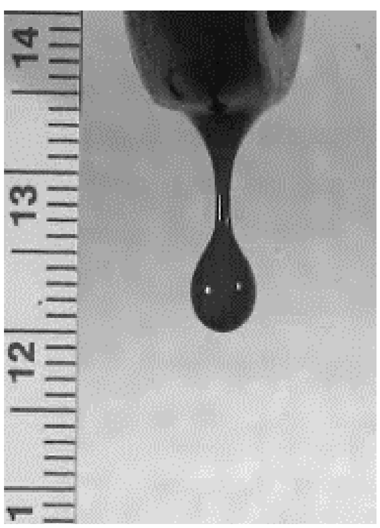

Figure 4: The blood droplet in flight, forming a teardrop shape (Brodbeck, 2012)
The teardrop shape loses its artistic form when it detaches from the blood origin.

Blood can strike on a variety of surfaces which can affect the spatter pattern's appearance. In BPA, there are two surface classifications, smooth surface, and rough surface. On the smooth surface (tile floor) the bloodstain remains intact and will be a well-formed stain. On any rough surfaces (e.g., asphalt) the blood will have an irregular shape with rough edges. As seen in figure 5, the bloodstain on paper creates an outer spine on impact. The blood droplet on the towel shows the variation in size and shape like the fabric creating a satellite stain from the parent stain. The shape of the spatter pattern aids the analyst in determining the directionality of the blood and where the bloodstain originated. Bloodstain patterns help to sequence events that have occurred during the incident—suggesting that bloodstains are predictable, reproducible, and able to be used to determine the point of origin for a blood source. Based on figure 6, the blood droplet has two ends, one end is circular, and the other end is called a tail/ tapered end. The resulting tail will point in the direction of the traveling blood. The blood travels from the bottom left to the upper right leading to the point of origin.

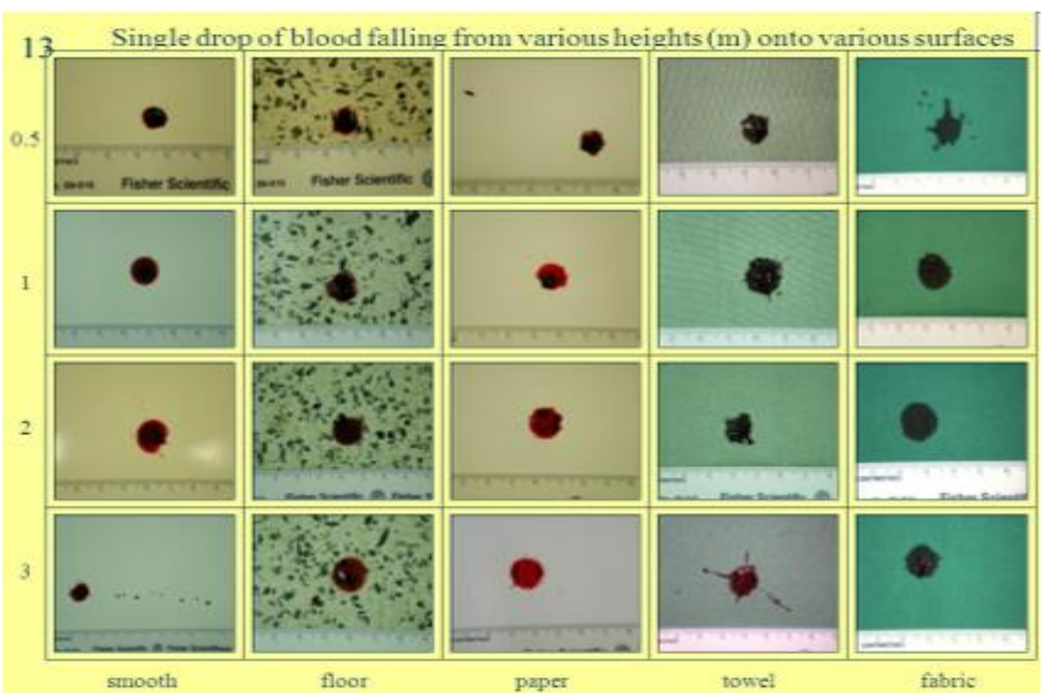

Figure 5: Bloodstain on different surfaces (Andrew R. W. Jackson, 2004; Gallagher, 2009). If the surface is not smooth, the droplet doesn't create a perfect circular shape on impact.

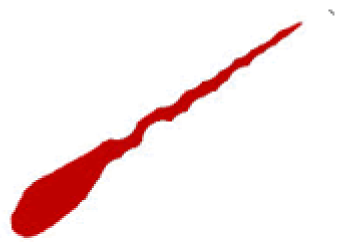

Figure 6: The direction of the bloodstain (Shanna Freeman, 2019).
The blood droplet travels from the bottom left to the upper right. The direction ultimately leads to the point of origin. The droplet caused due to a blunt object with different types of pattern velocity like LVIS, MVIS, or HVIS.

Impact Angle

An impact pattern is when a force is applied to liquid blood. The direction of blood forms the impact pattern at the plane of the surface, creating an angle of impact (I. F. Services, 2019). The angle of impact is solely responsible for determining the shape and elongation of the blood droplet. The shape may vary accordingly with the volume of blood traveling from the source to the surface. The shape of the droplet varies from spherical to elliptical based on the angle of impact. If the angle of impact is 90°, the shape of the droplet is round with zero absence of elongation, and if the angle of impact is 10°, the shape of the blood droplet is oval and elongated. As in figure 7, the 90-degree bloodstain is called a passive bloodstain, resulting from a self-inflicted wound. Thus, determining the direction of the blood drop by the angle of impact will help calculate the accuracy.

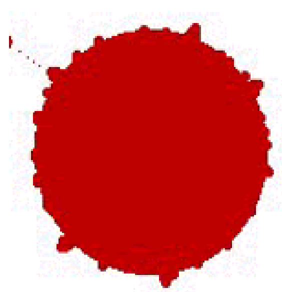

Figure 7: 90-degree Bloodstain (NFSTC, 2013).
This type of bloodstain is called a passive bloodstain. The stain is circular, resulting from a direct fall to the ground from a self-inflicted wound, stabbing, or accidental injury.

To determine the impact angle, the analyst uses trigonometric functions of any given blood droplet. The equation used for determining the impact angle is sin (á) = W/L, where W and L are the bloodstain's width and length. The width and length of the stain are measured to determine the angle of impact. As in figure 8, the number calculated is taken for an inverse sine function(arcsine). The bloodstain's length is the hypotenuse, while the width is the opposite side of the angle of impact (Shanna Freeman, 2019).

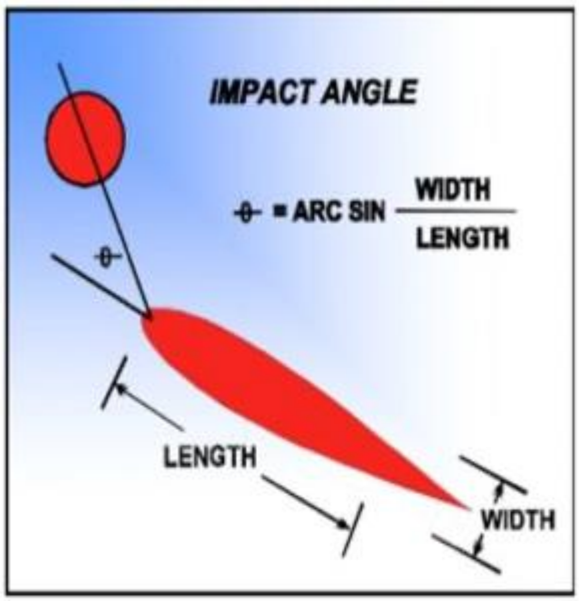

Figure 8: Impact angle (I. F. Services, 2019).
The formula for determining the impact angle. The arcsine is the inverse sine function.

The angle of impact works only with right angles, such as a wall or a floor. The width (long axis) is perpendicular, and the length (long axis) is parallel. Thus, the lesser the angle of impact results in an elliptical bloodstain shape. Figure 9 shows that the bloodstain is spherical/oval and elongated based on the relativity of the angle of impact. The blood droplet in contact with a non-horizontal surface will result in a higher acute angle with greater elongation, also the width and length increases. e.g., 50-degree shows a smaller droplet of blood detached from the parent/main bloodstain, which occurred during the moment of impact.

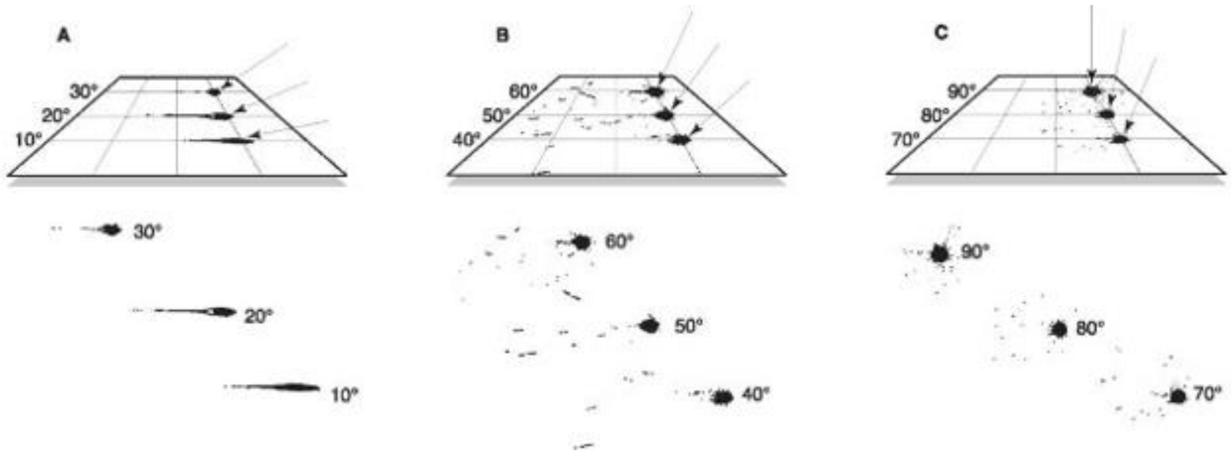

Figure 9: Different angles of Impact (Campbell, 2016)
The angles of impact of bloodstains against a target surface. The tail is an important tool when reconstructing bloodstain patterns because it points in the direction the droplet was traveling in when it impacted on to the target surface. The shape of the bloodstain is also important in the reconstructive process.

An analyst makes a general observation of the bloodstain by looking at it; if the tail is longer, the angle is smaller, which produces a more elongated stain such as the 10-degree stain (Museum, 2017). The steeper the angle of impact will create a more elliptical or elongated blood droplet. The angles at 50-degrees and less, to be shallow angles that produce insignificant results that correlate with the physical parameters of both the liquid blood and solid surfaces (Justice, 2018).

Review of Literature for Bloodstain Pattern Analysis

Bloodstain Pattern Analysis (BPA) was originated in 1895 by Dr. Eduard Piotrowski. The field of bloodstain pattern analysis often struggled to progress due to the lack of scientific investigations. The investigations from a rabbit massacre using trigonometry values have helped BPA to promote a new forensic science field in the scientific community. Herbert MacDonell, often known as the god father of BPA and is the founder of Bloodstain Evidence Institute, gave BPA its first legitimacy in the Texas court justice system. The history of BPA has evolved with time, resources, and the systematic origin of analysis. There appear to be different types of origin that BPA has acknowledged by systematic and non-systematic review.

In 1895, Dr. Eduard Piotrowski published a research study titled **"**Concerning the Origin, Shape, Direction, And Distribution of The Bloodstains Following Head Wounds Caused by Blows**,"** which has implemented a growing interest in the scientific community (Shanna Freeman, 2019). One of Piotrowski's studies states that bloodstains appear on a surface only during a second blow. For example, there should be an existence of a blood source for a bloodstain to appear. This theory questions whether the bloodstain spatters appearance could be due to blows or not (Brodbeck, 2012). Although Piotrowski's study and method were to be followed by several researchers, the analysis was non-systematic. In 1839, Victor Balthazard was the first forensic scientist to *use physical interpretations of bloodstains* and published a research study on impact angle (IABPA,2019). In 1955, Dr. Paul Kirk brought a systematic finding in the State of Ohio V. Samuel Sheppard case. The position of the assailant and the victim helped determine which hand could be used by the assailant to strike the victim. The case concluded that the attacker used his left hand; however, Sheppard was right-handed (Shanna Freeman, 2019).

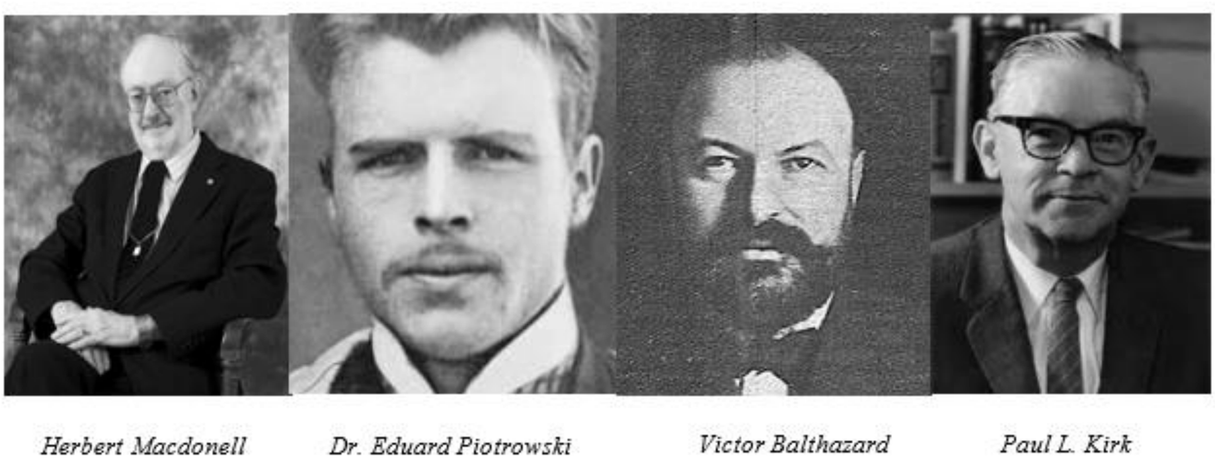

Figure 10: The founders of BPA (Wiki, 2012 -2018).
The founders of BPA who contributed to the significant study in scientific community.

In 1970, BPA has undergone major refinements in methods and variations in terminologies. Scientists often change the terminology or interpretation, such as the size of the bloodstain determines the type of force, which in turn gives us an idea of the speed of the weapon (Shanna Freeman, 2019). To apply scientific standards in BPA, different councils were formed such as the President's Council of Advisors on Science and Technology (PCAST), The International Association of Bloodstain Pattern Analysis (IABPA), and The Scientific Working Group on Bloodstain Pattern Analysis (SWGSTAIN).

President's Council of Advisors on Science and Technology

The PCAST is an advisory group of the United States' leading scientists and engineers appointed by the president to provide scientific and technological advice. The PCAST report explained how some disciplines lacked scientific reliability in the forensic science community. The report focused on two significant gaps: the need for clarity about the scientific standards for the validity and reliability of forensic methods; and the need to evaluate specific forensic methods to determine whether they are scientifically valid and reliable (PCAST, 2016). The PCAST report aimed to close any gaps related to feature-comparison methods (PCAST, 2016).

Feature-comparison methods determine whether an evidentiary sample collected from a crime scene is or is not associated with a source sample (collected from a suspect) based on similar features (PCAST, 2016). According to the PCAST report, BPA is a feature comparison technique. The BPA experiments are based on simulations of evidence under controlled conditions and mathematical measurements for determining the bloodstain patterns. BPA techniques can answer the questions of what may or may not have happened and the type of forced necessary to create these bloodstain patterns. The PCAST report has led to the National Research Council (NRC) report to establish a standard guideline for best practice. The PCAST report stated that a discipline's uncertainties could result in wrongful conviction, irregularities, and miscarriage of justice.

International Association of Bloodstain Pattern Analysis

In 1893, The International Association of Bloodstain Pattern Analysis (IABPA) was established and formed by Herbert Macdonell. The concept of the IABPA is to promote education in BPA by studying, researching, and testing (the areas in terminology, analysis, and training) (IABPA, 2008). The IABPA conducts its own BPA certification process. The IABPA focuses on the 2009 National Academy of Forensic Science (NAS) report on "Strengthening Forensic Science in the United States: A Path Forward" (The United States, 2019). The NAS report has paved the way for both the scientific community and the criminal justice system to follow a known number of limitations. The limitations rely on the experience and the education level of the expert. Also, the potential challenges represented by the 2009 NAS report have given BPA experts a knowledge base experience in courtrooms, testimony, pretrial, and proper communication about scientific knowledge.

Scientific Working Group on Bloodstain Pattern Analysis (SWGSTAIN)

The Scientific Working Group on Bloodstain Pattern Analysis (SWGSTAIN) is a group that consists of representatives and members from the IABPA (Encyclopedia, 2020). The members are experts from various sub-fields in BPA. The SWGSTAIN association is to enhance and promote the quality of the BPA methods; standardize a set of limitations and guidelines. In 2004, the SWGSTAIN drafted proposals on terminology, quality assurance, legal, ethics, education, and training in BPA ((FBI). 2002). The main objectives of SWGSTAIN are to analyze and compare BPA methods; to draw a blueprint on quality assurance programs BPA; to meet the challenges of admissibility on Frye, Daubert, and other standards; proficiency testing BPA methods; and to set a standardized "best practice" guideline for enhancing the discipline in BPA(FBI). 2002).

The BPA proficiency testing program aims to focus on an analyst's knowledge, skills, and abilities to fulfill the requirements intended to achieve in BPA. The proficiency testing should include pattern recognition, angle of impact, area of convergence, the origin of determination, clothing examination, stain selection, evidence integrity, evidence collection and documentation (photography), analysis, and reporting ((FBI). 2002; (SWGSTAIN), 2009). The test design should provide details on the blood source information and scenario information((SWGSTAIN), 2009). Eventually SWGSTAIN moved to the Midwest Forensic Center in Ames, Iowa when the FBI withdrew from the group.

In 2015 the National Institute of Standards and Technology (NIST) took control of the Bloodstain Pattern Analysis standards (BPA). They are a metrology laboratory and a non-regulatory of the United States Department of Commerce. Their mission is to promote innovation and industrial competitiveness. The Organization of Scientific Area Committees for Forensic Science (OSAC) are subcommittees of NIST, and they are developing new standards for the BPA discipline and work closely with the American Academy for Forensic Science.

List of Historical cases of bloodstain pattern analysis

The common forensic methods have led to some serious consequences. Ultimately stating to require further testing to establish a foundation and valid evidence collection. There are two cases (The Chamberlain Case, and The David Camm Case) discussed as an example to view where the collection and processing of evidence has failed.

The Chamberlain Case

The chamberlain case, also known as "The dingo ate my baby," took place in 1980 in Uluru (formerly known as Ayer's Rock), Australia. The chamberlain family (Lindy Chamberlain, Michael Chamberlain, and their two daughters 4-year-old Reagan and 9-week-old Azaria), camped in the Red Desert of Australia's Northern Territory (Haberman, 2014; Shanna Freeman, 2019). On the night of August 17th, 1980, baby Azaria disappeared from the tent, never to be found. Lindy Chamberlain claimed that a dingo took her daughter from the tent. The case led to a series of blood evidence, which led to a theory that Lindy Chamberlain killed her daughter and blamed it on a dingo. The court gave her a life sentence in which she spent three years in prison until the case reopened to investigate the evidence further.

Figure 11: The bloody jumpsuit of baby Azaria (Blanco, 2014).
The Evidence was recovered next to a dingo lair where baby Azaria disappeared

The local police improperly handled the blood evidence during the investigation, causing misrepresentation. The red stain collected from the family's car is assumed to be Azaria's blood when her throat was slit. Later concluded from the analysis, the red stain resulted from a spilled drink and sound detonating compound. On examination, a bloody handprint found on Azaria's jumpsuit reveals to be desert sand.

Figure 12: Azaria's blood-stained jacket (Chamberlain, 1991)
Recovered near a dingo lair, was a piece of crucial evidence for Lindy Chamberlain's release

The David Camm's Case

On September 28th, 2000, the Camm's family (Mrs. Camm and their two children) was found murdered at their home in Georgetown, Indiana. David Camm claimed that he was at a basketball event during the murder. A sweatshirt with blood droplets recovered at the crime scene later ruled out that it was not David's sweatshirt and had two unknown DNA (one male and one female). The white T-shirt that David wore on the day of the murder consisted of tiny blood droplets consistent with the gunshot. Speculations indicated the tiny blood droplets created due to High-Energy Spatter (HES) by a gunshot. Dr. Epstein, a bloodstain pattern analyst, confirmed that the stains in David's shirt were a contact stain; when he reached out to help his son, the shirt encountered Jill's bloodied hair.

Figure 13 The sweatshirt found at the crime scene (WLKY, 2013).

The analysis of the number of stains and size played a vital role in determining the type of stain. The bloodstain analysis also suggested that gunshot produces numerous tiny droplets, not a consistent number, found on David's T-shirt. There was a total of 7 small droplets found on the T-shirt. The bloodstain pattern evidence was inconsistent, and the jury found David guilty of murder. In 2002, the case reopened with the two unknown DNA on the sweatshirt, later verified on the felon database.

Figure 14: The T-shirt David Camm wore while returning from the basketball game (Howard Stringer, 2017; WLKY, 2013)

Factors That May Contribute to The Uncertainties in BPA

Expert testimony in BPA has contributed to the scientific foundation for analysis and interpretation of the forensic evidence (Scarraher, 2018). After Herbert MacDonell's first testimony against Reginald Lewis, the case went for a retrial in the Texas court of appeal. The case widely recognized BPA as a novel technique but was not scientifically reliable (Smith, 2018a). During an expert testimony, the expert submits a crime scene reconstruction to the court. The crime scene reconstruction is a forensic science method to create a sequence of events performed using the size, shape, and distribution of the bloodstain patterns collected at the crime scene. The purpose for reconstruction answers questions such as the distance of blood source to a target source, the direction of the blood droplets, different types of blood droplets, angle of impact, nature of the object used to cause the bloodshed event, and interpretation of patterns.

Challenges in BPA in the field of Forensic Science

Earlier, many BPA analysts were law enforcement officers and not scientists, which caused considerable controversy in BPA testimony. The testimony often led to circumstantial evidence, which is subjective in the scientific community. With expert testimony and no evidence to prove the expert's theory, several cases led to wrongful convictions that the court accepted. e.g., Bryan's and Rea's case, where the expert failed to provide sufficient scientific and experimental data to the testimony. Yet, the court accepted the circumstantial evidence by the expert. In Camm's case, a forensic expert and scientist named Robert Shaler proved that the prosecution and defense experts were incorrect as their testimony was based on specks of blood on Camm's T-shirt. Robert Shaler emphasized that the information provided for Camm's conviction was insufficient, and the experts themselves couldn't agree on the type of pattern (Collof, 2018). The wrongful conviction cases have emerged a more substantial standard and have published new guidelines for BPA.

Evolution of BPA in courtrooms

The evolution of BPA analysts' verdicts in courtrooms about the crime event had a more significant impact on solving a crime. The BPA analyst should not give their opinion based on a pattern until the analyst had reproduced the pattern. In 1880, the Supreme Court of Mississippi mentioned the first use of blood spatter at trial (Smith, 2018a). In 1954, Sam Sheppard's case gained significant attention in BPA analysis, where Paul Leland Kirk, BPA analyst, studied the interpretation of events at the crime scene. In 1957, the Supreme Court of California accepted BPA and affirmed that Kirk was a qualified expert in the field of BPA (Smith, 2018b). In 1966, The Supreme Court of Alaska accepted BPA for expert testimony following the case of a victim shot in a fishing ship (Smith, 2018b). The statement included an Alaska State Police officer in determining the victim's position when shot. In 1979, Compton Vs. Commonwealth, the Supreme Court of Virginia, accepted BPA expert testimony. The Danville police officer testifies for the bloodstain evidence collected from the crime scene, which possessed a bloodless circle that helped determine the victim's position during the crime event. In 1980, Macdonell's admission as an expert was unsupported by the defendant in the Illinois appellate court. Macdonell testifies that the bloodstains on the defendant's clothing resulted from the impact spatter from the defendant's wife's attack. In 1981, the Supreme court of Maine supported the BPA expert testimony on the State vs. Hilton case (Smith, 2018b). In 1983, Courts in Tennessee, California, Illinois, Oklahoma, and Maine supported Macdonell's studies in BPA and accepted BPA in trials. In 1985, the Supreme court of Mississippi focussed on the expert's qualification based on Macdonell's training, which involved a week-long training considering it objectionable for a retrial. In 1987, the court in

Indiana accepted BPA based on the expert's knowledge compared to the average layperson. The comparability itself was sufficiently weak, yet it sufficed the requirements as an expert witness. For example, the detective on Fox vs. State testified as an expert witness who had attended only one course in BPA and hasn't testified before (Smith, 2018b). In 1990, the courts in Minnesota, Idaho, and Michigan relied on Texas courts for the admissibility in BPA expert testimony. The Supreme Court of Minnesota accepted expert testimony from a serology expert who took courses in BPA. The court didn't require the specified BPA expert but recognized experts with known knowledge in BPA. In 1995, the Supreme Court of North Carolina accepted expert testimony from Duane Deaver, a forensic investigator who gave incorrect details of bloodstain evidence collected at the crime scene. Deaver testified that the defendant had no bloodstains in his clothing and later found tiny blood spots on the defendants' boots (Smith, 2018b).

In 2001, an officer who had insufficient credentials appeared in court for expert testimony in BPA. Camm's case is a perfect example of misrepresentation of patterns which could result in wrongful conviction (Reform,2017). When the court system had its acceptance of BPA expert testimony, it became clear that the credentials of BPA experts were contradicting. In 2009, the National Academy of Sciences found the uncertainty of BPA in forensic science, and most of the expert testimonies were subjective rather than scientific((TIL), 2020). The uncertainties led the National Academy of Science to establish a set of standards for BPA. The federal court ruled that the BPA experts who had testified performed inadequate testing and were highly subjective. For example, in 2018, the Texas commission implemented an accreditation requirement on BPA based on Joe Bryan's case.

Effects of Bloodstain Pattern Analysis

BPA is a growing field in the scientific community which involves uncertainty. The reliability in BPA has questioned courtroom testimony based on the expert's credentials. During the growing phase of BPA, an officer who has completed training or workshop (48 hours week-long course) qualified as an expert. Soon, the testimonies derailed due to the lack of expert evidence when questioned. The certainty of the expert's testimony had been based on circumstantial evidence and turned to be subjective. An analysis might involve human error based on the analyst's experience in the field. A study conducted by Osborn et al. in BPA has indicated that an expert's subjective analysis (20% of the experts in BPA) has misidentified a bloodstain pattern (Osborne, 2016). One study involved the classification of bloodstain patterns, a total of 730 bloodstain pattern samples based on different surfaces and six different types of patterns (Impact Spatter, Gunshot Spatter, Cast-Off, Satellite Spatter, Transfer Pattern, and Expirated Spatter) (Terry Laber, 2014). The analysts chose a single pattern by nominating more than one. The study concluded that 13.1% of the pattern classification did not include the correct pattern based on the surfaces (Terry Laber, 2014). The accuracy of the pattern classification of the variables was varied or biased (Taylor, Laber, Kish, Owens, & Osborne, 2016). The different types of patterns indicated different percentages of misinterpretation.

Another study indicated that the analysts' difficulty recognizing patterns resulted in the analyst's conclusion being subjective and inconclusive. The analyst's proportion of misclassification was comparatively less when given a crime scene/scenario. Whereas, given only the pattern, the significance in determining the classification was less, which indicated a confirmation bias. This study concluded that the identification of pattern classification using traditional BPA methods involved 4% error rates for expirated blood spatter and 8% error rates for impact spatter (Terry Laber, 2014). The error rates were dependent on the target surfaces, where analysts easily identified the type of stain on non-absorbent surfaces than fabrics. The misclassification rates varied based on the kind of bloodstain pattern, especially impact spatter.

In cognitive science, experts are more susceptible to bias and contextual information. The proficiency testing in traditional BPA showed high variation in human errors and misinterpretation of type of stains. A reliable methodology to improvise a more standard practice increases accuracy and reliability (Terry Laber, 2014).

Bloodstain Pattern Analysis Cases involving the lack of human error

In 2016, according to the National Registry of Exonerations (NRE), numerous prisoners were released due to false convictions (Pokin, 2017). The NRE record for 2016 tallied to be 168 individuals were exonerated based on the forensic evidence submitted (Pokin, 2017). In 2009, Brad Jennings was convicted for the murder of his wife, Lisa Jennings. At first, Lisa's death (gunshot wound) was a suicide because of insufficient evidence. Based on Lisa Jennings's younger sister, Marsha Iler, who testified that Brad killed Lisa, officer Sgt Dan Nash re-examined the crime scene photos. Upon the analysis of the blood spatter and Marsha's confession. Officer Nash ordered a gunshot residue test on Brad's bathrobe. (Pokin, 2019). The defense argued that Officer Nash had withheld information on the analysis and was not an expert in BPA. In 2015, the evidence against Officer Nash for providing false information surfaced to the court. The blood spatter evidence provided by Officer Nash was inaccurate. The defense attorney, Robert Ramsey, argued on Officer Nash's BPA expertise as he attended a week-long coursework/workshop and a certification of training. As Nash stated, the mist blood spatter found on Brad's bathrobe resulted from a gunshot. Brad was found guilty by the blood spatter evidence submitted by Nash and sentenced to 25 years in prison. According to Brady's violation (act established for accumulating and withholding evidentiary information during trial), Brad Jennings was found not guilty and was released. The blood spatter pattern (mist pattern) found on Brad's bathrobe was inconsistent with a high-velocity impact spatter and was a transfer pattern. The Jennings case was one of the NRE cases where false convictions, inconsistent expertise in BPA, and insufficient evidence. Officer Nash's record indicated that Tom Bevel, leading expert in BPA, trained him.

In 1996, Warren Horinek was convicted of murdering his wife, Bonnie. Warren stated that Bonnie shot herself in her throat, and the autopsy indicated a single gunshot wound to the chest. The gunshot wound to Bonnie's chest was self-inflicted based on the proximity of the gunshot (Mann, 2010). Many witnesses testified against Warren, stating his abusive relationship with Bonnie, and based on the circumstantial evidence, Warren was found guilty of murder. The prosecution's final witness was Tom Bevel, a private bloodstain pattern expert in Oklahoma (Mann, 2010). On the analysis conducted by Bevel of Warren's T-shirt (evidence collected from the night of Bonnie's death), the clothing was covered in blood and had dozens of specks of blood on the shirt's left shoulder (Mann, 2010). Bevel explained that the specks of blood are the origin (100 blood spots found on the left side of the T-shirt) from a high-velocity impact spatter (Mann, 2010) concluded that the bloodstain was caused due to a gunshot wound at close range.

Figure 15: The Warren Horinek case evidence (Mann, 2010; Pokin, 2017)
*(left)*Warren Horinek with the bloodied T-shirt and (right) specks of blood found on the wall.

Jim Varnon, a retired police officer, doubted Bevel's testimony and implied that specks of blood could be due to CPR or contact with bloodied objects. Varnon presented his case to Herbert MacDonell (Bevel was a student/trainee of MacDonell) and Anita Zannin (analysts), who concluded that Bevel's testimony was incorrect (Mann, 2010). Zannin indicated that high velocity spatter can be caused by gunshot and a punctured lung, such as expirated spatter. MacDonell illustrated an experiment that co-relates to Zannin's analysis, where he made a student place a small amount of blood and breathed on a white T-shirt (Mann, 2010). Bevel had two different causes for his testimony against Warren: the size of the bloodstain matters and its appearance. The expirated blood will be lighter than standard blood color and will most likely have bubbles present in the bloodstain. The lack of bubble-like presence could cause confusion between an expirated spatter and a gunshot spatter. The other cause is the lack of blood spatter trail; the specks of blood were only on a T-shirt and not towards Bonnie's face as it was covered entirely with blood. The theory had a reasonable explanation for the testimony of Bevel. The Horinek case is an excellent example of inconsistent testing, and different standards in terminology could lead to a wrongful conviction.

Human error in bloodstain pattern analysis prevented by computerized technology

Every expert in BPA has different standards in their credentials and expertise, resulting in specific errors allowing automated methods to become an essential subject in forensic science. Automated methods can significantly reduce human errors. e.g., A case involving a gunshot wound to the head and decapitation results in different patterns of blood overlapping. A gunshot pattern will occur in high velocity spatter, whereas a decapitation results in arterial spurts, smears, and low-velocity droplets (Karger, 2008). Image processing helps to divide blood spatter patterns into local and globular quantitative data. The study applies by assigning quantitative values to each pattern, which distinguishes them broadly based on the applied data (Arthur, 2017).

The automated methods also include a Multi-resolution 3D processing/scanning tool, which enhances and accurately examines the crime scene photos. The enhancement of the crime scene photos helps the analysts to distinguish the pattern. The tool's drawbacks are that it takes a prolonged time to analyze and does not involve the analysts' direct analysis of the crime scene. To determine the point of origin would cause a negative impact using the Multi-resolution 3D processing/scanning tool. New automated methods such as *Hemovision* and Directional Analysis have emerged for determining the area of convergence of BPA (Illes & Boue, 2013; Joris, 2015). Improvising automated methods could have a positive impact on BPA and reduce false convictions. Hence, computerized methods are highly improving compared to manual methods.

Introduction to Artificial Intelligence (AI)

The knowledge of computer vision has seeded into the term Artificial Intelligence in several ways of machine learning programs. The emergence of artificial neural networks, computing resources, and extensive data collection has advanced how a human brain works and processes the collected data. Biological experiments first conducted the study of machine learning—the knowledge of neural networks implemented by the recreation of human neurological structures to digital format. The experiment (neurophysiological research) involved analyzing the various stimuli of neurons in cats and learning how the neurons help to store sophisticated features like shape and then into more complex data such as visual representations (Dr. Sharam Tafazoli, 2019). Due to the emergence of A.I., there has been exponential growth and potential in the field. Artificial Intelligence was coined in 1956 by John McCarthy at the Dartmouth conference (Dr. Sharam Tafazoli, 2019; Eudreka, 2019). *A.I.* is defined as science and intelligence in creating machines that perform human intelligence tasks. General intelligence or human intelligence tasks involve visual perception, speech recognition, decision-making, and translation between languages. *A.I.* is a discipline involving machine learning, deep learning, knowledge base, expert systems, computer visions, and natural language processing.

The growth of A.I. has progressed due to the available computational power, advanced algorithms (better algorithms help in computational analysis for deep learning with increased accuracy), and more module data (generating large data sets). A.I. helps in the classification of data and enabling the data to be more efficient. A.I. classified into three types, Artificial Narrow Intelligence (ANI), Artificial General Intelligence (AGI), and Artificial Super Intelligence (ASI). ANI, also known as weak A.I., focuses on a specific problem or task. AGI, also known as strong A.I., can perform particular human-like abilities involving human intelligence. ASI is when a computer's capabilities surpass human knowledge and skills. Hence, only ANI is used and exists with full ability.

Platform, IDE, Language, and Algorithm

AI programming has an increasing rate of technological efficiency and benefits created/funded by researchers and many other foundations. A developer in computational analysis develops different software using various algorithmic languages due to a new AI program (Victor, 2018). There is no single programming language that can have all the solutions, each AI program has a specific approach for a particular project. Selecting a programming language, entering relevant data, and implementing algorithms can create a program that meets specific requirements (Duomly, 2020).

Anaconda

Anaconda is an open-source distribution of python applicable for data science, deep learning, and machine learning. Anaconda has more than 300 data science libraries, which aids in

AI algorithms. Anaconda Navigator is a desktop GUI that helps the user quickly access and edit files. The Anaconda is called the package manager, which allows installing multiple programs at once. Anaconda consists of both python and Jupyter notebooks. Using Anaconda navigator 2.0, launching the Jupyter Notebook has become an easy task.

Jupyter Notebook

Usually, for developing a program, IDE (Integrated development environment) should be installed. It is an environment that includes everything necessary for developing a program. It has a text editor (for writing code), running the program, and a debugger (which allows quick editing of all the bugs in the program). In this project, instead of using a traditional IDE, a Jupyter notebook is used. The Jupyter notebook is a Web-based interactive environment to write and test the program quickly.

Python

Python, also known as the fastest-growing programming language, was developed in 1991 and highly favored compared to C++. Python is the most helpful language for AI and is the leading coding language for Natural Language Processing (NLP) because it is a very convenient, simple syntax, efficient, and natural language to learn (Zola, 2018). Implementing machine learning in Python can result in predefined functions of algorithms and an extensive data set library (Nadim, 2019). Python uses Linux, Windows, IOS, Platform Independence, UNIX, and Extensive Frameworks for Deep Learning and Machine Learning (Claire, 2017; Victor, 2018). Programming in Python supports object-oriented, functional, and procedure oriented (Nadim, 2019; Zola, 2018). Python has cons, including a slower execution of data/lack of speed than Java, and is not suitable for mobile development (Duomly, 2020; Garrett, 2020).

K- Nearest Neighbor (KNN)

KNN is a machine learning algorithm used for solving classification and regression problems (Harrison, 2018). KNN is a supervised learning algorithm that depends on labeled input data to understand and learn a function and produces output data when given new unlabeled data (Harrison, 2018). For example, when a child (taken as a computer) is trained for what an apple looks like, different pictures of apples, oranges, and grapes are shown by implementing several input data given, requiring a specified output. A classification problem has distinct categories of values as output. For example, a binary classification can be image of blood present in clothing or blood being not present in clothing.

A generated data would base on the classifications of the input data. There are two sections, a predictor, and a label. We are predicting if there is image of blood on the victim's clothing (1) or image of blood is not present on the clothing (0) based on the type of victim's clothing (considered as the predictor). The output classification algorithm is representing an integer number (0, 1). The integer numbers are representational and not for mathematical operations. The regression problem has an actual number as its output data. Regression analysis will have a dependent variable and independent variable. The independent variable can also be a more than one variable. The dependent variable is the output when an independent variable is written as input. The KNN algorithm assumes that identical elements/data are in proximity. The KNN algorithm calculates the distance between any two data points. The possibility of calculating the distancing based on the specific data solving technique/method. The preferable method is the Euclidean distance, also known as the straight-line distance calculation.

Review of Literature for Artificial Intelligence

Artificial Intelligence (A.I.) originated from the classical ages of Greek Mythology, which had their notion of machine learning (Dr. Sharam Tafazoli, 2019). Even though A.I. started as a hypothesis, it has evolved into the most basic machine learning intelligence method in today's world. In 1950, Dr. Alan Turing speculated about creating a machine and questioned if the designed machine could think. Alan Turing's speculation turned into creating a Turing test. The Turing test is defined as testing a machine's ability to think like a human and is considered as the original proposal for the philosophy of A.I. According to Turing, if a machine could carry an indistinguishable conversation with a human, it was reasonable to assume that the machine was thinking and would qualify for the Turing test. However, there has not been a machine that has a hundred percent qualified for the Turing test until now.

In 1951, Christopher Strachey, a computer scientist from the University of Manchester, created the first program known as the checker's program using the Ferranti Mark 1 machine programmed for the A.I. to play and compete with humans' game of chess. In 1956, the term Artificial Intelligence, coined by John McCarthy at the Dartmouth Conference (Edureka, 2019). In 1959, the first A.I. laboratory was established and set up by the MIT lab. The MIT AI lab started its research on A.I. programs, also known as the research era of A.I. The lab conducted neurophysiological research on cats to determine how the neuron's stored data based on the various stimuli—the experiments conducted for digital networks. Many universities recognized the growth of A.I. and promoted research by funding. During the 1970-the 1990s, there was a significant fall-back in A.I., also known as A.I. Winter, a period where there were false expectations of success. The challenge of developing computing resources was not appreciated or considered, which led to severe financial setbacks in much research. In 2012, ImageNet Large Scale Visual Recognition

Challenge (ILSVRC), an image classification competition, involves higher accuracy and error rates. Deep neural networks are a gold standard in image recognition tasks (Dr. Sharam Tafazoli, 2019).

Benefits and Effects of AI

Implementing and amplifying human intelligence with computational machine learning has a great potential for civilization as far as the developed technology is beneficial (Tegmark, 2016). The goal to keep A.I. profitable from economic perspectives to the law involves validity, security, and control. Developing A.I. has led to improvising features in day-to-day life, from controlling our cars to power grid systems. A.I. performs cognitive tasks by outperforming specific human intelligence and triggering self-improvement (I.J. Good, 1965). Even though ANI is the currently used A.I., the development and achievement of AGI can be better than human intelligence and performs all cognitive tasks. Many researchers have believed that AGI development can be a cognitive task and would be highly beneficial for civilization.

While A.I. could be beneficial, it could also be dangerous as the researchers also believe that the development of AGI could progress to ASI by self-achieving cognitive tasks by the A.I. itself. This programming could lead to two risks (a) A.I. programmed to cause negative consequences, such as an autonomous weapon is programmed to kill and cause mass casualties (Tegmark, 2016). (b) A.I. is processed to do the beneficial activity but follows a negative path to achieve the goal (Tegmark, 2016). The side effects of superintelligence can lead to the achievement of the performed task through a real threat. A.I. has not achieved to outperform human-like thinking abilities. When the A.I. becomes a superintelligence, it would be beneficial and safe until the performed goal of both the A.I. and human are on the same pathway. In terms of law enforcement, A.I. has the potential of situational awareness and better responses in a dangerous situation. The future of A.I. can assist in the nation's crime laboratories (Rigano, 2019).

Factors That May Contribute to Uncertainties in the Region of AI

The potential of AI is vastly evolving in forensic science, as the use of AI has played a vital role in the criminal justice system. Human intelligence is considered learning from experience, whereas AI has regarded as the machine's ability to learn and mimic its software experience (Marr, 2016). Humans recognize patterns, emotions, objects, places, and people, whereas AI mimics these features in software algorithms such as image processing, detecting complex medical conditions, and online search tools.

Artificial Intelligence in the field of forensic science

In a legal system, scientific methods should have proper forensic statistics. A.I. provides faster results if the provided database has much extensive information. During a trial or conviction, the information pertained should be disclosed and not withheld by Brady's violation. Due to withholding information, there will be miscommunication and cause a wrongful conviction. A.I. can help overcome this issue and bridge the gap between forensic investigators and the court. A.I. can also help develop a graphical model for a case scenario that would help improve judgments during trial and support. Manual video and Image analysis have caused human shear error due to the volume of information and limited expertise in this specific field to process the data. A.I. can reduce errors and make the process easier and quicker. e.g., A recent study introduced an A.I. algorithm in Gunshot analysis in forensics for the discovery of pattern signatures (Labs, 2016; Marr, 2016).

Digital forensics is a growing field that requires the analysis of complex sets of extensive data. A.I. performs as a great tool in analyzing the large complex data sets by simplifying the format and delivering a metadata analysis (P, 2016). Pattern recognition identifies a specified type of pattern in a large data set. A.I. performs this task in a very accurate manner as it matches with the maximum possible data types available. A.I.'s recognition of patterns can reduce false positives and negatives (P, 2016).

Role of Artificial Intelligence in Bloodstain Pattern Analysis

Numerous researchers have invested in merging machine intelligence and BPA for better accuracy. The traditional BPA method involves manual techniques resulting in a long and tedious approach. AI reduces the processing time compared to conventional methods, e.g., A study conducted by Giovanni. Et al. stated that integrating computational intelligence with image processing techniques increases examining bloodstains (Giovanni A, 2014). Yu Liu et al., (2020) discusses the crime scene reconstruction of bloodstain pattern (Attinger, Liu, Bybee, & De Brabanter, 2018; Yu Liu, 2020). The type of computational analysis used was machine learning for the classification of patterns. They mainly focus on the automated classification of bloodstains produced by a gunshot or blunt impact (beating or stabbing). Yu Liu. et al. studied the difference in the accuracy of bloodstain patterns depending on the type of target surface and the distance. The results were significant, and the researchers constructed a new automated method for BPA.

Hypothesis statement

BPA analysts evaluate both the quantitative and qualitative features associated with bloodstain patterns, and their analysis of these bloodstain features has evolved. One reoccurring theme throughout the evolution of the science of BPA is the improvement in the accuracy of its techniques and the reduction of human error. Recent advances in image analysis using Artificial Intelligence have prompted the BPA research community to investigate the use of AI to BPA. As a tool, AI image analysis has the potential to model the complex data associated with bloodstain patterns accurately and, therefore, decrease the error rate of BPA. The purpose of this study aims to utilize AI algorithms to assist in the analysis of bloodstain patterns. Our AI-assisted method will be evaluated for accuracy and then compared to the current manual methods for BPA. Bloodstain patterns of various impact angles were created under controlled conditions. The experimental methodology used for this study was based on impact angle experiments commonly used to train BPA analysts. Bloodstain pattern images produced from various impact angles were used as the primary input data in the AI algorithm. While it is understood that BPA analysts utilize a variety of physical characteristics for a bloodstain, our research methodology only focused on the angle of impact that originated from medium velocity impact spatter. A novel AI-assisted methodology for analyzing bloodstain patterns will be provided to the forensic science community through our scientific evaluation.

Chapter II

Pilot Study: Impact Angle Experiment

The research performed in this study was conducted at The University of Central Oklahoma's Forensic Science Institute in the evidence bay. The evidence bay was designed for BPA and is an excellent controlled environment to produce blood spatter patterns. For the pilot study impact angle experiment was performed and cow blood was utilized throughout the experiment. The cow blood was collected from a local butcher shop and was approved by the University of Central Oklahoma before use. An anticoagulant (EDTA) was added to the blood before storage to prevent the blood from coagulation. The amount of anticoagulant added was sufficient to prevent the blood from clotting but did not alter the physical properties of the blood. The cow blood was refrigerated at 20°C in 20 mL containers and was used for all our experiments. When conducting experiments with blood, safety is an essential concern. Animal blood is an excellent alternative to human blood for BPA, and the practice of using non-human blood is expected in the field, as it decreases but not eliminates pathogens or risks (IABPA, 2008, 2019; B. A. Larkin & Banks, 2013, 2016; B. A. J. Larkin, 2015). The impact angle experiment was conducted to produce bloodstains in which blood is dropped from a known distance onto a target surface, fixed at a known angle ranging from 10 to 90 degrees. The bloodstain images were edited using the photoshop tool editor and the KNN analysis was conducted.

Method

The impact angle experiment was conducted to produce bloodstains in which blood is dropped from a known distance onto a target surface, fixed at a known angle ranging from 10 to

90 degrees. The target surface was a white sheet of paper which was secured to a paper clip board, laid flat at the time of deposition. Every target surface was marked with the known angles.

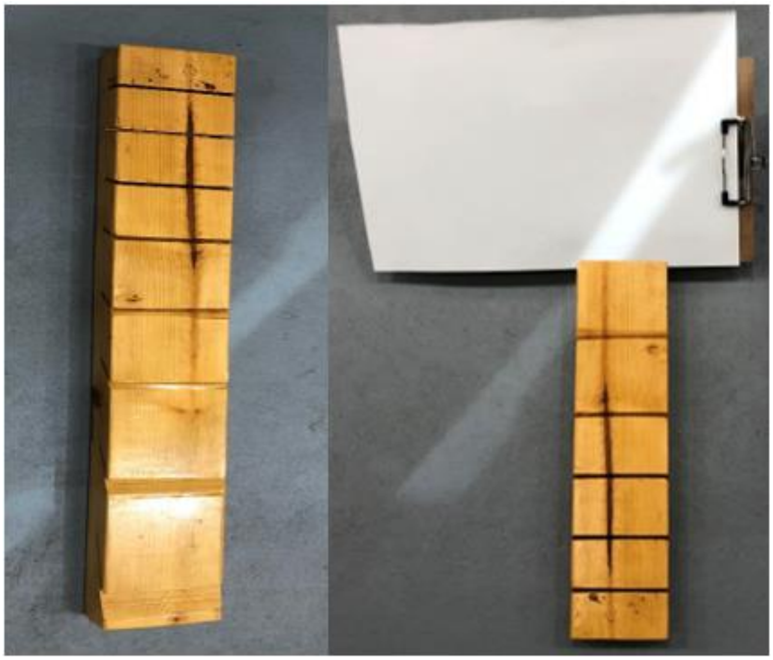

Figure 16: Impact angle experiment materials.
(Left) Impact angle board with angled slot; (Right) Impact angle board with a target surface (a paper board clipped to a clipped board) placed on 40-degree angle slot. The angle of Impact board is a flat wooden board which has 9 cuts on it. Each cut on the wooden board is at different angles (10°, 20°, 30°, 40°, 50°, 60°, 70°, 80°, 90°). A wooden clip board with a white paper is placed on the angle of impact board. When the liquid blood with known volume and height is dropped on the paper, based on the angle at which the clip board is placed at the angle of stain is formed.

A micropipette was used to transport a known or a measured volume of liquid. The disposable plastic tip was changed every three drops to avoid any dry blood disruption. The cow blood was transferred from 20 mL container to a small plastic tube. After transferring the blood to a smaller plastic tube, the pipette was filled with 50µl of liquid blood and was placed 30.5 inches over the target surface. Several drops fell on each target surface, forming separate stains. The impact velocity depends on the height where the blood is dropped from. The height was chosen based on previous studies for impact angle experiments (B. A. Larkin & Banks, 2013, 2016; B. A. J. Larkin, 2015). Temperature is a factor that affects the viscosity of the blood causing stain distortion (B. A. J. Larkin, 2015). To avoid this problem, during the experimentation, room temperature (25-30°C) was maintained. Each bloodstain was set for a minimum of five minutes after the last drop before target movement. After the bloodstains have set, the target was moved to a different angle slot (10, 20, 30, 40, 50, 60, 70, 80, and 90 degree). A sample size of eight bloodstain per target surface and a total of five target surface per impact angle were collected.

Angle	**90°**	**80°**	**70°**	**60°**	**50°**	**40°**	**30°**	**20°**	**10°**
Height (L)	30.5 inches								
Volume (V)	50μl								
Sample size (Z)	6-8 bloodstain per sample sheet and 5 sample sheet per impact angle								

Table 1: Various impact angle as a function of the impact-to-target distance (30.5 inches)

From the table 1, a total of 90 sheets of A4 sized paper were used for the experimentation, each sheet had six to eight bloodstains. For every angle, there was 10 individual sheets. The bloodstains were all collected and dried for two days at the evidence bay. The sample was later collected from the evidence bay and scanned at 300dpi resolution and transferred to a folder for editing.

Adobe Photoshop 2020 Editor

The scanned PDF bloodstain images were opened in the Photoshop and a new tab known as import pdf appears and all the pages with the bloodstain images were visible on the import pdf tab. The bloodstain images were opened on the Photoshop tool as seen in Figure 17. The size of each individual bloodstain in the Photoshop editor was 32 width X 192 height at 300dpi. The polygonal Lasso tool (L) was selected to create straight edged selections of the bloodstain images. Each of bloodstain was selected individually and cropped using the Lasso tool (as seen in figure 19). In the Photoshop document a new file was created with specified size (32 width X 192 height), resolution of 300dpi, and color mode (grayscale). The Gray scale image (10-degree bloodstain) was then selected and pasted on the Photoshop homepage.

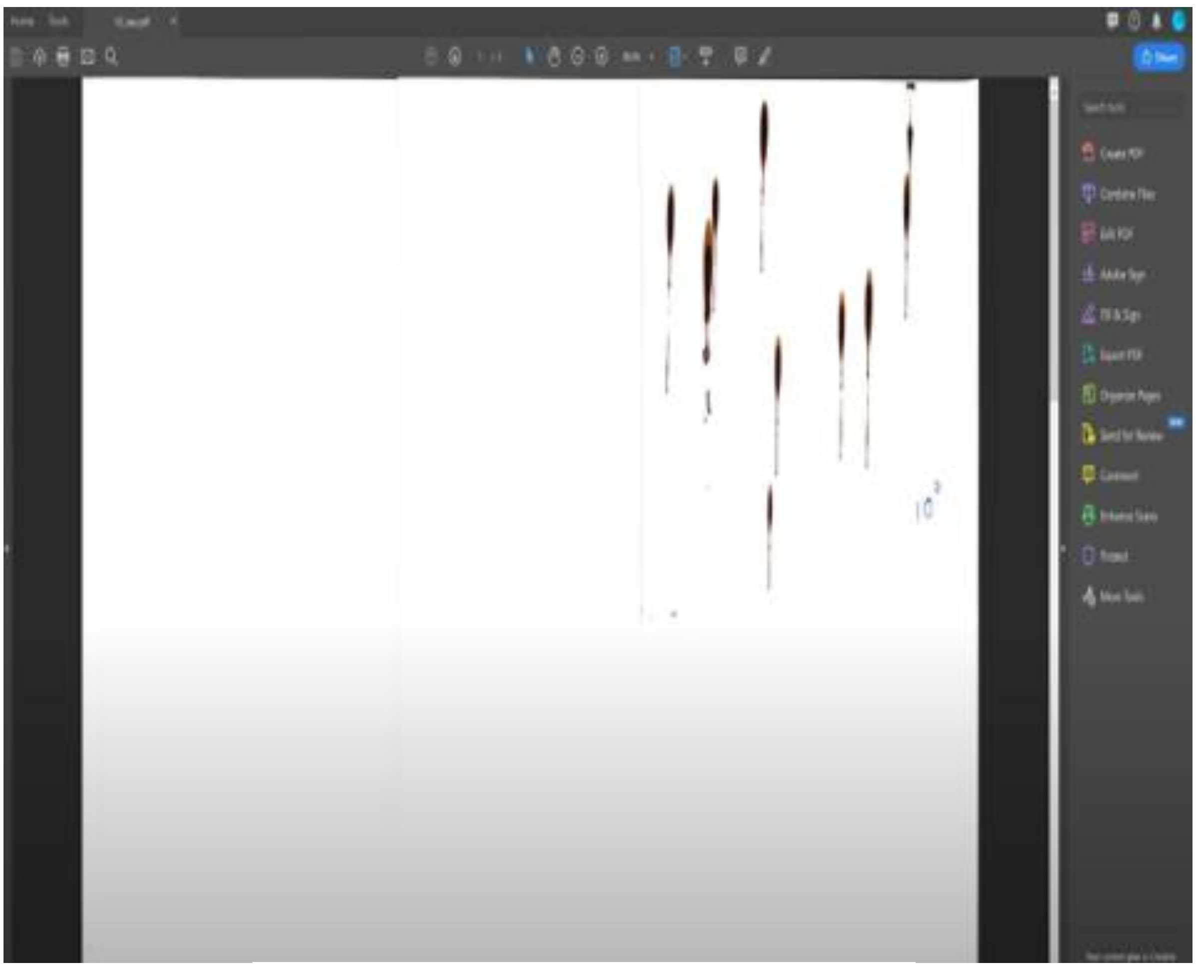

Figure 17: Screenshot of the Photoshop editor tool.
The 10-degree bloodstains are uploaded to the Photoshop.

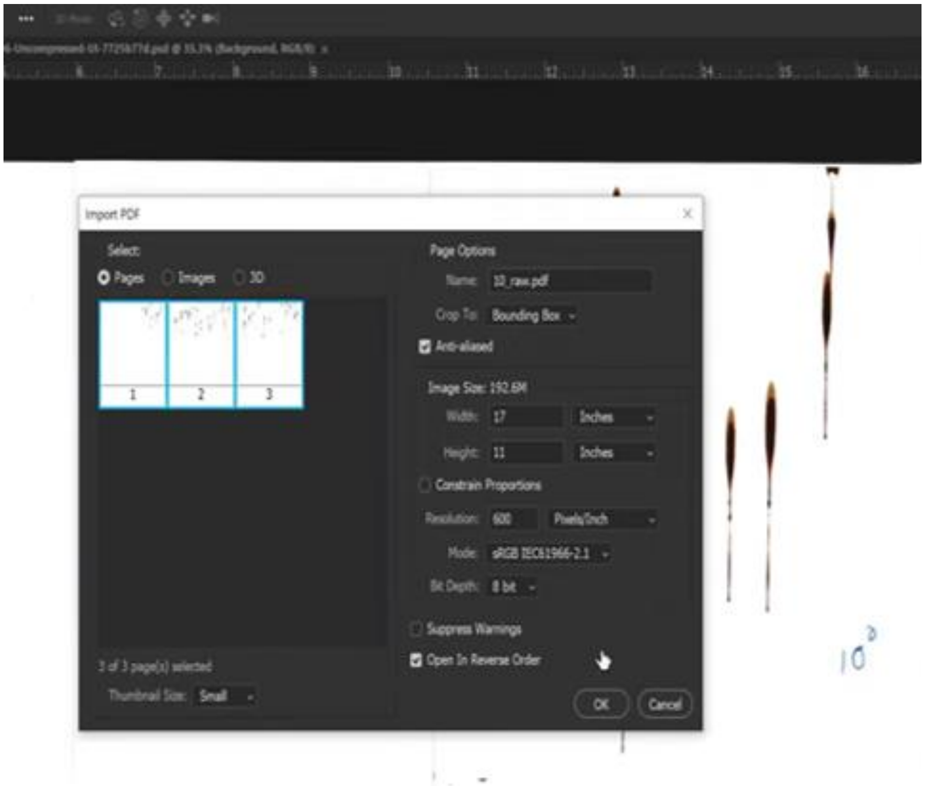

Figure 18: Adobe photoshop 2020 editor.
When the photoshop editor tool was opened the import pdf file appears on the screen with bloodstain images uploaded in pdf format.

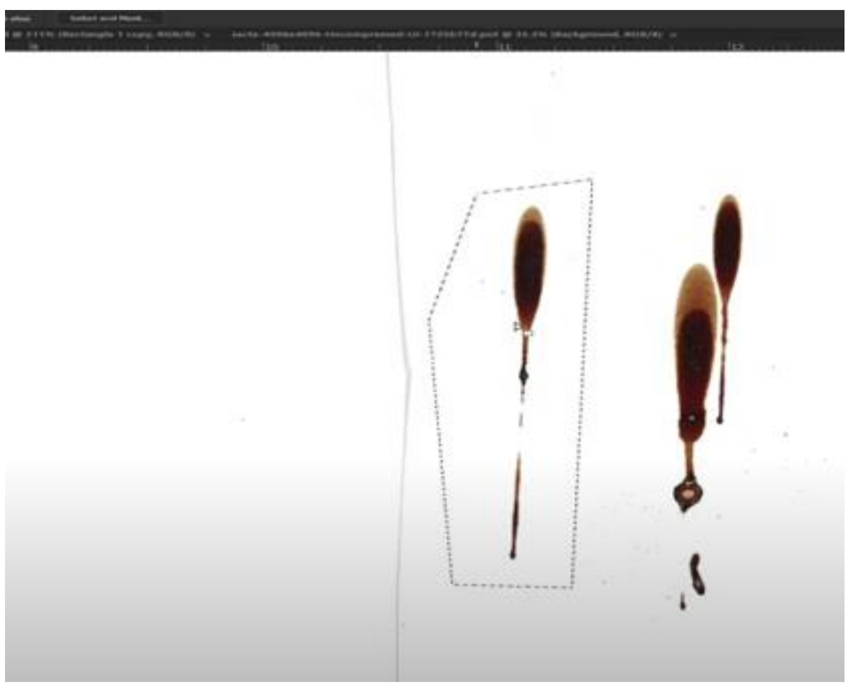

Figure 19:Polygonal Lasso tool (L)
Individual bloodstain selected using the polygonal lasso tool which was available on the tool bar in the photoshop editor.

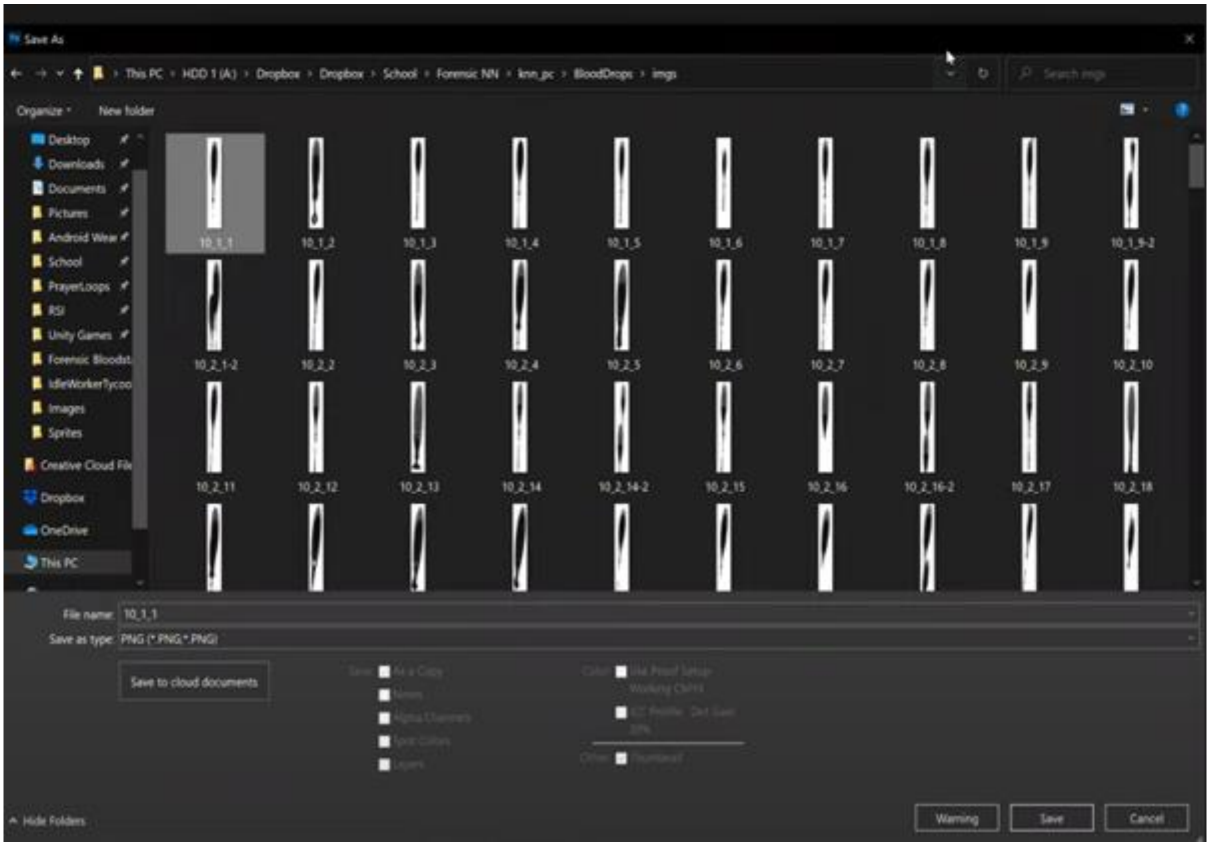

Figure 20: The bloodstain images were edited using the photoshop tool.
The naming convention of the bloodstain images were based on the angle and the sample set.

Jupyter Notebook

The Jupyter is an open-source computational notebook used for writing programs. The Jupyter Notebook App was launched by clicking on the Jupyter Notebook icon installed by Anaconda in the start menu on Mac OS or the windows or it can be launched by typing in a terminal. As shown in Figure 18, the anaconda navigator was used to open Jupyter notebook and launched a new browser window showing the Notebook Dashboard (a sort of a control panel which allows to select/ choose which notebook to open). When started, the Jupyter Notebook App accesses only files within its start-up folder which includes any sub-folder. No configuration was necessary if the notebook was placed in folder or subfolders.

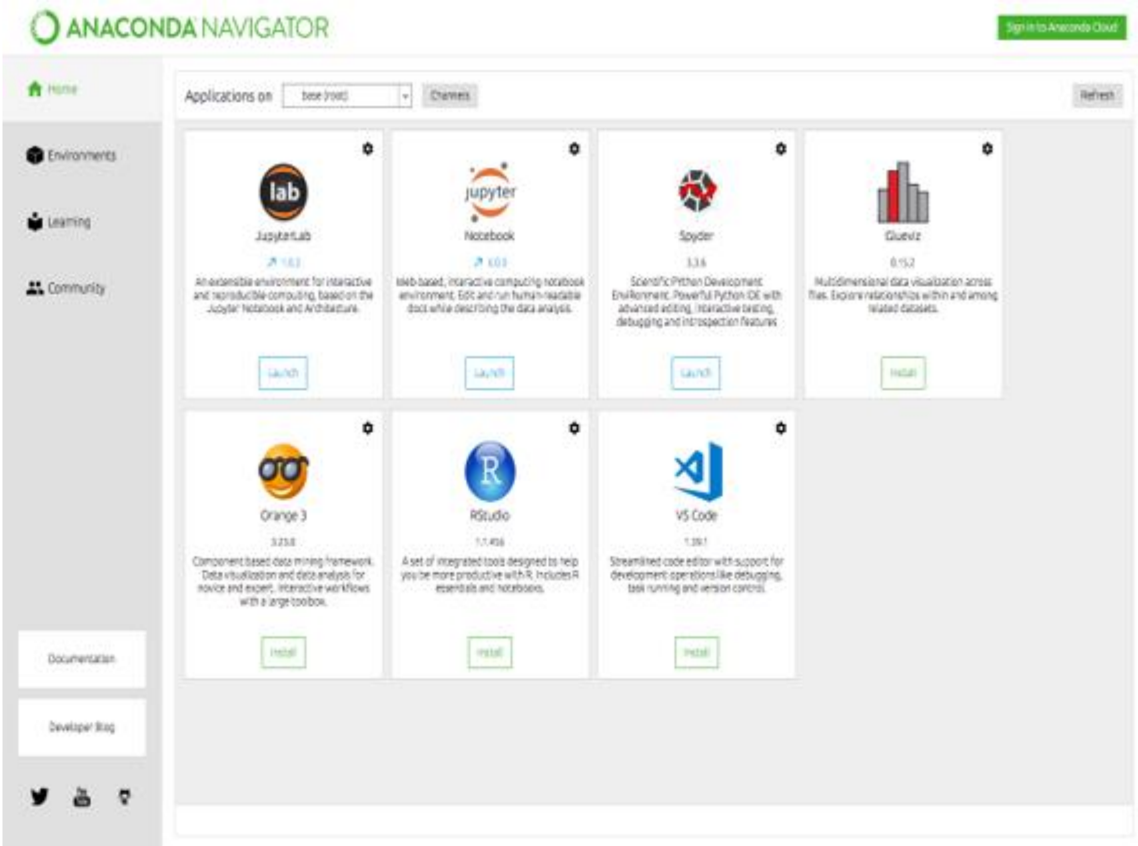

Figure 21: Image taken from the Anaconda Navigator 2.0 Documentation.
The display shows the Anaconda Navigator helps to launch Jupyter Notebook.

In the Notebook Dashboard navigate to find the notebook: clicking on its name opened a new browser tab. By clicking on the menu *Help -> User Interface Tour* for an overview of the Jupyter Notebook App user interface. The notebook document was run step-by-step by pressing *shift + enter*. The whole notebook was run in a single step by clicking on the menu *Cell -> Run All*. To restart the kernel that is the computational engine, the menu *Kernel -> Restart* was selected. Once the program was run and the output was detailed, the program was shut down by terminating the software. From the Figure 20, a screenshot taken during the analysis and the image of the different angle of impact was stored in this program. The 5th row consists of the KNN associated with the python which helps in the run analysis of the program. The program (a) The data set of the bloodstain images was addressed to be saved in file hdf5. The program was written according to the shape of the bloodstain. The train and a test set were a feature which was used for displaying the approximated value.

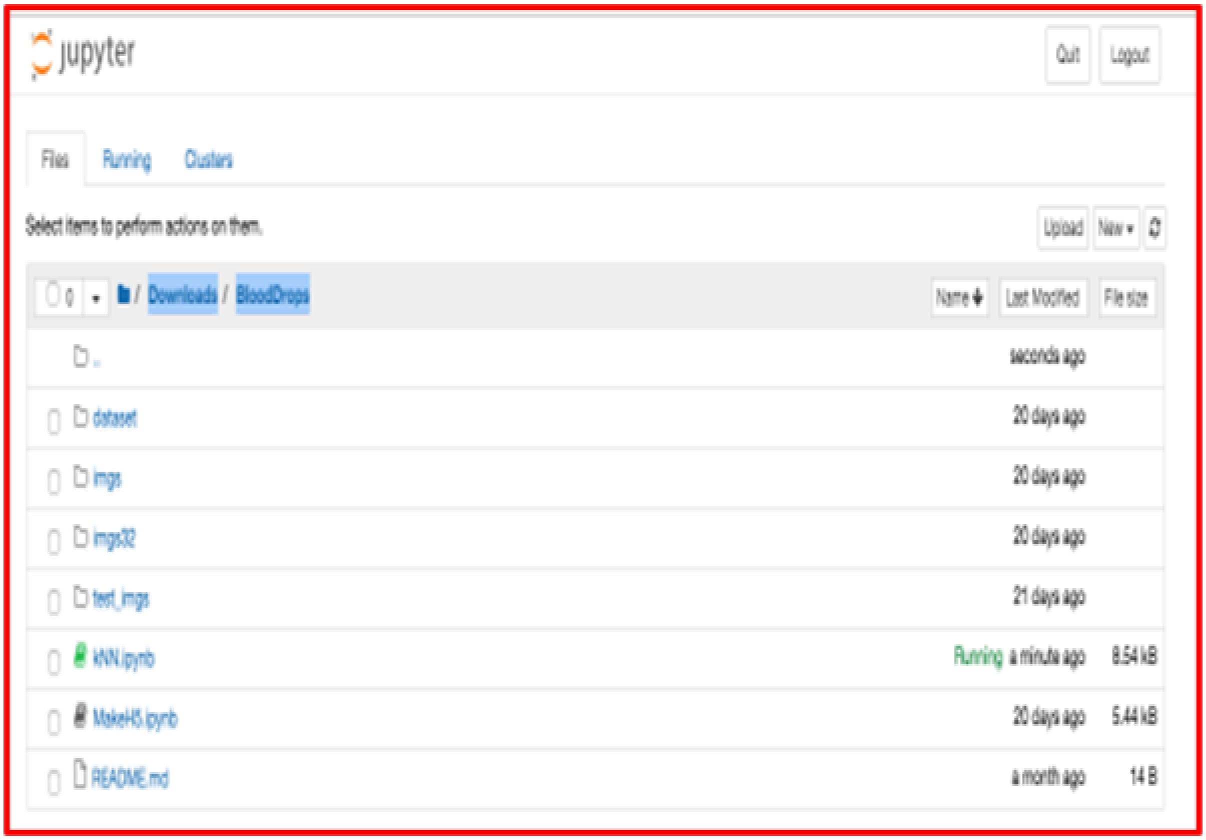

Figure 22: Image taken from the Jupyter Notebook.
The Jupyter Notebook contains all the bloodstain images from the impact angle experiment.

KNN (K-Nearest Neighbor)

In determining the angle of the bloodstain using the KNN, the bloodstain characteristics (data) should be known. There are 10 angles each one with classification. The new bloodstain angle (in this case, the class) can be known by comparing to its K nearest neighbors, and the majority class of its K neighbors would be the class of the new bloodstain. For example, if most of the K neighbors is 10°, then the angle of the new blood stain is 10°. KNN compares the new (unclassified) data with all existing data to measure the distance between the data to make the classification. The KNN steps are receiving an unclassified data, measuring the distance from the new data to all other data that is already classified, getting the *K* (where *K* is a parameter that was defined for this experiment) nearest neighbors, checking the list of *K* classes that had the shortest distance and counting the amount of each class that appears, acquiring the correct class which is the class that appeared most times.

Results and Discussion

For this pilot study, a large data set (90 samples containing six bloodstains per angle) of bloodstain pattern images were taken as the primary input for the AI algorithm. The AI algorithm assessed the bloodstain images, converting the data into an understandable result, which reduced time and human resources. Using the KNN algorithm, the impact angle from 90° to 10° accuracy was determined. The program's written according to the shape of the bloodstain using the Jupyter notebook. All the images of the impact angle (dataset) were stored in an HD5 file and the KNN algorithm was implemented using Python. During the experiments, the program divides the dataset into independent train and test sets. The test set is a set of examples used to assess impact angle (specific classification). The train set is used to facilitate the KNN algorithm to classify a new blood stain into one of the 10 possible angles. The classification report consists of precision, recall, f-1 score, and support. The precision is the number of the indeed identified positive results divided by the number of all positive classifications, includes those that were unidentified correctly. The recall is the number of correctly identified positive results divided by the total number of samples identified as positive to calculate the accuracy. The support is the number of samples of the correct response that lie in the class. In binary classification, the F1 score, also known as F-measure, measures a test’s accuracy. F-measure calculates the precision and recall of the test.

```
Test Result:

accuracy score: 0.8304

Classification Report:
              precision    recall  f1-score   support

          10       1.00      1.00      1.00        13
          20       0.87      1.00      0.93        13
          30       0.90      0.90      0.90        29
          40       0.75      0.86      0.80         7
          50       0.91      0.74      0.82        27
          60       0.73      1.00      0.84         8
          70       0.44      0.80      0.57         5
          80       1.00      0.25      0.40         4
          90       0.50      0.33      0.40         6

    accuracy                           0.83       112
   macro avg       0.79      0.76      0.74       112
weighted avg       0.85      0.83      0.82       112


Confusion Matrix:
 [[13  0  0  0  0  0  0  0  0]
 [ 0 13  0  0  0  0  0  0  0]
 [ 0  1 26  0  2  0  0  0  0]
 [ 0  0  0  6  0  0  1  0  0]
 [ 0  1  3  1 20  2  0  0  0]
 [ 0  0  0  0  0  8  0  0  0]
 [ 0  0  0  0  0  0  4  0  1]
 [ 0  0  0  0  0  0  2  1  1]
 [ 0  0  0  1  0  1  2  0  2]]
```

Figure 23: Image taken from the classification report
The variables are precision(mm), recall(mm) and F1 score(mm). The report indicates that the accuracy score was 0.8304.

As in Figure 21 which consists of a confusion matrix is 9x9, where the diagonal is the total value expressed for its accuracy. The confusion matrix shows how the classification's derived from the impact angle. The diagonal in the confusion matrix represents the correct classifications. The rows and columns represent the impact angle; for example, the third row has 26 on the diagonal and 1 to its left, which indicates that one is classified to be 20-degree. The result consists of an approximate accuracy of 0.8304, which is 83.04 %.

Conclusion

AI is a valuable tool that the BPA analyst can use to analyze a crime scene's bloodstain pattern. The pilot study has demonstrated the accuracy (83.04%) and certainty of using AI algorithms to analyze bloodstain patterns. The KNN algorithm was written according to the shape of the bloodstains. The size (32 width X 192 height) of the bloodstain image has been a constant parameter while performing the KNN analysis. The accuracy could vary if there were noise present in the bloodstain images. In the case of impact, angle bloodstains were a more extensive set of stains and had a suitable resolution for the KNN analysis. The total number of bloodstains samples could be a factor to achieve higher accuracy. This study was based on small sample size (10 samples per angle), limiting the analysis. However, the research conducted has given positive results, which supports further analysis in BPA. Thus, using the AI tools in BPA has significantly reduced time, error, and extensive expertise.

Impact Spatter Study – 120 Degree

Cow blood was utilized throughout this study. The blood was freshly drawn in a container for the experiment; an anticoagulant EDTA was added to the blood prior to storage to prevent the blood from coagulation. The volume of the anticoagulant depends on the volume of blood collected. The cow blood was refrigerated at 20°C in a 20 mL container and used for all experiments. For a conducting a preliminary bloodstain pattern experiment, animal blood is the most economical and resourceful way. Animal blood (cow, swine, porcine, bovine) stands as a great substitute for human blood. When considering animal blood, the source where it is obtained raises several questions, such as obtained from a slaughterhouse, either it is ethical or not, screened, or unscreened, and is it safe for BPA.

Impact Spatter Experiment

Materials required for the experiment are Butcher paper, mouse trap, impact angle board, poster boards, protractor, and blood. To produce spatter patterns was by applying medium energy force of blood. Butcher paper was placed under the mouse trap, and under the impact angle board to collect any blood spatter hitting the floor. Poster boards were cut in the size of an A-4 sheet to place on the impact angle board. As in figure 21, the mouse trap was placed at a height of 35 inches from the ground, set up on a table, parallel to the impact angle board. The impact angle board was placed at a height of 29.3 inches from ground set up on a table. The A-4 size poster boards were clipped to a clip board which was placed on the impact angle board at different angles. A *1000* µl blood liquid volume of blood was taken in a micropipette and deposited onto the open front edge (on the white portion) of the mouse trap to create a blood pool ranging in 1 inch diameter. From figure 20, the mouse trap was setup an angle of 20 degree using a protractor to create medium energy force of blood. Allowing the top of the mouse trap to drop closed, impacting the surface of the blood pool. The bloodstains were created on the A-4 size poster boards placed at an angle. The distance between the mouse trap and the impact angle board was 12 inches. The experiment was repeated for different angles from 10-degree to 90-degree.

Figure 24: Photographs of a mouse trap and impact angle board
(a) Mouse trap and angle board before placing a clip board (b) Mouse trap and angle board after placing a clip board at different angles.

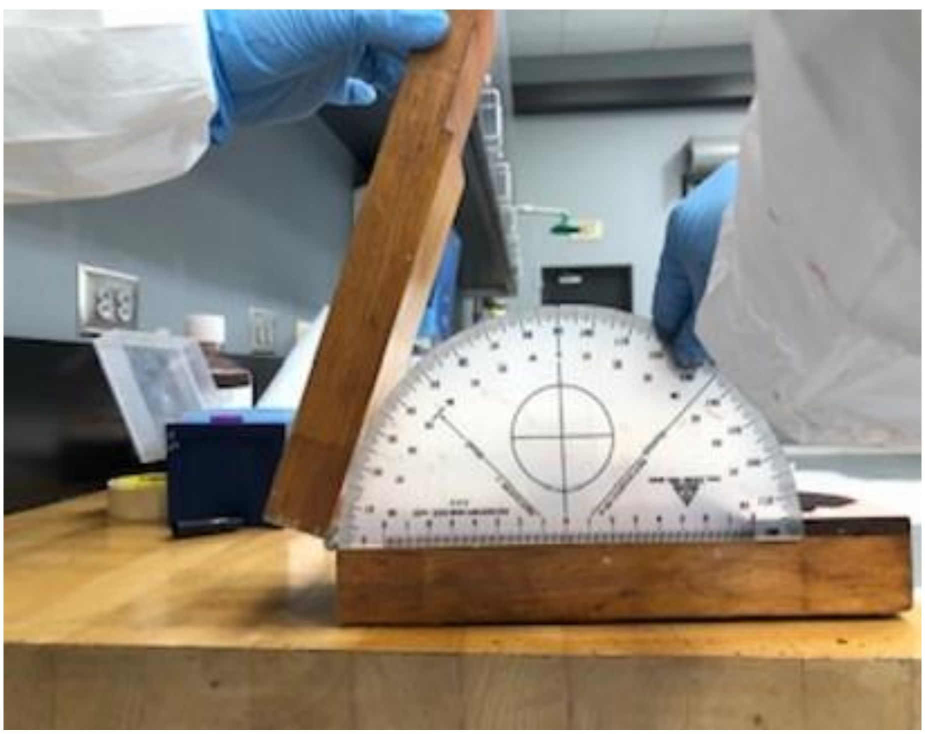

Figure 25: Image of mouse trap and a protractor.
Aligning the mouse trap to 120 degree using a protractor for creating medium impact spatter.

Figure 26: Image taken from the experiment set up.
The mouse trap is set up at a height of 35 inches on the table with 1000 μl blood and on impact hits the target surface which is the impact angle board (at a height of 29.3 inches) containing the clip board placed at an angle.

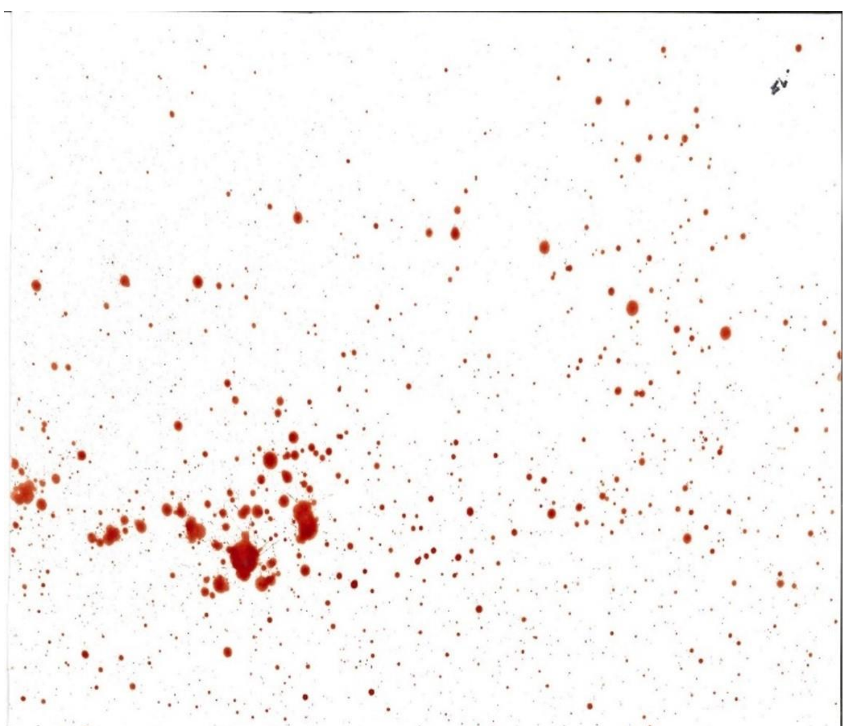

Figure 27: Example of a Scanned Image of the impact spatter – 80 degree

A total of 36 sheets of A4 sized poster boards were used for the experimentation, each poster boards had 30-50 bloodstains. For every angle, there was 4 individual sheets. The bloodstains were all collected and dried for a day at the evidence bay. The sample was later collected from the evidence bay and every individual bloodstain was cut separately and scanned for the AI algorithm process. From Figure 22, all the bloodstain images were scanned and converted into PDF file.

Artificial Intelligence Algorithm

The experiment was performed using the AI tools (KNN, confusion matrix, Jupyter notebook) which was downloaded from the Anaconda Navigator that was available online. Using the KNN algorithm, the impact angle (90° - 10°) accuracy was determined. The program's written according to the impact spatter shape of the bloodstain using the Jupyter notebook. All the images of the impact angle (dataset) were saved in an HD5 file and the KNN was implemented using Python. To better evaluate whether the KNN algorithm could learn the patterns, the data set was divided into a train and a test set. The test set is a set of examples used to evaluate whether KNN could accurately classify new data. The train set is to train the algorithm to learn how to classify blood stains.

Result and Discussion

Medium energy impact spatter are bloodstain patterns with a preponderant stain size of generally 1mm to 4mm in diameter. These are patterns are created because of some application of force. They are considered as the result of energy of up to 25ft/s. There was an absolute range set in medium energy spatter as the stains varied significantly for every impact angle. There was an observable relationship between the overall stain pattern and the location of the mouse trap as there was a radiating effect. The radiating effect results in a higher level of dispersion from the impact point. As we encounter impact spatter patterns frequently at crime scenes. Differentiating spatter patterns based on the preponderant size of the stains is the most common method employed. Thus, the overlapping in stains is mostly encountered. Any decision often made to identify a pattern as consistent or inconsistent should be based on specific characteristics based on the stain. For an example, when the distance was at 18 inches the stains appeared to be more dispersed and had a less of a misting effect. For each impact angle bloodstain, a total of four sheets containing at least 30-40 individual stains were experimentally created. The images of bloodstains were then sent for the AI algorithm to process. Each of the images were converted to grayscale before the analysis. Gray scale images are simply images in the colors of black and white. The importance of these images being converted to gray scale is to provide less information for each pixel. The bloodstains images at first appears to be in red, where grayscale would convert the red components to gray to have equal intensity.

After converting the images to grayscale, the bloodstain images were processed by the KNN algorithm the images were classified into a test set and a training set. The test set is a set of examples used to assess impact angle (specific classification). The train set feature is for fitting the dataset to the specified parameters. With the limited number of test cases, the training set was organized as each category having 7 samples. Therefore, the total number of training examples were 7 x 9 = 63. We used the rest of 98 samples as independent testing data. (KNN K = 6). The KNN performs a mathematical calculation to measure the distance between the data to make the classification. Using the Jupyter notebook in the Anaconda navigator, the program is processed with the images. Thus, displaying the result in the form, a confusion matrix. In this scenario, we have classified the results into three different cases.

Case Example 1

In case example 1, the blood stains were very similar when it goes above 70 degrees, the samples were grouped together of 70, 80, and 90 degrees as in the same range. The accuracy was 76.53%. (KNN K = 6). The above confusion matrix is 7x7, where the diagonal is the total value expressed for its accuracy. The confusion matrix showed how the classification's derived from the impact spatter for each angle.

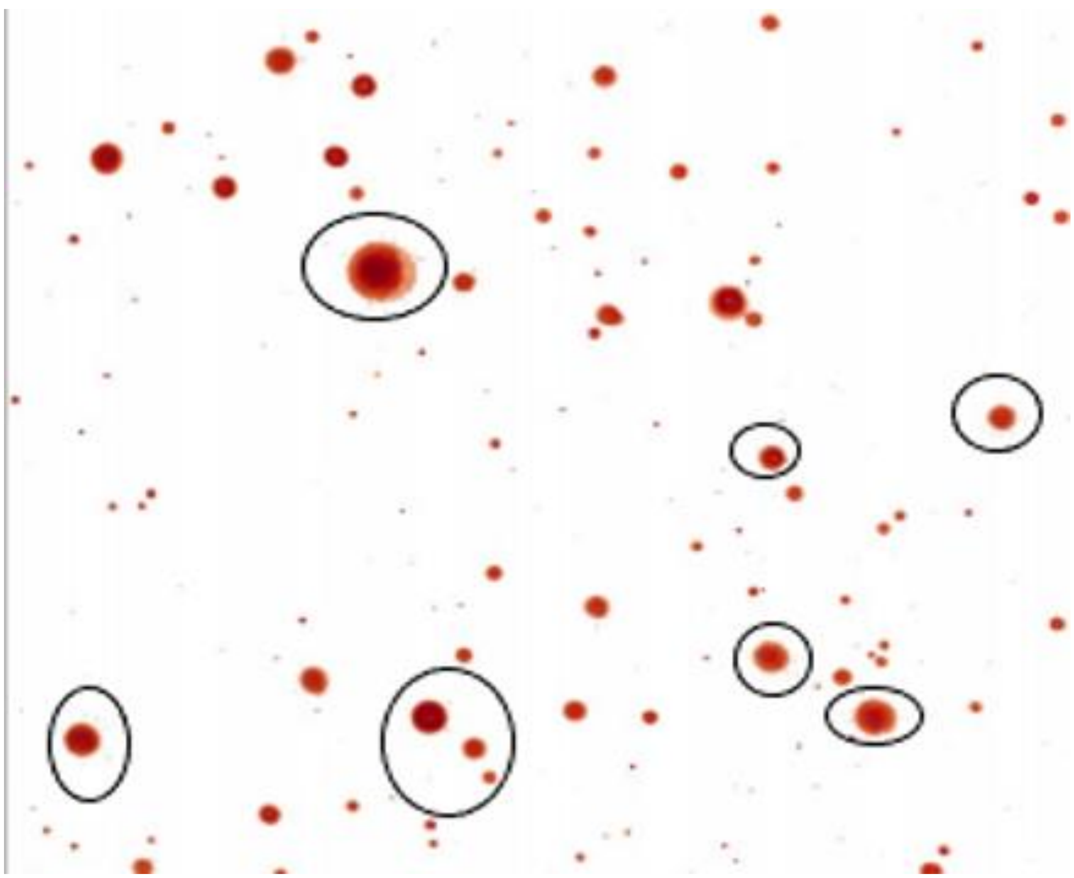

Figure 28: Image taken from the 70 - degree impact spatter bloodstain pattern. The circled bloodstains were selected for KNN analysis.

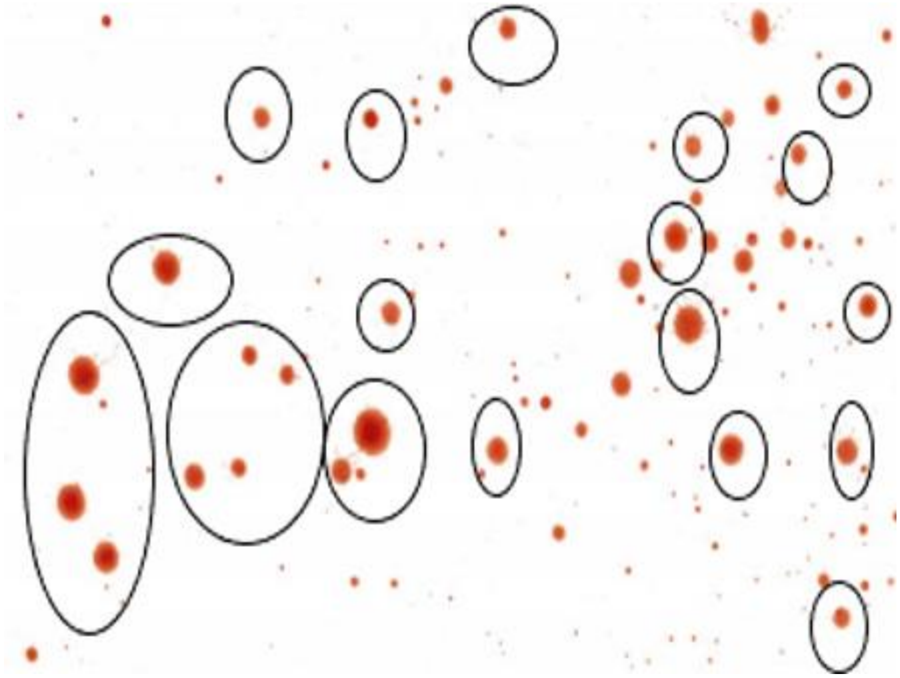

Figure 29: Image taken from the 80 - degree impact spatter bloodstain pattern. The circled bloodstains were selected for KNN analysis.

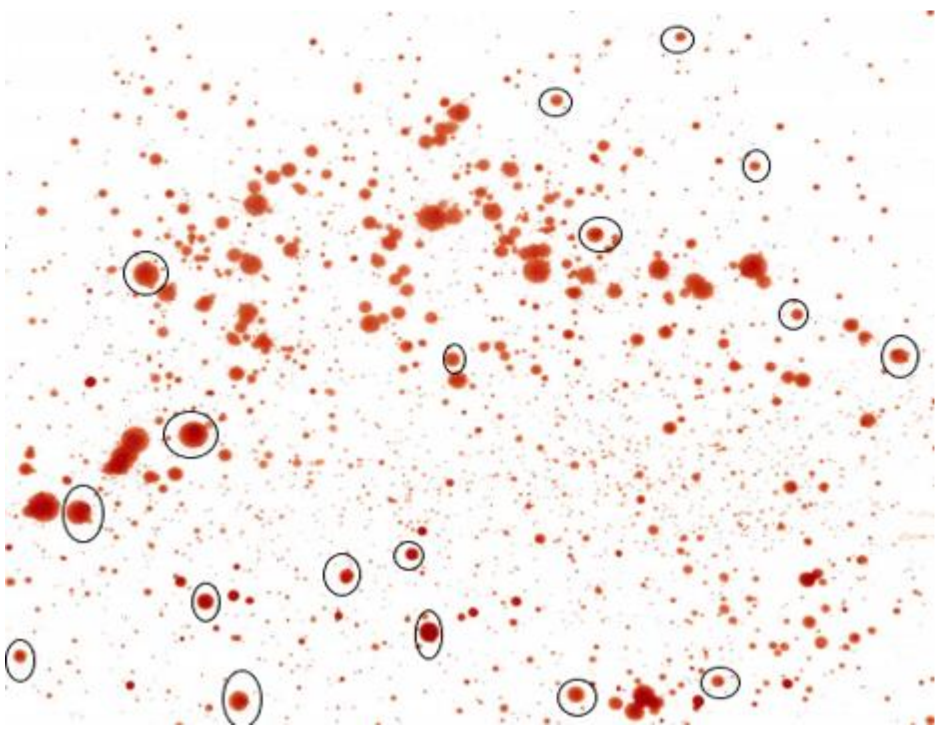

Figure 30: Image taken from the 90 - degree impact spatter bloodstain pattern. The circled bloodstains were selected for KNN analysis.

```
Test Result:

accuracy score: 0.7653

Classification Report:
              precision    recall  f1-score   support

          10       0.83      1.00      0.91         5
          20       0.91      0.83      0.87        12
          30       0.71      0.75      0.73        16
          40       0.75      0.50      0.60        18
          50       0.62      0.80      0.70        10
          60       0.67      0.40      0.50        10
          70       0.82      1.00      0.90        27

    accuracy                           0.77        98
   macro avg       0.76      0.75      0.74        98
weighted avg       0.76      0.77      0.75        98


Confusion Matrix:
 [[ 5  0  0  0  0  0  0]
 [ 1 10  1  0  0  0  0]
 [ 0  1 12  3  0  0  0]
 [ 0  0  4  9  3  1  1]
 [ 0  0  0  0  8  1  1]
 [ 0  0  0  0  2  4  4]
 [ 0  0  0  0  0  0 27]]
```

Figure 31: Image taken from the test result for case 1.
The classification report indicates the precision, recall, f1-score, and support

The above confusion matrix is 7x7, where the diagonal was the total value expressed for its accuracy. The confusion matrix showed how the classification's derived from the impact spatter for each angle. The diagonal in the confusion matrix represents the correct classifications. The rows and columns represent the impact angle; for example, the fourth row has 9 on the diagonal and 4 to its left, which indicates 4 blood stains were classified to be 30 degrees. The result consists of an approximate accuracy of 0.7653, which is 76.5 %. The precision (0.76) is the number of the indeed identified positive results divided by the number of all positive classifications, includes the tests which were unidentified correctly. The recall (0. 77) is the number of correctly identified positive results divided by the total number of samples identified as positive to calculate the accuracy. The support (98) is the number of samples of the correct response that lie in the class.

Case Example 2

In case example 2, the bloodstains were grouped under a different category to see if a higher accuracy can be achieved. The Figures 27 and 28 consist of the 30-degree and 40-degree impact spatter bloodstains, respectively. Each individual viable stain was circled for the AI algorithm to process. As the current samples of 30 and 40 degrees were very similar, thus the samples of 30 and 40 are in the same group, the accuracy was 84.69%. The above confusion matrix is 6x6, where the diagonal is the total value expressed for its accuracy. The confusion matrix shows how the classification's derived from the impact spatter for each angle. The diagonal in the confusion matrix represents the correct classifications. The rows and columns represent the impact angle; for example, the third row has 29 on the diagonal and 1 to its left, which indicates that one is classified to be 20. The result consists of an approximate accuracy of 0.8469, which is 84.69 %.

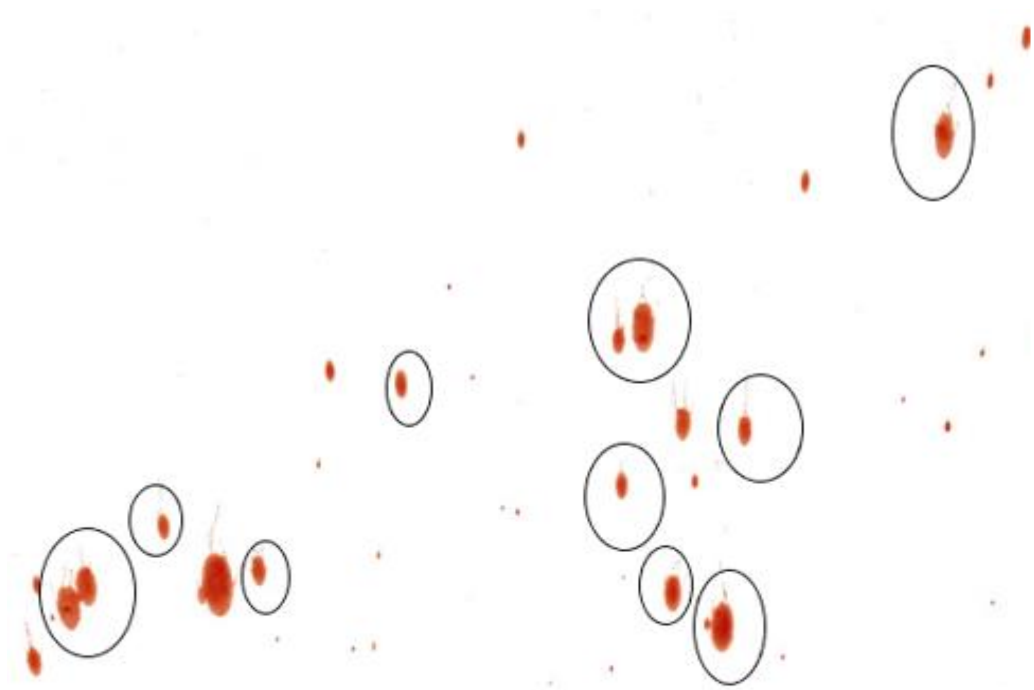

Figure 32: Image taken from the 30 - degree impact spatter bloodstain pattern. The circled bloodstains were used for the KNN analysis

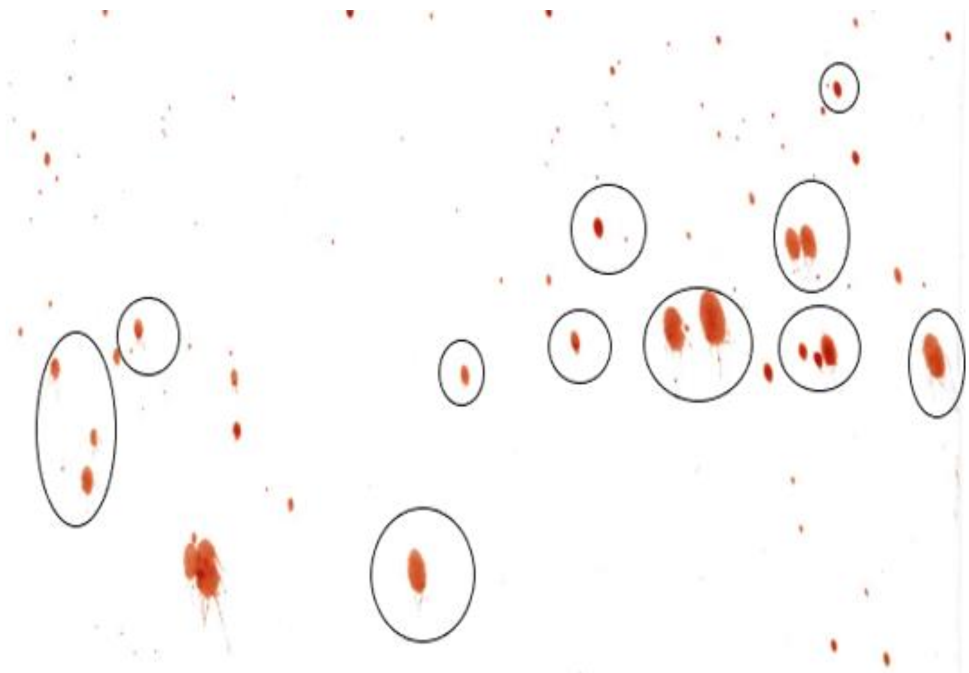

Figure 33: Image taken from the 40 - degree impact spatter bloodstain pattern. The circled bloodstains were used for the KNN analysis

The precision (0.85) is the number of the indeed identified positive results divided by the number of all positive classifications, including the tests that were unidentified correctly. The recall (0. 85) is the number of correctly identified positive results divided by the total number of samples identified as positive to calculate the accuracy. The support (98) is the number of samples of the correct response that lie in the class.

Case Example 3

In case example 3, the samples of 60, 70, 80, and 90 degrees were grouped into the same group, the accuracy rises to 87.76% (KNN K = 4). The grouping was based on the shape of the stain, as the degree was higher, the similar it appears in certain samples. The confusion matrix is 5x5, where the diagonal is the total value expressed for its accuracy. The confusion matrix shows how the classification's derived from the impact spatter for each angle.

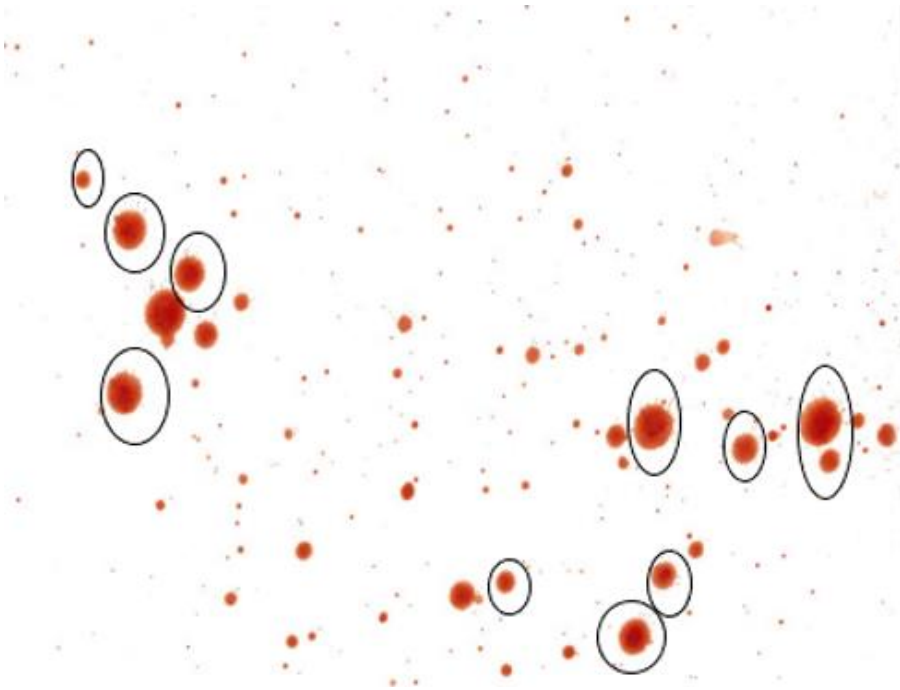

Figure 34: Image taken from the 60 - degree impact spatter bloodstain pattern. The circled bloodstains were used for KNN analysis

```
accuracy score: 0.8469

Classification Report:
              precision    recall  f1-score   support

          10       0.83      1.00      0.91         5
          20       0.91      0.83      0.87        12
          40       0.97      0.85      0.91        34
          50       0.67      0.80      0.73        10
          60       0.67      0.40      0.50        10
          70       0.82      1.00      0.90        27

    accuracy                           0.85        98
   macro avg       0.81      0.81      0.80        98
weighted avg       0.85      0.85      0.84        98


Confusion Matrix:
 [[ 5  0  0  0  0  0]
 [ 1 10  1  0  0  0]
 [ 0  1 29  2  1  1]
 [ 0  0  0  8  1  1]
 [ 0  0  0  2  4  4]
 [ 0  0  0  0  0 27]]
```

Figure 35: Image taken from the test result for case 2.
The classification report consists of the precision, recall, f1-score, and support.

```
Test Result:

accuracy score: 0.8776

Classification Report:
              precision    recall  f1-score   support

          10       0.83      1.00      0.91         5
          20       0.85      0.92      0.88        12
          40       1.00      0.85      0.92        34
          50       0.64      0.70      0.67        10
          70       0.87      0.92      0.89        37

    accuracy                           0.88        98
   macro avg       0.84      0.88      0.85        98
weighted avg       0.89      0.88      0.88        98


Confusion Matrix:
 [[ 5  0  0  0  0]
 [ 1 11  0  0  0]
 [ 0  2 29  1  2]
 [ 0  0  0  7  3]
 [ 0  0  0  3 34]]
```

Figure 36: Image taken from the test result for cased 3.
The classification reports shows that 60, 70, 80, and 90 degree are grouped together as 70 degree.

The diagonal in the confusion matrix represents the correct classifications. The rows and columns represent the impact angle; for example, the third row has 29 on the diagonal and 2 to its left, which indicates that one is classified to be 20. The result consists of an approximate accuracy of 0.8776, which is 87.7 %. The precision (0.89) is the number of the indeed identified positive results divided by the number of all positive classifications, including the tests that were unidentified correctly. The recall (0. 88) is the number of correctly identified positive results divided by the total number of samples identified as positive to calculate the accuracy. The support (98) is the number of samples of the correct response that lie in the class. The questioned sample (Q1 and Q2) was given as a proficiency testing for the AI algorithm to process. The Q1 and Q2 sample were considered as a classification of 30-dgree and 40-degree impact angle. Originally, the questioned sample was experimentally constructed at an angle of 30-degree. Therefore, giving an accuracy of 84% which is case 2.

Impact Spatter Study – 160 Degree

Introduction to Image J Processing Software

In this experiment, we used Image J that is a powerful tool to automatically extract blood stain images. The version is available online as Fiji-ImageJ or Fiji Downloads which can be downloaded by clicking on the windows download tab. The file was downloaded which consists of 300 megabytes. Once the files downloaded >> click on the Image J >> a window tab appears >> click on file >> open recent samples/open samples >> opens a bloodstain image. Based on Figure 33, the bloodstain image was selected (example: 90-degree bloodstain image), and the particle analysis was performed. The image area was cropped by only focusing only the area without margins or handwritings. The next step to be followed was to preprocess the image by clicking >> Image on the tab >> Adjust >> Color Threshold. The process will change the image into a binary image to remove the grayscale data. Click Tab >> Close color threshold tab >> Click Analyze >> Analyze particles. The tab requiring the *size* of the particles was displayed, the *shape* of the particle with a more circular pattern or irregular pattern, and outlines >> Bare outlines >> OK. As in Figure 40, a new window displays all the outlines producing 1622 particles, basically analyzing all the particles, and naming each particle. A specific particle can be viewed by accessing the manager window. By adjusting the size of the particle, the number of particles displayed on the window may vary. If the size was adjusted to more than 100 -100000, there are fewer particles. The results display various parameters for each angle. The measurements were set up before setting up the analysis. There are 20 different measurements where all the measurements are selected and saved. Each excel file has 35 parameters, but we used area, major, and minor.

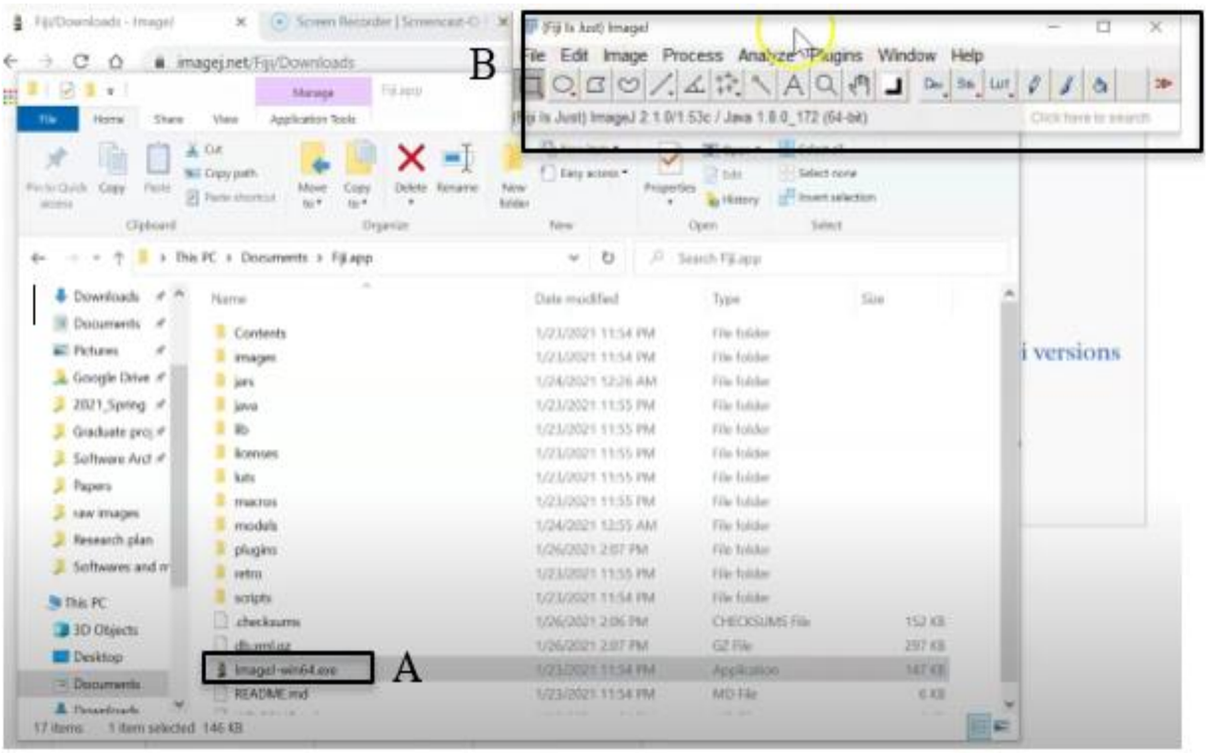

Figure 37 The ImageJ software.
A is the downloaded ImageJ software; B is the window tab that appears after clicking ImageJ software.

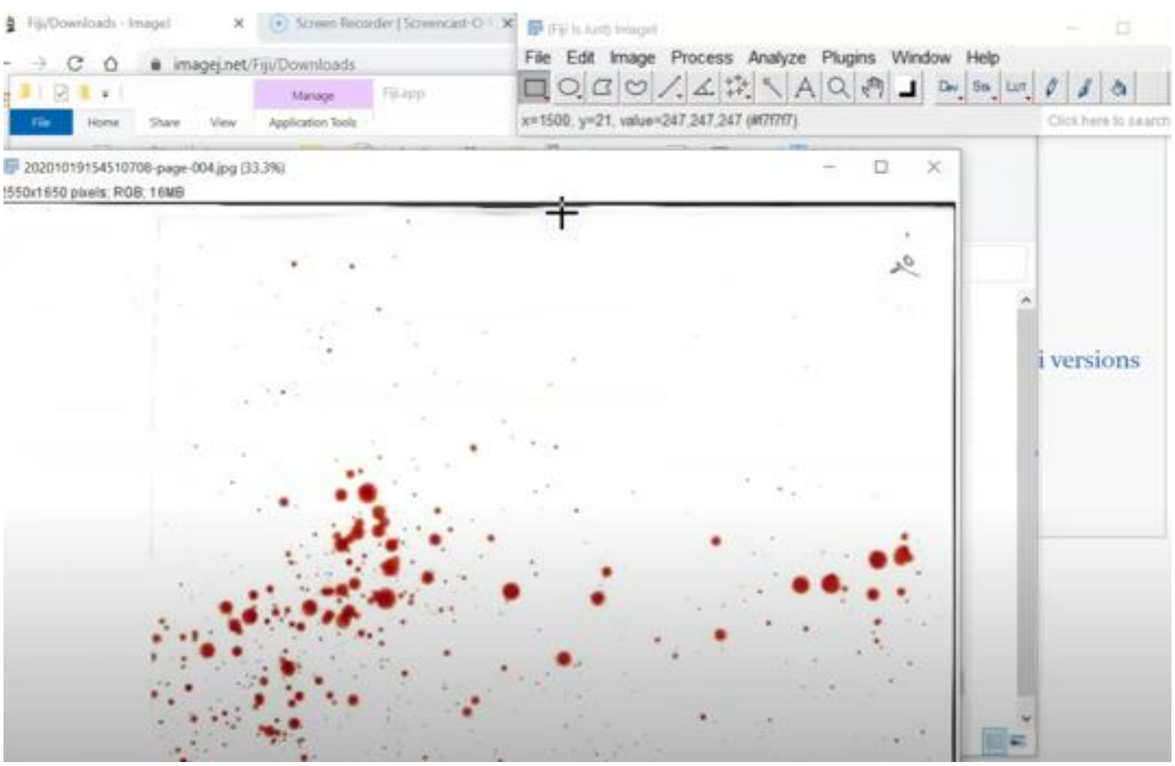

Figure 38: Example of the 90-degree sample taken for the image J processing.
The image shows that 70-degree bloodstain is selected for the ImageJ analysis.

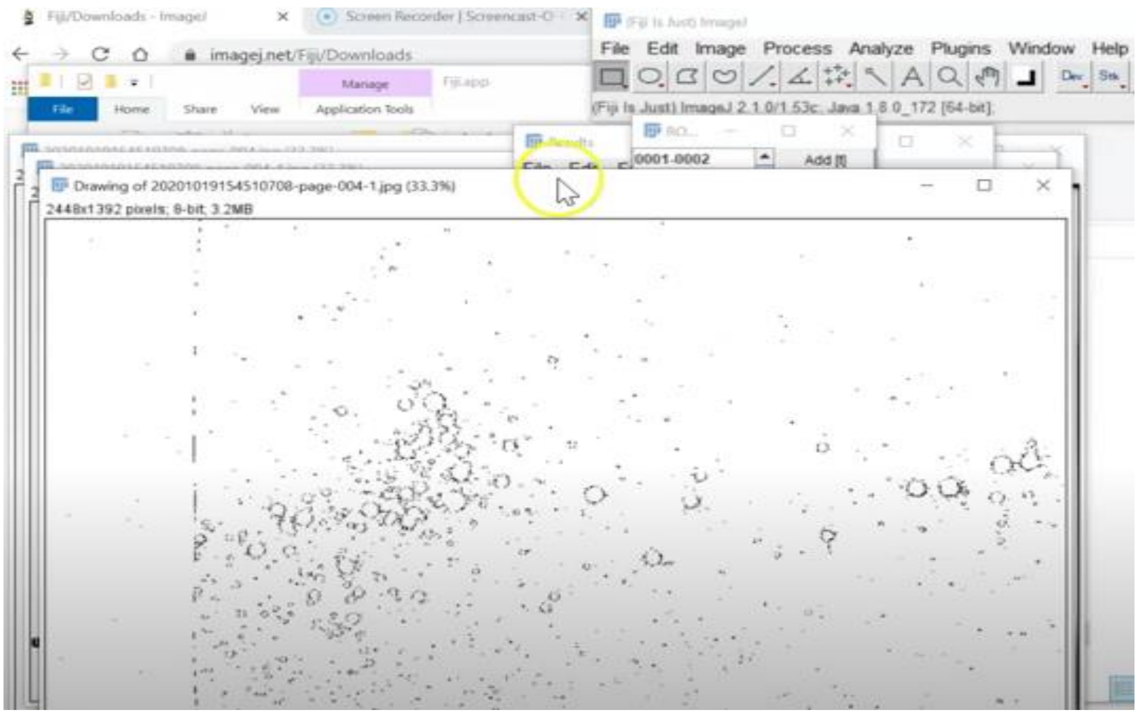

Figure 39: Window displays the outlines of the 1622 particles.
A new window displays all the outlines producing 1622 particles, basically analyzing all the particles, and naming each particle.

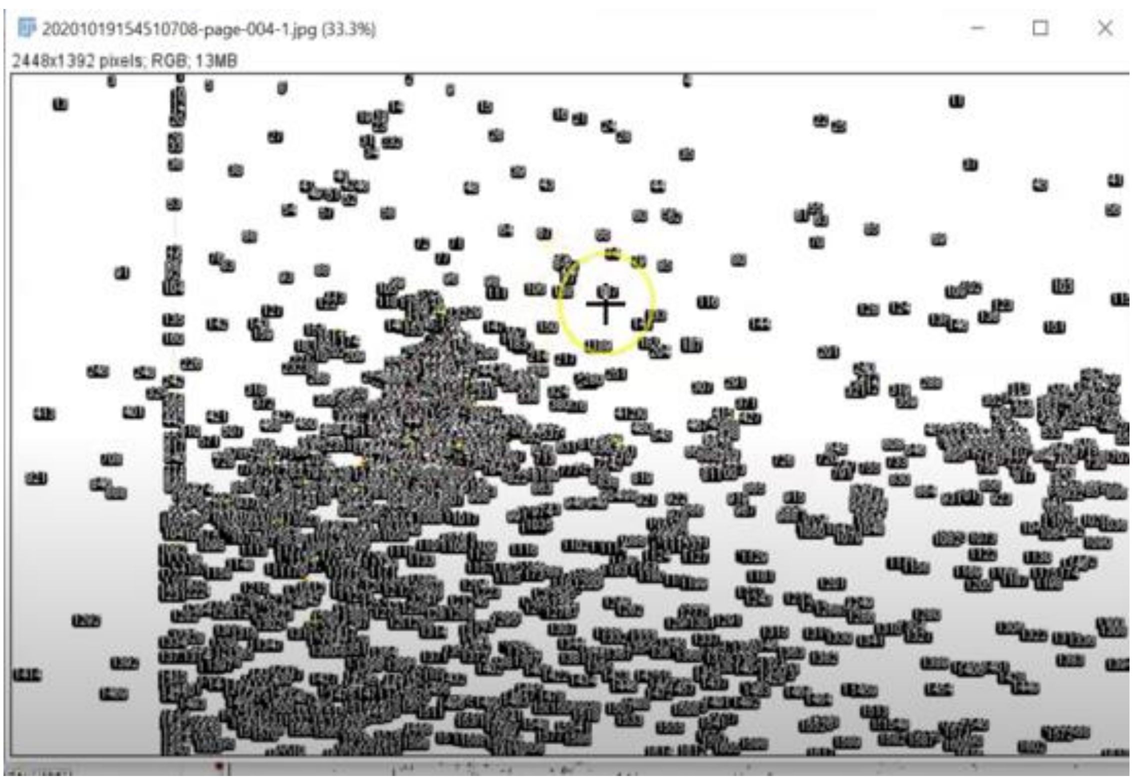

Figure 40: Window displays that each particle is labelled based on the order of the size.
All the bloodstains are labelled as particles under the various parameters.

Introduction to Manual Analysis

The direction of blood striking an object is determined using the pattern it produces. The pointed end always faces the direction the blood was travelling. The impact angle of blood on a flat surface can be determined by measuring the degree of circular distortion. The formula for calculating the sine of the angle is width divided by the length of the blood droplet. The angle, known by eliminating the sine by calculating the inverse of sine.

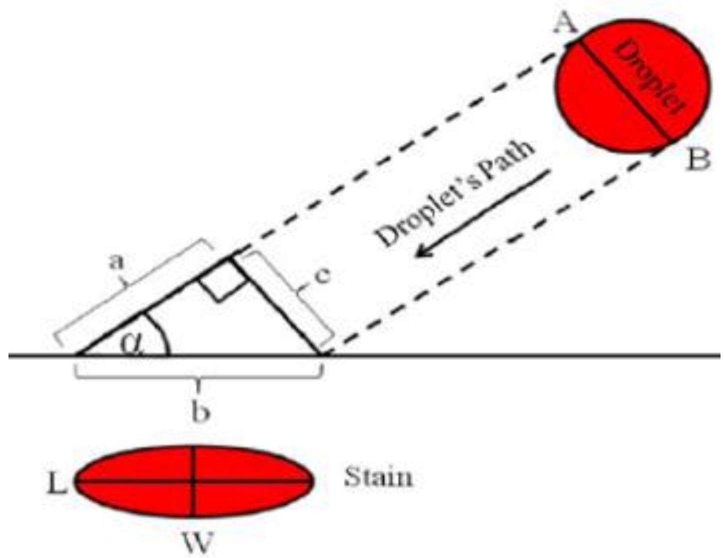

Figure 41: Schematic image of the bloodstain from a blood droplet with an impact angle (Kittipat,2010). Formula: The sine of the angle is width divided by the length of the blood droplet.

Materials and Methods

Image J Processing Software

For Bloodstains with different shapes and sizes, the images were converted into a binary image. Then the images were analyzed, ImageJ identifies six different areas. Each bloodstain image was cropped and saved in a file_1 (Input Image). As it would be a time-consuming process to individually extract/crop bloodstain images a macro program was used. The program takes all the images which were extracted from file_1 (Input Image), performs the analysis, and stores them into the new folder. The program is simply accessed by clicking the run analysis. The Figure 37 represents all the three steps: different size and shape particles. The particles converted to binary, and the image J identifies six different areas of the particle.

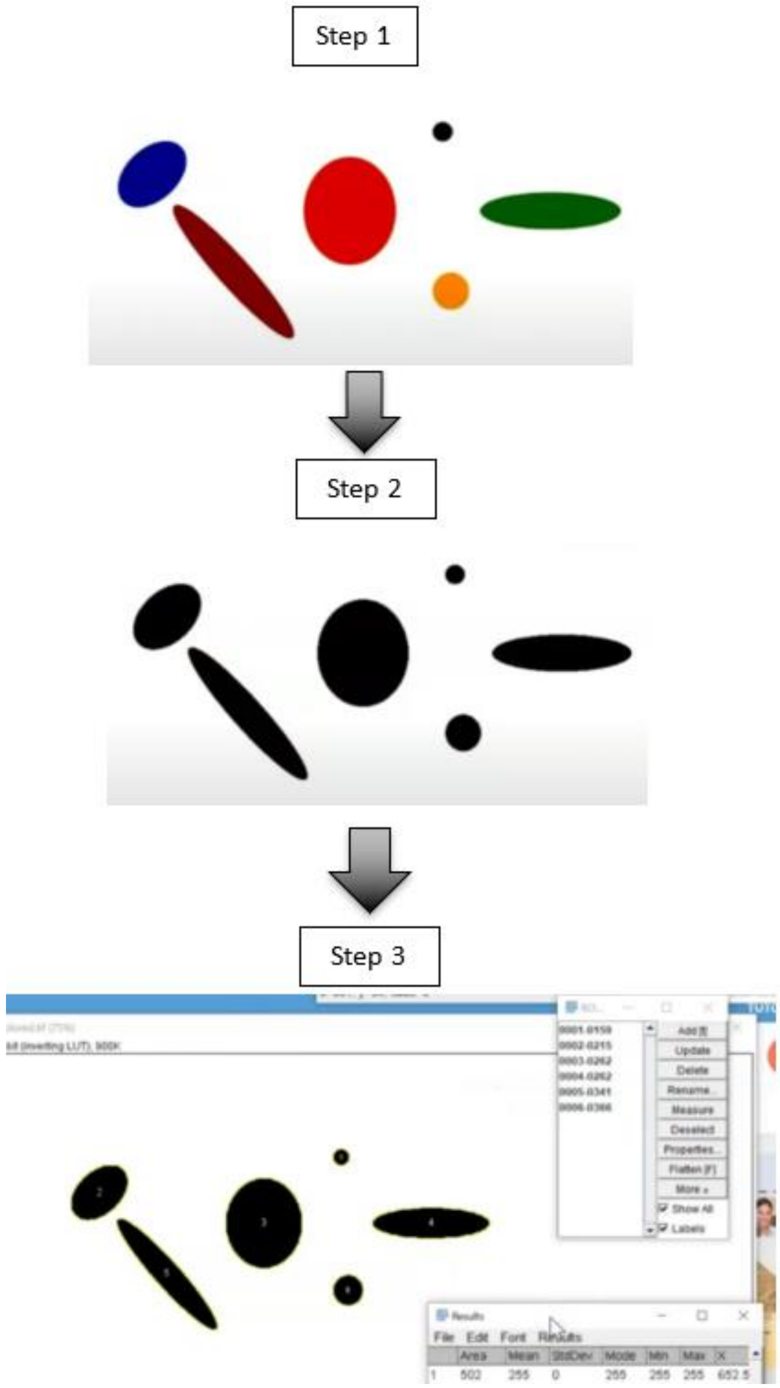

Figure 42: Different steps of the Image J processing.
Step1: The different size and shape particles. Step 2: The particles converted to binary. Step 3: The image J identifies six different areas of the particle.

Manual Analysis

To produce spatter patterns by applying medium energy force of the blood was conducted by the following experimental setup. Butcher paper was placed under the mousetrap, and the impact angle board. Poster boards were cut in the size of an A-4 sheet. The mousetrap was placed at a height of 35 inches from the ground placed on a table. The impact angle board was placed at a height of 29.3 inches from the ground set up on a table. The A-4 size poster boards were clipped to a clipboard which is placed on the impact angle board at different angles. A *1000* µl blood liquid volume of blood is taken in a micropipette and is deposited onto the open front edge (on the white portion) of the mouse trap to create a blood pool ranging in 1-inch diameter.

The mousetrap was setup an angle of 160 degrees using a protractor to create a medium energy force of blood. Allowing the top of the mousetrap to drop closed, impacting the surface of the blood pool. The bloodstains were created on the A-4 size poster boards placed at an angle. The distance between the mousetrap and the impact angle board was 12 inches. The experiment was repeated for different angles from 10-degree to 90-degree. The width and length of a bloodstain were measured using the following steps are to be followed: Step 1: After, the bloodstains have dried and set. The bloodstains were measured using a traditional method. Step 2: The curved edge of the bloodstain (right) was matched with the shape on the distorted end (tail). The length and the width were measured. The length was always longer than the width. Step 3: Using the Formula, the impact angle was calculated for each bloodstain.

$$\boxed{\text{Sin}^{-1}\text{ (width/length) = Impact Angle}}$$

Figure 43: 10-degree angle measured for the width and length of the angle. A scale (mm) is used for measuring the length and width of the stain to calculate the impact angle.

Result and Discussion

Manual Analysis

The orderly collapse of a droplet on a target surface had produced different characteristics shape based on the impact angle. As the shape of the bloodstain is circular, the impact angle increases (example: 90-degree). As the shape of the bloodstain is elliptical, the impact angle decreases (example: 10-degree). The 10 degrees had been calculated from the ground, which was always measured from the ground. The target surface affects the shape and size of the stain. In this case, the target surface was a flat paper surface that does not alter the shape/size of the stain. The impact angle was calculated for each bloodstain, a sample size of thirty. The average was calculated along with their accuracy. According to the manual analysis, the accuracy ranged from 97.8233 to percentage for the different impact angles. The manual analysis showed a better accuracy for certain impact angles such as 90 degrees, based on the bloodstains chosen manually.

Sample number	10-degree	20-degree	30-degree	40-degree	50-degree	60-degree	70-degree	80-degree	90-degree
S1	12.83	21.63	35.6	41.81	54.90	56.44	69.08	78.52	90
S2	12.83	22.76	30	41.81	48.59	61.04	70.25	80.30	90
S3	9.59	21.63	34.8	38.68	50.28	61.04	69.08	77.16	90
S4	9.59	21.34	30	41.81	50.28	61.04	70.25	77.16	90
S5	7.18	23.24	30	45.58	50.28	61.04	70.25	77.16	90
S6	9.59	21.63	30	44.42	53.75	62.73	70.25	80.30	90
S7	9.59	21.63	30	41.81	53.75	56.44	70.25	80.30	90
S8	14.47	19.39	30	41.81	50.28	56.44	70.25	80.30	90
S9	11.53	23.24	33.05	41.81	50.28	61.04	70.25	80.30	90
S10	9.59	21.34	33.7	38.68	46.65	56.44	69.08	80.30	90
S11	9.59	21.34	30	41.81	50.28	57.79	71.24	78.52	90
S12	11.53	21.34	30	41.81	46.65	56.44	71.24	78.52	90
S13	9.59	19.47	30	36.86	53.75	56.44	71.24	77.16	90
S14	11.53	21.34	26.38	41.81	53.75	56.44	71.24	77.16	90
S15	9.59	22.76	30	41.81	51.78	56.44	69.08	80.93	90
S16	11.53	19.47	35.37	41.81	46.65	56.44	70.25	79.52	90
S17	9.59	21.63	34.84	41.81	50.28	61.04	70.25	78.52	90
S18	11.53	22.76	30	41.81	50.28	61.04	70.25	80.30	90
S19	9.59	23.24	30	41.81	50.28	61.04	70.25	80.93	90
S20	7.18	21.63	30	41.81	50.28	61.04	70.25	79.52	90
S21	11.53	21.34	30	41.81	50.28	61.04	70.25	79.52	90
S22	9.59	21.34	33.74	38.68	50.28	61.04	70.25	80.93	90
S23	11.53	21.63	30	36.86	50.28	61.04	71.24	80.30	90
S24	12.12	19.47	30	41.81	48.59	64.15	70.25	79.52	90
S25	9.59	19.47	30	41.81	48.59	64.15	70.25	77.16	90
S26	11.53	21.34	30	43.43	48.59	64.15	70.25	80.93	90
S27	9.59	21.34	30	41.81	50.28	58.99	71.89	80.93	90
S28	11.53	21.63	30	36.86	54.90	61.04	70.25	80.93	90
S29	11.53	22.02	30	41.81	46.65	58.99	70.25	78.52	90
S30	9.59	22.02	30	36.86	50.28	61.04	70.25	80.30	90
AVERAGE	**10.539**	**21.480**	**30.916**	**41.103**	**50.391**	**59.782**	**70.313**	**79.397**	**90**
ACURRACY	**89.22**	**70.39**	**81.68**	**78.89**	**96.08**	**97.82**	**93.72**	**93.97**	**100**

Table 2: Manual analysis of impact angle.
Bloodstains are manually selected from the bloodstain samples and their angle of impact is calculated. Using Numerical formula, the impact accuracy is calculated with the average accuracy.

Comparison of the Second Impact Spatter Experiment and Third Impact Spatter Experiment

There were some variations on the preparation, for the first preparation (based on impact angle experiment) there were large bloodstains, compared to the second or the third preparation (based on impact spatter experiment). The second and third experiment was based on the same procedure, but a simple modification on the angle of spatter. The mouse trap was setup at angle of 120 degree for the first impact spatter experiment and for the second impact spatter experiment at 16

0 degree. For the 10-degree angle, the predicted angle is higher than the reference line. The x-axis is the expected impact angle (10, 20, 90), and the y-axis is the measured impact angle based on the size of each blood drops. Ideally, the expected impact angle should be the same as the measured impact angle. If the angle is the same, the line would be diagonal, but the actual data indicates the dotted blue line. Based on Figure 39, when conducting the linear regression for the second and third preparation, the coefficient (R^2) result ranges from 0.9643 and 0.9512. Both the results achieved a similar regression coefficient.

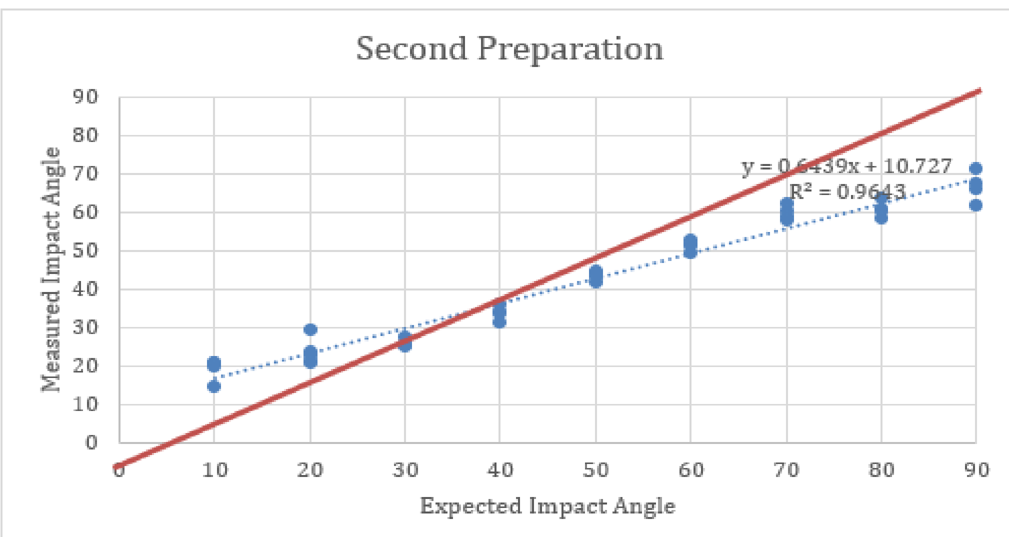

Figure 44: Measured Impact Angle vs Expected Impact Angle for second Preparation. The coefficient result for second preparation is 0.9643.

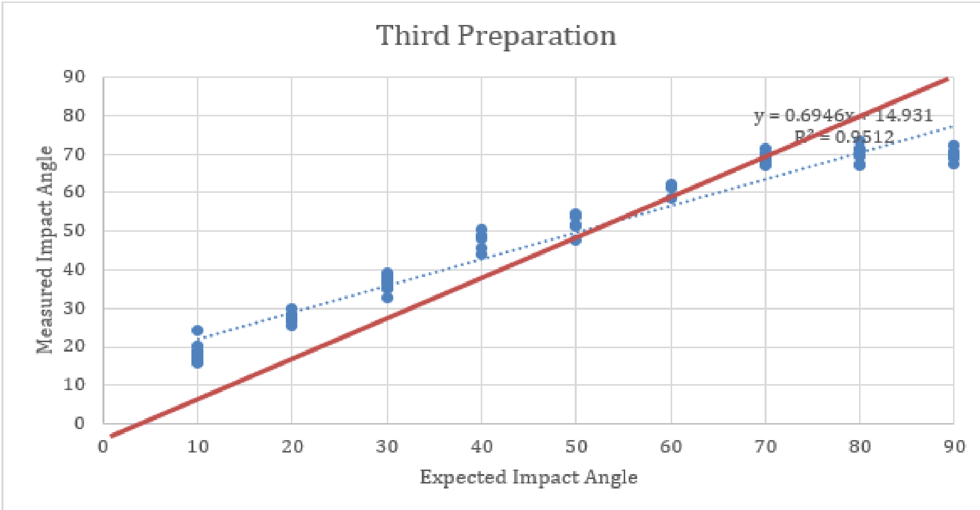

Figure 45: Measured Impact Angle vs Expected Impact Angle for third Preparation. The coefficient result for third preparation is 0.9512.

- Classical method of impact angle measurement achieves a high overall accuracy.
- The classical method works the best when impact angle < 70, but is less accurate when impact angle > 70

The Expected vs. Measured Impact Angles are as follows: The second preparation and third preparation achieved similar regression results. The second preparation resulted in R^2 = 96.43%, third preparation resulted in R^2 = 95.12% accuracy. Bloodstain images were taken and analyzed using Image J. The area of each blood drop was calculated for the impact angle. The area was plotted for the impact angle of each blood drop. The x-axis is the area of each blood spot, where the blood spots are smaller in size and plotted further left. The y-axis is the impact angle which each droplet has, when the droplet is small the variation is larger. The plots are scattered from 0 to 90 degrees as the size of the blood droplet increases, the prediction of the impact angle is more consistent. The purple line is the reference line for example, the sample from 40 degrees, has the blood spots towards the left. Ideally, all the blood spots should be on the reference line. As in for the analysis, the spots are either above or below the reference line. The difference becomes clearer when the impact angle is less than 60 degrees. Scatterplots of each degree images from the 3rd prep set determine the sizes of each bloodstain in comparison to each other.

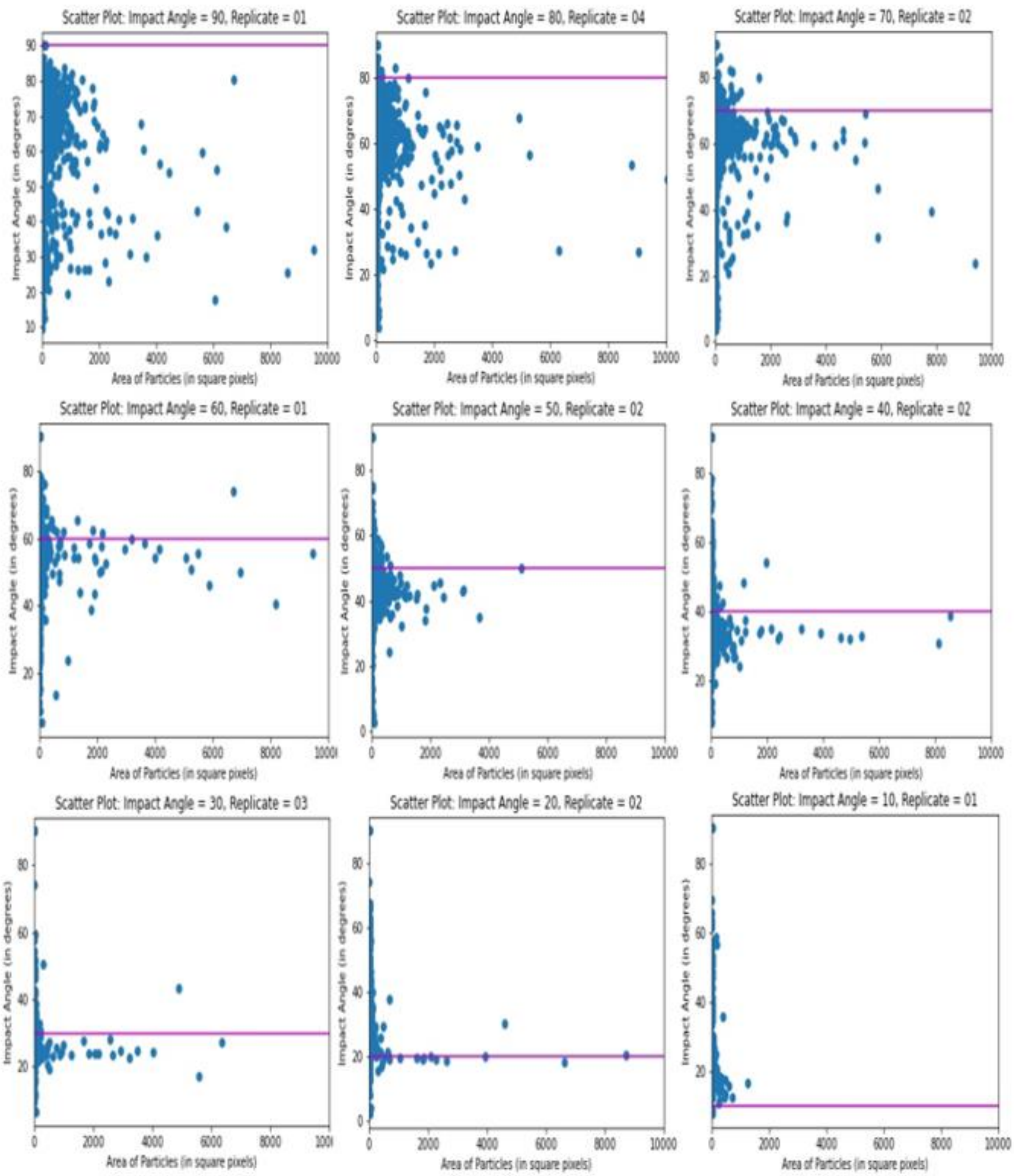

Figure 46: Scatter plots. The Scatter plots range from 10 to 90 degrees.
The plots are created from bloodstain images (impact spatter experiment 3). The Scatterplots of each degree images from the 3rd[d] preparation set determines the sizes of each bloodstain in comparison to each other.

Image J processing

The macro program results in an input image of the sample elements and the bloodstain images extracted from the impact spatter experiment. The output sample extracts single element from the original image that has binarized. The result had parameters that include area, mean, standard deviation, mode, width, height, major, and minor axis. The result gave all the parameters of each particle which has been identified. The unidentified particles can be eliminated by setting a threshold.

Figure 47: Image J extracts single elements based on the particle size and shape.
The results of ImageJ processing with parameters are stored in the excel file. For Bloodstains with different shapes and sizes, the images were converted into a binary image. Then the images were analyzed, ImageJ identifies six different areas. Each bloodstain image was cropped and saved in a file_1(Input Image).

	Area	Mean	StdDev	Mode	Min	Max	X	Y	XM	YM	Perim.	BX	BY	Width	Height	Major	Minor
1	30	114	27.665	99	76	178	1974.167	11.067	1974.101	10.911	19.314	1971	8	6	6	6.503	5.874
2	37	115.649	26.147	97	80	174	2413.014	24.095	2413.058	24.113	22.485	2410	21	6	7	7.049	6.683
3	20	112.45	18.112	97	83	155	2028.25	25.25	2028.328	25.249	15.314	2026	23	5	5	5.142	4.953
4	10	113.7	29.878	66	66	163	2011.7	27	2011.654	27.168	10.485	2010	25	3	4	4.111	3.097
5	32	107.281	28.12	80	74	176	2046.031	28.531	2046.039	28.385	19.556	2043	25	6	7	6.943	5.868
6	30	109.733	26.03	102	73	173	562.967	32.233	562.91	32.237	19.899	560	29	6	6	6.517	5.861
7	63	119.714	23.489	98	91	176	2254.849	39.563	2254.844	39.61	28.142	2251	35	8	9	9.444	8.494
8	24	116.833	26.771	83	83	175	1819.208	41.542	1819.192	41.564	17.314	1816	39	6	5	5.766	5.299
9	52	117.327	30.078	79	79	178	1938.212	48.654	1938.24	48.686	25.799	1934	44	8	9	8.372	7.908
10	97	102.144	29.202	101	68	177	716.407	52.345	716.371	52.305	36.385	711	47	11	11	11.657	10.594
11	15	107.4	29.914	55	55	167	606.1	54.9	605.982	54.86	13.071	604	53	4	4	4.659	4.099
12	31	129.839	18.078	113	99	171	1795.21	55.79	1795.186	55.9	19.314	1792	53	6	6	6.387	6.179
13	25	107.68	27.363	88	71	178	2528.26	55.82	2528.311	55.837	17.899	2526	53	5	6	6.405	4.969
14	16	108.625	37.5	85	70	178	463	60	463.022	60.026	13.657	461	58	4	4	4.514	4.514
15	118	101.059	30.926	75	61	176	658.161	69.932	658.161	69.961	39.213	652	64	12	12	12.602	11.922
16	62	125.177	20.628	110	96	175	2084.968	69.5	2084.907	69.478	27.799	2080	65	9	9	9.257	8.528
17	55	109.055	29.743	82	79	177	1749.355	73.736	1749.173	73.652	27.213	1745	69	9	9	8.405	8.332
18	154	103.669	29.187	77	68	177	2379.565	76.357	2379.495	76.253	45.456	2373	69	13	15	14.926	13.137

Figure 48: The analysis results.
The result has parameters that include area, mean, standard deviation, mode, width, height, major and minor axis. The result gives all the parameters of each particle which has been identified. The unidentified particles can be eliminated by setting a threshold.

KNN (K- Nearest Neighbor)

For each impact angle bloodstain, a total of four sheets to 8 sheets containing at least 30-40 individual stains were experimentally created. The images of bloodstains were then sent for the KNN algorithm to process. Each of the images was analyzed by ImageJ processing. The bloodstains images at first appear to be in red, where Image J would convert the red components to binary data set to have equal intensity. After converting the images to binary, the bloodstain images were processed in the KNN algorithm. The images were classified into a test set and a training set. The test set is a set of examples used to assess impact angle (specific classification). The train set feature is for fitting the dataset to the specified parameters. Using the python editor called Jupyter Notebook, the NumPy and Python libraries were run to create a normalization of the images. The HDF5 or the Hierarchical Data Format 5 had been designed to store and organize large amounts of data such as image files. The process was performed in the MarkH5 code which is available on GitHub. The bloodstain samples were randomly divided into 80% training samples and 20% testing samples. The samples were then run through the MarkH5 code to format all the images into the HDF5 files. In this program, the images had been organized to their respective labeling (10-90 degrees), despite if the images were training or testing set images.

The KNN performed a mathematical calculation to measure the distance between the data to make the classification. The NumPy and Python libraries were used to create the KNN algorithm. The KNN code takes in the formatted and labelled HDF5 files and creates a classification of the training images. The labelled training images and the specific degree was sorted into a classification matrix based on the blood drop’s appearance. Meanwhile, the program analyses the test images to test against the classifications created to check whether the algorithm can predict the angle of the test image. The algorithm can only predict the correct classification using the blood droplet's appearance. Afterward, the test image's labels were used to correct the program's prediction on whether the algorithm had predicted correctly or not, which results in building up or down the test accuracy. Based on the parameters, we had classified the case results into two with noise and without noise. With noise, the test accuracy result was 60.16%, and without noise, the test accuracy result was 82.09%. KNN is a noise-sensitive classifier as its accuracy highly depends on the image quality of the training data set (Cover, 2006). Data regions that have a mislabeled data or overlap between data regions could led to a less accurate score (refer to Figure 48). There are two types of strategies implemented to show a great example between the accuracy score with noise and without noise. For bloodstain images which are processed with high resolution at 600 dpi still produce noise. The resolution in noise can be achieved with clean data set, adjusting with various parameters such as reducing the area in size using image J.

Case Result 1: With Noise

Case 1 shows accuracy results of 60.16% obtained by using 13 sets of images out of 54 data set images. The blood drops (splatters) obtained from these 13 images using the ImageJ software tool separated into train images (80% of the entire data set) and test images (20% of the whole data set). The training dataset was optimized to train the KNN model, while the test data used to test the KNN Model. The accuracy obtained was low because the data was unclean. The information was unclean because the dataset had noise data such as overlapping blood splatters (weakness from ImageJ software), unwanted blood drops, and noise from the ink used in labelling the angles on the images. This noise data affected the results highly by reducing the accuracy of KNN in classifying the blood drops into various angles.

```
Test Result:

accuracy score: 0.6016

Classification Report:
              precision    recall  f1-score   support

          10       0.27      0.53      0.36        74
          20       0.40      0.60      0.48        94
          30       0.08      0.02      0.03        98
          50       0.33      0.22      0.26        60
          70       0.84      0.80      0.82       437

    accuracy                           0.60       763
   macro avg       0.38      0.43      0.39       763
weighted avg       0.59      0.60      0.59       763


Confusion Matrix:
 [[ 39  21   2   1  11]
 [ 17  56  10   2   9]
 [ 42  24   2   9  21]
 [  6   9   5  13  27]
 [ 38  29   7  14 349]]
```

Figure 49: Test result with noise accuracy.
The accuracy results in 60.16%, using 13 images out of 54 data set bloodstain images. The data the KNN analyzed was unclean which leads to a low accuracy being achieved.

Case Result 2: Without Nosie

Case 2 shows accuracy results of 82.09.16% obtained by using 13 sets of images out of 54 data set images. The blood drops (splatters) obtained from these 13 images using the ImageJ software tool were separated into train images (80% of the entire data set) and test images (20% of the whole data set). The training dataset is utilized for training the KNN model, while the test data was utilized to test the KKN Model. The results showed high accuracy because the data was cleaned by removing the noise blood splatters and ink used in labelling the angles on the images.

```
Test Result:

accuracy score: 0.8209

Classification Report:
              precision    recall  f1-score   support

          10       0.71      0.81      0.76        58
          20       0.80      0.62      0.70        60
          30       0.34      0.48      0.40        27
          50       0.72      0.46      0.56        67
          70       0.90      0.95      0.92       363

    accuracy                           0.82       575
   macro avg       0.70      0.66      0.67       575
weighted avg       0.82      0.82      0.82       575


Confusion Matrix:
 [[ 47   9   0   0   2]
 [  6  37  16   1   0]
 [ 11   0  13   1   2]
 [  0   0   2  31  34]
 [  2   0   7  10 344]]
```

Figure 50: Test result without noise.

The accuracy results of 82.09% obtained by using 13 images out of 54 data set images. The results show high accuracy because the data was cleaned by removing the noise blood splatters and ink used in labelling the angles on the images.

Chapter III

Thesis Conclusion

The scientific community requires increased standards for the accuracy of BPA by reducing human error. Investing in AI to accurately model the complex data of BPA will reduce human error comparatively. The purpose of this study aims to utilize AI algorithms to assist in the analysis of bloodstain patterns. The initial goal for this study was to determine whether bloodstains can be classified using automated methods such as AI. The preliminary test involved using impact angle experiments creating bloodstains in controlled conditions. The result consists of an approximate accuracy of 83.04 %. Based on the preliminary study, an impact spatter experiment was conducted to create new bloodstain images and determine the new accuracy using the KNN algorithm. Different parameters were altered to achieve better accuracy, and the images of the patterns were used as the primary input data in the AI algorithm. Based on this study, a standard methodology can be practiced in the forensic science community.

The Difference in the KNN Accuracy

Impact spatter experiments (experiment I and experiment II) were conducted to obtain images of the bloodstains. From the first impact spatter experiment, the accuracy differed upon different case examples. In the case of example 1, the accuracy was 0.7653, which is 76.53 %. As the bloodstains are very similar when it goes above 70 degrees, the samples of 70, 80, and 90 degrees are grouped in the same range. In the case of example 2, the accuracy was 0.8469, which is 84.69 %. The 30 and 40 degrees are very similar, the samples of 30 and 40 are in the same group. In the case of example 3, when the angles go above 60, the samples ranging from 60 to 90 degrees are grouped into the same group, the accuracy rises to 87.76% (KNN K = 4). Thus, the experiment concludes that having viable bloodstain samples can provide better accuracy.

In impact spatter study (120-degree), the total sample size was 98, which precludes further AI analysis. Also, only a selective number of individual stains were taken into consideration for the AI algorithm to process the accuracy. Suppose there was a large set of sample size, which would create a better accuracy. The resulting impact angle accuracy may vary if they are not grouped but analyzed individually because the stains are similar in shape at certain angles; for example, 30 and 40 degrees are similar.

The first impact spatter experiment has provided an accuracy of 84.69%. Blood drops were extracted manually from the given set of sample images. The blood drops were selected manually based on how well the blood drop looked like, rather than an actual blood drop to the human eye, introducing potential bias. The bloodstains were scanned at a 300dpi resolution which could have possibly been a factor for the accuracy to be lower. Photoshop was used to extract the blood drop to resize, rotate, and binarize the blood drop to create a high accuracy result. The accuracy obtained does not seem like a reliable result because the accuracy result cannot be replicated. If only provided with the same sample set of images tested for 84.691%, the accuracy can be replicated. The advantage of the result eliminated the noise and unwanted blood drops that could not be used for analysis. However, the analysis also got rid of blood drops that could potentially help achieve higher accuracy.

The second impact spatter experiment resulted in different accuracy based on different parameters. The blood drops were scanned at a 600dpi resolution and processed using ImageJ analysis. The accuracy is classified into four different cases. Each case categorizes the accuracy based on the difference in parameters that had been altered. The experiment has provided accuracies based on limiting noise, using different parameters, and analyzing an extensive data set of bloodstain images. Based on the accuracy of altering the parameters, two types of strategies had implemented to show a great example of accuracy score with noise and without noise. With noise, the accuracy was 0.6016, which is 60.16%, and without noise, the accuracy was 0.8209, which is 82.09%. For bloodstain images that are processed with high resolution at 600 dpi still produce noise as a factor for lower accuracy. The resolution in noise can be achieved with clean data set, adjusting with various parameters such as reducing the area in size using image J.

Case 1: Accuracy of 48.94%

```
Test Result:

accuracy score: 0.4894

Classification Report:
              precision    recall  f1-score   support

          10       0.33      0.67      0.44         6
          20       0.27      0.27      0.27        11
          30       0.50      0.43      0.46         7
          50       0.50      0.11      0.18         9
          70       0.75      0.86      0.80        14

    accuracy                           0.49        47
   macro avg       0.47      0.47      0.43        47
weighted avg       0.50      0.49      0.46        47


Confusion Matrix:
 [[ 4  2  0  0  0]
 [ 3  3  3  0  2]
 [ 3  1  3  0  0]
 [ 2  4  0  1  2]
 [ 0  1  0  1 12]]
```

Figure 51: Case 1 result of the accuracy of 48.94%.
The accuracy was 48.94%. The result had low accuracy because the blood drops were extracted with no parameters using the ImageJ software. The advantage of this run was to see how well the KNN algorithm could run on an "unclean" data set that was not normalized and had no human bias interference at all.

Bloodstain images were manually extracted with no parameters using the software called ImageJ. This allowed for all the noise to be included in the extracted sets. The blood drops were not rotated nor binarized but were resized into the KNN program as an acceptable input. The reasons for decreased accuracy (48.94%) are the non-binarization of tiny blood drops that were less than 0.2mm in size, the manually written notes on the image set, and the double splotched of blood drops. The elimination of the initial input data correctly has resulted in producing an unreliable accuracy and caused an error.

Case 2: Accuracy of 64%-74%

The bloodstain images originally scanned in a PDF format were converted to a JPEG format. The PDF file contained lesser resolution, which introduced more noise during the KNN analysis. Converting the images to JPEG reduced noise and resulted in better accuracy. The images (a total of 2400 blood drops) were extracted through the ImageJ software and including a parameter of 500 pixels to infinity pixels. Using ImageJ, the noise had reduced from the extracted data set. In this case, two additional parameters had set up to determine two different accuracies. The first copy of the whole data set was rotated, resized, and binarized, which had a 64% accuracy. The second copy of the whole data set was only resized and binarized, which had a 74% accuracy.

The accuracy was not reliable entirely because there was a loss of quality in the images when converting the files from PDF to JPEG. Also, manually eliminating the written notes of 10-90 degrees and double splotches were not applicable in this case. The advantage binarization had significantly improved the first copy’s accuracy as well as the noise reduction. The second copy showed that there was a 10% improvement when the blood drops were rotated. For better accuracy, the images were directly scanned as JPEG, so there was no need for conversion from PDF to JPEG, unlike the first copy (accuracy of 64%). In this case, entire data set images (12-13 images out of the 54) failed to be downloaded, resulting in selective images being extracted. ImageJ extraction was performed using the same parameters to eliminate noise and do the resizing and binarization.

Case 3: Accuracy of 80%-86%

The bloodstains for case 3 were manually selected for the KNN analysis. The result was not reliable because the images were manually selected and only the selected images were used for the KNN instead of the whole data set given. There was no quantifiable parameter as the dataset was selected, so there was no way to replicate this with another random set of data sets from the images unless the same sample sets were selected again.

```
Test Result:

accuracy score: 0.8643

Classification Report:
              precision    recall  f1-score   support

          10       0.67      0.90      0.76        58
          20       0.77      0.68      0.73        60
          30       0.70      0.52      0.60        27
          50       0.75      0.75      0.75        67
          70       0.95      0.94      0.94       363

    accuracy                           0.86       575
   macro avg       0.77      0.76      0.76       575
weighted avg       0.87      0.86      0.86       575


Confusion Matrix:
 [[ 52   6   0   0   0]
 [ 13  41   5   1   0]
 [ 10   1  14   1   1]
 [  0   1   0  50  16]
 [  3   4   1  15 340]]
```

Figure 52: Case 3 result of an accuracy of 86.43%.
The result was not reliable because the images were manually selected and only the selected images were used for the KNN instead of the whole data set given.

However, the manually selected images are hard to define how or why those images would be selected other than they have given the highest accuracy. The only theory that would be applicable for selecting the specific set of bloodstains would be based on the bloodstain's appearance. The advantage is that in this case the set of samples images have given the highest accuracy result.

Case 4: Accuracy of 78%-79%

In this case, all the samples (a total more than 2400 blood drops) were selected, and the image extraction was analyzed using ImageJ to get the extracted blood drops. Meanwhile, the noise reduction and manually eliminating any written notes were made. The automation script analysis was performed to randomly distribute 80% to the train set and 20% to the test set. An accuracy of 78% was achieved with the automation script. An accuracy of 79% was achieved by manually selecting the 80% train and 20% test images.

```
Test Result:

accuracy score: 0.7864

Classification Report:
              precision    recall  f1-score   support

          10       0.82      0.97      0.89        29
          20       0.82      0.82      0.82        34
          30       0.80      0.82      0.81        45
          40       0.68      0.58      0.62        26
          50       0.53      0.55      0.54        29
          60       0.31      0.25      0.28        20
          70       0.90      0.90      0.90       126

    accuracy                           0.79       309
   macro avg       0.70      0.70      0.70       309
weighted avg       0.78      0.79      0.78       309


Confusion Matrix:
 [[ 28   1   0   0   0   0   0]
 [  3  28   3   0   0   0   0]
 [  0   5  37   2   1   0   0]
 [  1   0   4  15   6   0   0]
 [  1   0   2   3  16   5   2]
 [  1   0   0   0   3   5  11]
 [  0   0   0   2   4   6 114]]
```

Figure 53: Case 4 results in an accuracy of 78.64%.
An accuracy of 78% was achieved with the automation script. The accuracy, in this case, has been the most reliable as most of the noise was reduced, and human bias was eliminated.

```
Test Result:

accuracy score: 0.7902

Classification Report:
              precision    recall  f1-score   support

          10       0.94      0.94      0.94       116
          20       0.78      0.87      0.82       108
          30       0.82      0.82      0.82       177
          40       0.58      0.35      0.43        95
          50       0.53      0.75      0.62       110
          60       0.42      0.21      0.28        86
          70       0.89      0.94      0.92       433

    accuracy                           0.79      1125
   macro avg       0.71      0.70      0.69      1125
weighted avg       0.78      0.79      0.78      1125


Confusion Matrix:
 [[109   7   0   0   0   0   0]
 [  5  94   9   0   0   0   0]
 [  2  19 145   8   1   1   1]
 [  0   1  15  33  44   1   1]
 [  0   0   5  11  82   9   3]
 [  0   0   1   2  21  18  44]
 [  0   0   1   3   7  14 408]]
```

Figure 54: Case 4 results in an accuracy of 79.02%.
This accuracy was achieved when running the whole data after noise reduction. An accuracy of 79% when manually just choosing 80% train and 20% test images.

Thus, the use of additional parameters removes out the noise that is quantifiable and reasonable. The randomization using automation also further reduces bias to select which set of bloodstains are 80% training and the rest of the images to test. Ultimately, it is advantageous because the 78% accuracy is the most reliable accuracy test result. The low score can be reasoned to be external factors of not having the perfect blood drops in every given angle because in a standard bloodstain pattern image, not all blood drops will exhibit their given impact degree.

During both the manual (traditional method) and automated (KNN) analysis, there was a potential to introduce bias in selecting bloodstain droplets. To eliminate bias in the automated method, all the bloodstain droplet images were analyzed by the KNN algorithm, where an accuracy of 78.64% was achieved. The manual analysis resulted in an accuracy of 89.08%. The bloodstain droplet selected for the manual analysis was random; not all the bloodstain droplets were analyzed. A sample of 30 bloodstains was randomly chosen from the sample images and by using the traditional method to calculate the impact angle. The strategy adopted was to see how accurate the automated method accuracy is comparatively high or less to a trained analyst accuracy. Both the accuracy was achieved by two different scenarios, one (automated) by eliminating bias and the other (manual) includes bias. The KNN also achieved 86% accuracy when the bloodstain droplet images were randomly selected for manual analysis. When both methods introduce a potential bias, the accuracy achieved was 86% for automated and 89.08% for manual analyses. When there is no potential bias in automated, resulting in 78.64%, the difference would be (86%-78.64%) 7.36%. Therefore, the difference between the analysis results in an accuracy difference of 3.08% (potential bias) and 7.36% (no potential bias). Ultimately, the comparison is relatively differing with 7.36% based on using the KNN algorithm, considering this technique giving the most reliable result.

Also, KNN is not a complex algorithm to go further in-depth in classifying the blood drops with intense image analysis and parameters. KNN has no parameter in its classification, so it is the most straightforward AI algorithm and can be a cause to score such a low accuracy as it cannot handle the intricacy of the images. However, as a preliminary study, it has provided valuable results and positive indications for future research. Future research could be establishing an AI algorithm for BPA concerning different impact angles, different objects, different surfaces, different impact spatter distances (LES, MES, and HES), and different sizes.

Proposed Future Study: Study Design and Methodology

The experiments' goal is to establish a significant classification of bloodstain patterns from different energies created by different weapons, sizes of bloodstains, and distances. Generally, a low-energy spatter pattern is associated with dripping or pooling of blood. A medium-energy impact spatter pattern is associated with a blunt force injury, and a high-energy impact spatter pattern is related to a gunshot wound. The differentiation of these impact spatter patterns is qualitative, inconsistent, and highly controversial. The classification of impact spatter patterns is contentious in the judicial system. The differentiation between a blunt force pattern (MES) and a gunshot pattern (HES) which are highly debatable due to the known error rate (e.g., the Warren Horinek case). Often, impact spatter patterns are determined by the size (diameter) and the impact energy. Many experts have suggested that impact spatters are becoming more subjective based on the classification of the terminology.

Experimental Aims and Objectives

Aim and Objectives

To determine different variables in bloodstain pattern analysis for the developed AI algorithm. The objectives of the future study are to develop a novel experiment setup, to determine different sizes of impact spatter patterns, to determine the types of bloodstains on different types of surfaces, to determine different distances based on impact spatter energy pattern and, to determine different objects impact energy and impact stains.

Experimental Hypothesis

EH_o: The impact force applied to the object would not cause variation or affect the distance traveled by the blood drop.
EH_1: The impact force applied to the object would cause variation or affect the distance traveled by the blood drop.

Size

The size of bloodstain can differ by the impact force and the type of object used to strike. The blunt force impact can range from 0.5 mm to 0.7 mm, whereas a gunshot can range from 0.4mm – 0.5mm as the impact velocity (low to high) increases, the bloodstain's size decreases. The size also depends on the amount of force used during the time of the impact. A blunt force spatter pattern can also consist of the same size droplets as a gunshot pattern. LES has relatively large size bloodstains ranging from 4mm or more in diameter. LES increases in size as the distance on impact increases, but the spatter's size remains constant after 4ft. MES ranges from 1mm to 4mm in diameter. The HES ranges from 1mm or less in diameter.

Materials and Method

Materials required are animal blood, different types of objects (screwdriver, hammer, rod, etc.), target surface (paper), camera, scale, measuring tape, and butcher paper. In this experiment, the blood is dropped to a surface from a standard height with different objects. The surface containing the bloodstains is dried and photographed. The images are analyzed for the size of the droplet. This development of a quantitative methodology using the AI algorithm will generate a better consistency of the test accuracy.

S (mm)	0.1	0.2	0.3	0.4	0.5	0.6	0.7	0.8	0.9	1	2	3	4	5	6	7	8
V	5 to 50µl																
L	30.5 inches																
Z	25 samples per size																

Table 3: Various sizes (diameter) as a function of impact-to-target distance (L).
The different sizes differ with varying velocities of impact (LES, MEIS, and HEIS). The volume of the blood is standard throughout the experiment. The sample size (z) is 25 samples per size.

Surface

Bloodstain pattern analysis on surfaces can help determine scenarios consistent with the crime scene. The blood lands' surface plays a vital role in the shape, size, and distribution of the bloodstain. During analysis, the rough surface's appearance will seem distorted, and hard to determine which angle the blood has traveled. For example, when passive bloodstain land on a fabric (irregular surface) may classify as projected bloodstain due to misinterpretation. Using a computerized method to distinguish stains based on the surfaces will help reduce the error rate. The type of surface that the blood strikes will affect the appearance of the resulting stain on impact. There are two types of surfaces: a rough surface and a smooth surface. A drip stain on a soft surface will be more uniform and circular. The stain will have a smooth edge. A drip stain on a rough or coarse surface will create an irregular stain pattern with rough or jagged edges.

Materials and Methods

Materials required are carpet, tile, paper, fabric, glass, metal, wood, cardboard, plastic, animal blood (50 µl), measuring tape, pipette, and butcher paper. A known blood volume (50 µl) is dropped from a known height (30.5 inches) on different target surfaces using a pipette. The bloodstain can dry on the surface, and the bloodstains are photographed. The AI algorithm assesses the image and produces an estimated accuracy.

Surface	Carpet	Tile	Paper	Fabric	Glass	Metal	Wood	Cardboard	Plastic
Volume	50µl								
Height	30.5 inches								
Sample size (z)	25 -50 samples per surface								

Table 4: Various surface as a function to impact-to-target distance.
The Z is the sample size. The bloodstain images are analyzed for different surfaces listed in the table

Distance

The parameters in this experiment are the object's initial energy, impact force when the object strikes the target source, and the distance from the target paper to the target source. The distance travelled by a bloodstain can play a significant role in the size, shape, and distribution. The experiment would help determine how accurate different distances can produce stains using the same object for each impact spatter.

Materials and Methods

Materials required are measuring tape, animal blood, LES weapon, MES weapon, HES weapon, target paper, blood-soaked sponge, camera, and butcher paper. A known volume (200 - 1000 of blood is soaked in a sponge and placed on a target surface. Using different impact objects, strike the object onto a target paper from a known distance (30cm – 120cm). The controlled variables, such as the distance and the object used, would be investigated to its relation to the shape, size, and stain distribution.

Part 1: Determining the distance for Low-Energy Spatter (LES) bloodstains and using the captured image as a primary input for the AI algorithm to assess.

Distance	30cm	40cm	50cm	60 cm	70cm	80cm	90cm	100cm	110cm	120cm
Volume	200µl - 1000µl (may vary)									
Weapon	LES weapon (0-5ft/s)									
Sample Size (z)	25 samples per distance									

Table 5: Various distances (D) as a function to impact-to-target object/weapon (LES)
The volume of the blood is standard throughout the experiment. The sample size (z) is 25 samples per size.

Part 2: Determining the distance for Medium-Energy Spatter (MES) bloodstains and using the captured image as a primary input for the AI algorithm to assess.

Distance	30cm	40cm	50cm	60 cm	70cm	80cm	90cm	100cm	110cm	120cm
Volume	200μl -1000μl (may vary)									
Weapon	MEIS weapon (5-200ft/s)									
Sample	25 samples per distance									

Table 6: Various distances (D) as a function to impact-to-target object/weapon (MES)
The volume of the blood is standard throughout the experiment. The sample size (z) is 25 samples per size.

Part 3: Determining the distance for High-Energy Spatter (HES) bloodstains and using the captured image as a primary input for the AI algorithm to assess.

Distance	30cm	40cm	50cm	60 cm	70cm	80cm	90cm	100cm	110cm	120cm
Volume	200μl - 1000μl (may vary)									
Weapon	HEIS weapon (over 100ft/s)									
Sample	25 samples per distance									

Table 7: Various distances (D) as a function to impact-to-target object/weapon (HES)
The volume of the blood is standard throughout the experiment. The sample size (z) is 25 samples per size.

Objects

The term energy does not measure the speed of blood traveling; it describes the amount of force applied. In the experiment, different impact energies created using other weapons. The impact energies of various weapons include a baseball bat, hammer, screwdriver, syringe, are used systematically. The patterns created are digitalized and quantified using the AI algorithm to determine the accuracy. The experiment involves energies from 5ft/s to 120ft/s.

Materials and Methods

Materials required are animal blood, different types of weapons (knife, rock, wooden bat, hammer, rod, screwdriver), target surface (sponge/bloodied object), target paper, measuring tape. A known volume of blood is taken and soaked in a sponge (target surface). When the object strikes the target surface, producing bloodstain patterns on the target paper. The individual bloodstains are photographed and used as a primary input for AI to assess for accuracy.

Objects	**Hammer Full (A)**	**Baseball bat (B)**	**Blood flicked off finger (C)**	**Blood dropped into blood (D)**	**Mouse trap (E)**	**Rock (F)**	**Syringe (G)**
Volume (V)	200 µl -1000 µl						
Distance (L)	12 inches						
Sample size (Z)	25 samples per object						

Table 8: Various objects (O) as a function of the impact-to-target distance (L)
The volume (V) varies from 200 µl -1000 µl, depending on the target surface's absorbance. The sample size (Z) ranges from 25 samples per energy. The pattern ranging at or less than 5ft/s is a low energy spatter (L = 0 ft to 5ft), pattern ranging from 5ft/s < 25ft/s is a medium energy impact spatter (L= 5ft to 20ft), and pattern ranging over 100ft/s is high energy impact spatter (L = 50ft or more). For energy at 5ft/s, blood dropped into the blood or a footstep pattern. For energy ranging from 15ft/s-100ft/s, blood flicked off a finger or blunt object can be used for creating the bloodstains. A syringe can substitute for 100ft/s or more, and based on the force applied, the impact energy will differ accordingly. In the initial analysis, one foot (L= 12 inches), selected as the standardized distance.

References

(FBI)., F. B. o. I. (2002). Bylaws of the Scientific Working Group on Bloodstain Pattern Analysis (SWGSTAIN). *Forensic Science Communications, 11*. doi: http://www.fbi.gov/hq/lab/fsc/backissu/july2002/swgstain.htm

(SWGSTAIN), S. W. G. o. B. P. A. (2009). Scientific Working Group on Bloodstain Pattern Analysis:

Recommended Terminology. *Forensic Science Communications 11*.

Andrew R. W. Jackson, J. M. J. (2004). Bloodstain Droplets. *Jackson & Jackson: Forensic Science*.

Arthur, R. M. H., P. J.; Hoogenboom, J.; Baiker, M.; Taylor, M. C.; de Bruin, K. G. (2017). An image-processing methodology for extracting bloodstain pattern features. *Forensic Science International, 277*, 122-132. doi: http://dx.doi.org/10.1016/j.forsciint.2017.05.022.

Bou Zeid, W. V., J.; Brutin, D. (2013). Influence of evaporation rate on cracks' formation of a drying drop of whole blood. *Colloids and Surfaces A: Physicochemical and Engineering Aspects, 432*, 139-146. doi: http://dx.doi.org/10.1016/j.colsurfa.2013.04.044.

Brodbeck, S. (2012). Introduction to Bloodstain Pattern Analysis. *SIAK-Journal − Journal for Police Science and Practice, (Vol. 2), 51-57*. doi: http://dx.doi.org/10.7396/IE_2012_E.

Chamberlain, L. (1991). Through my eyes. *Simply streep*.

Claire, D. (2017). Top 5 best Programming Languages for Artificial Intelligence field. *Towards data science*.

Collof, P. (2018). She Was Exonerated of the Murder of Her Son. Her Life Is Still Shattered. *The new york times*.

Colloff, P. (2018). Blood will tell you Part I. *Propublica*.

contributors, W. (2020). Sam Sheppard. *Wikepedia, The Free Encyclopedia*.

Dr. Sharam Tafazoli, D. A. A. (2019). How Artificial Intelligence Revolutionized Computer Vision: A Brief History. *Motion Metrics*.

Dryzal, D. (2018). “Bloodstain Pattern Analysis: Applications and Challenges. *The D.U.Quark,, 2*(2), 22-29.

Duomly. (2020). The best programming language for Artificial Intelligence and Machine Learning. *DEV*.

Dutelle, A. W. (2011). An Introduction to Crime Scene Investigation. *Jones & Bartlett Publishers*.

Eckert, W. G. a. S. H. J. (1999). *Interpretation of Bloodstain Evidence at crime Scenes*. CRC Press.

Encyclopedia. (2019). Cast-off Blood. *ENCYCLOpedia.com*.

Englert, R. P., K. (2010). Blood secrets: chronicles of a crime scene reconstructionist. *Macmillan*.

Ericksen, K. (2017). 7 Ways the CSI Effect is Altering Our Courtrooms (For Better and For Worse). *Rasmussen College*.

Eudreka. (2019). Artificial Intelligence. *Edureka*. doi: https://www.edureka.co/masters-program

Evans, C. (2004). "Murder 2: The Second Casebook of Forensic Detection." *John Wiley & Sons*.

Forensics, C. S. (2015). Interpreting bloodstain patterns. *Crime Scene Forensics, LLC*. doi: http://www.crimescene-forensics.com/Crime_Scene_Forensics/Bloodstains.html

G. Paul Neitzel, M. S. (2017). The Fluid Dynamics of Droplet Impact on

Inclined Surfaces with Application to

Forensic Blood Spatter Analysis. *National Criminal Justice Reference Service (NCJRS)*.

Gallagher, S. (2009). Blood 4: Passive Bloodstains. *Crime Scene Forensics, LLC*.

Gardner., V. T. B. a. R. M. (2001). Bloodstain Pattern Analysis: With an Introduction to Crime Scene Reconstruction. *CRC Press, 2nd edition*.

Garrett, W. (2020). The best AI programming languages to use. *Algorithmia*.

G. Acampora, A. Vitiello, C. Di Nunzio, M. Saliva and L. Garofano, "Towards Automatic Bloodstain Pattern Analysis through Cognitive Robots," *2015 IEEE International Conference on Systems, Man, and Cybernetics*, Kowloon, 2015, pp. 2447-2452, doi: 10.1109/SMC.2015.428.

Haberman, C. (2014). Vindication at Last for a Woman Scorned by Australia's News Outlets. *The new york times*.

Harrison, O. (2018). Machine Learning Basics with the K-Nearest Neighbors Algorithm. *Towards data science*.

HemoSpat. (2020). Bloodstain Pattern Analysis Terminology. *Bloodstain Pattern Analysis Software*

.

Hoelz, B. W. P. (2009). Artificial Intelligence applied to Computer Forensics. *Research gate*.

Holowko, E., Januszkiewicz, K., Bolewicki, P., Sitnik, R., & Michonski, J. (2016). Application of multi-resolution 3D techniques in crime scene documentation with bloodstain pattern analysis. *Forensic Sci Int, 267*, 218-227. doi: 10.1016/j.forsciint.2016.08.036

Howard Stringer, R. K., Erin Moriarty, Peter Van Sant, Richard Schlesinger, Maureen Maher, Tracy Smith, Jim Axelrod, Anne-Marie Green, Michelle Miller. (2017). Crime Document Murder on Lockhart Road. *48 hours*.

Hueske, E. E. (2005). "Practical Analysis and Reconstruction of Shooting Incidents." *CRC Press*.

IABPA. (2008). International Association of Bloodstain Pattern Analysts. *Evidence Technology Magazine*. doi: www.iabpa.org

IABPA. (2019). Bloodstain Analysis. *weebly.*

Illes, M., & Boue, M. (2013). Robust estimation for area of origin in bloodstain pattern analysis via directional analysis. *Forensic Sci Int, 226*(1-3), 223-229. doi: 10.1016/j.forsciint.2013.01.030

Jiaying Wu, M. S. S. M., Ph.D.; and Ruksana Baby, M.S. (2018). Impact Spatter Bloodstain Patterns on Textiles. *Journal of Forensic Sciences*. doi:doi: 10.1111/1556-4029.13951

Joris, P. D., W.; Jenar, E.; Suetens, P.; Vandermeulen, D.; Van de Voorde, W.; Claes, P. (2015). HemoVision: An automated and virtual approach to bloodstain pattern analysis. *Forensic Science International, 215*, 116-123. doi: http://dx.doi.org/10.1016/j.forsciint.2015.03.018.

Justice, N. I. o. (2018). Researchers Develop Insight into Blood Droplet Behavior for Bloodstain Pattern Analysis. *nij.ojp.gov*. doi: https://nij.ojp.gov/topics/articles/researchers-develop-insight-blood-droplet-behavior-bloodstain-pattern-analysis

Kristine Boos, Amanda Orr, Mike Illes, Theresa Stotesbury. 2019. Characterizing drip patterns in bloodstain pattern analysis: An investigation of the influence of droplet impact velocity and number of droplets on static pattern features, Forensic Science International, Volume 301, Pages 55-66, ISSN 0379-0738, https://doi.org/10.1016/j.forsciint.2019.05.002.

Kaitlin Leslie, T. L., Larry E. Barksdale, David O. Carter. (2019). Some Error Rates Associated with Bloodstain Pattern Analysis. *Department of Entomology, University of Nebraska-Lincoln, 68583-0816*

Karger, B. R., S.; Fracasso, T.; Pfeiffer, H. (2008). Bloodstain pattern analysis—Casework experience. *Forensic Science International, 181*(1), 15-20. doi: https://doi.org/10.1016/j.forsciint.2008.07.010

Kittipat, Boonkhong & Karnjanadecha, Montri & Aiyarak, Pattara. (2010). Impact angle analysis of bloodstains using a simple image processing technique. Songklanakarin Journal of Science and Technology.

Laan, N., de Bruin, K. G., Slenter, D., Wilhelm, J., Jermy, M., & Bonn, D. (2015). Bloodstain Pattern Analysis: implementation of a fluid dynamic model for position determination of victims. *Sci Rep, 5*, 11461. doi:10.1038/srep11461

Laan, N. S., F.; Nicloux, C.; Brutin, D. (2016). Morphology of drying blood pools. *Forensic Science International 267* 104-109. doi: https://doi.org/10.1016/j.forsciint.2016.08.005.

Labs, C. R. (2016). “Development of Computational Methods for the Audio Analysis of Gunshots”. *Cadre Research Labs* (LLC, NIJ award number 2016-DN-BX-0183).

Laux, D. F., J. Y.; Brutin, D. (2016). Ultrasonic monitoring of droplets’ evaporation: Application to human whole blood. *Ultrasonics Sonochemistry 32*, 132-136. doi: https://doi.org/10.1016/j.ultsonch.2016.03.003.

Mann, D. (2010). A Bloody Injustice. *Observer*.

Marr, B. (2016). “What Is the Difference Between Deep Learning, Machine Learning and AI?” *Forbes*.

Museum, C. (2017). Blood Evidence: Blood Stain Pattern Analysis. *Crime Museum, LLC*.

Nadim, J. (2019). Top 5 best Programming Languages for Artificial Intelligence field. *GeeksforGeeks A computer science portal for geeks*.

NFSTC. (2013). A Simplified Guide to Bloodstain Pattern Analysis. doi:

www.forensicsciencesimplified.org

Osborne, N. K. P. T., M. C.; Healey, M.; Zajac, R. (2016). Bloodstain pattern classification: Accuracy, effect of contextual information and the role of analyst characteristics. *Science & Justice, 56*, 123-128. doi: http://dx.doi.org/10.1016/j.scijus.2015.12.005.

P, S. (2016). AI in Forensic Science. *News Medical Life Sciences*.

PCAST. (2016). REPORT TO THE PRESIDENT - Forensic Science in Criminal Courts: Ensuring Scientific Validity of Feature-Comparison Methods. doi: Obamawhitehouse.archives.gov

Pokin, S. (2017). Uncertainties associated with bloodstain-pattern analysis are enormous': national study. *Spring Field News-Leader*.

Pokin, S. (2019). Federal lawsuit vs. Highway Patrol detective now includes former supervisor as defendant. *Springfield News-Leader*.

Reform, F. S. (2017). Chapter 9- Bloodstain Pattern Analysis. *Science Direct*, Pages 271-297.

Rigano, C. (2019). “Using Artificial Intelligence to Address Criminal Justice Needs,” *NIJ Journal 280*. doi: https://www.nij.gov/journals/280/Pages/using-artificialintelligence-to-address-criminal-justice-needs.aspx.

Scarraher. (2018). THE EVOLUTION OF BLOOD-STAIN PATTERN ANALYSIS VERDICTS IN THE COURTROOM. *csafe- Centre for statistics and applications in forensic evidence*.

Seamons, K. (2018). A Serial Killer Murdered Her Son. She Was the One Found Guilty. *Newser*.

Services, F. S. (2020). Bloodstain Pattern Analysis. *Bureau of Criminal Apprehension*.

Services, I. F. (2019). Bloodstain Pattern Analysis. Retrieved from INFO@IFSCOLORADO.COM

Shanna freeman, N. g. (2019). How Bloodstain Pattern Analysis Works. *How stuff works?*

Smith, L. (2018a). How a Dubious Forensic Science Spread Like a Virus. *Propublica*.

Smith, L. (2018b). How an Unproven Forensic Science Became a Courtroom Staple. *The new york times*.

staff, I. (2019). Ten Years Later: The Lasting Impact of the 2009 NAS Report. *Innocence project*.

T. Cover and P. Hart. (2006). Nearest neighbor pattern classification. IEEE Trans. Inf. Theor., 13(1):21--27

Taylor, M. C., Laber, T. L., Kish, P. E., Owens, G., & Osborne, N. K. (2016). The Reliability of Pattern Classification in Bloodstain Pattern Analysis-PART 2: Bloodstain Patterns on Fabric Surfaces (). *J Forensic Sci, 61*(6), 1461-1466. doi:10.1111/1556-4029.13191

Tegmark, M. (2016). Benefits and Risks of Artificial Intelligence. *Future of life*.

Terry Laber, P. K., Michael Taylor, Glynn Owens, Nikola Osborne, James Curran (2014). Reliability Assessment of Current Methods in Bloodstain Pattern Analysis *NCJRS*. doi:

www.ncjrs.gov

Tom Bevel, R. M. G. (2009). Bloodstain Pattern Analysis with an Introduction to Crime Scene Reconstruction (Practical Aspects of Criminal and Forensic Investigations). *3rd edition*.

Tour, M. H. (2018). Bloodstains: A brief Forensic History. *Medical History Tour*.

Turvey, B. E. (2013). An archive of cases that involve intentionally deceptive or misleading reports by forensic experts. *Forensic Fraud*.

United States : Chairwoman Johnsons Statement on Ten-Year Anniversary of Release of National Academies Forensics Study. (2019). MENA Report.

Victor. (2018). AI Programming: 5 Most Popular AI Programming Languages. *EXISTEK*.

Wirtzfeld, A. (2018). The History of Forensic Science - Blood Spatter Analysis. *Prezi*.

Wonder, A. Y. (2001). Blood dynamics. *Academic press*.

Zola, A. (2018). The 5 Best Programming Languages for AI. *Springboard Blog*.

(TIL), T. I. L. (2020). TIL that, in 2009, the National Academy of Sciences found only DNA analysis could rigorously and consistently match evidence to a single person/source with high confidence. Other methods, especially pattern matching (fingerprints, handwriting, bite marks, footprints, hair, fibers, etc.), could not. doi:https://www.reddit.com/r/todayilearned/comments/gokzdc/til_that_in_2009_the_national_academy_of_sciences/

Bou Zeid, W. V., J.; Brutin, D. (2013). Influence of evaporation rate on cracks' formation of a drying drop of whole blood. *Colloids and Surfaces A: Physicochemical and Engineering Aspects, 432*, 139-146. doi:http://dx.doi.org/10.1016/j.colsurfa.2013.04.044.

Connolly, C., Illes, M., & Fraser, J. (2012). Affect of impact angle variations on area of origin determination in bloodstain pattern analysis. *Forensic Sci Int, 223*(1-3), 233-240. doi:10.1016/j.forsciint.2012.09.009

Encyclopedia, W.-T. f. (2020). Scientific Working Group – Bloodstain Pattern Analysis doi:https://en.wikipedia.org/wiki/Scientific_Working_Group_%E2%80%93_Bloodstain_Pattern_Analysis

Englert, R. P., K. (2010). Blood secrets: chronicles of a crime scene reconstructionist. *Macmillan*.

IABPA. (2008). International Association of Bloodstain Pattern Analysts. *Evidence Technology Magazine*. doi:www.iabpa.org

IABPA. (2019). Bloodstain Analysis. *weebly.*

Laan, N., de Bruin, K. G., Slenter, D., Wilhelm, J., Jermy, M., & Bonn, D. (2015). Bloodstain Pattern Analysis: implementation of a fluid dynamic model for position determination of victims. *Sci Rep, 5*, 11461. doi:10.1038/srep11461

Laan, N. S., F.; Nicloux, C.; Brutin, D. (2016). Morphology of drying blood pools. *Forensic Science International 267* 104-109. doi:https://doi.org/10.1016/j.forsciint.2016.08.005.

Larkin, B. A., & Banks, C. E. (2013). Preliminary study on the effect of heated surfaces upon bloodstain pattern analysis. *J Forensic Sci, 58*(5), 1289-1296. doi:10.1111/1556-4029.12185

Larkin, B. A., & Banks, C. E. (2016). Exploring the applicability of equine blood to bloodstain pattern analysis. *Med Sci Law, 56*(3), 190-199. doi:10.1177/0025802414542456

Larkin, B. A. J. (2015). Bloodstain pattern analysis: scratching the surface. *CORE*, 50-256. doi: https://e-space.mmu.ac.uk/579548/1/complete%20thesis.pdf

Laux, D. F., J. Y.; Brutin, D. (2016). Ultrasonic monitoring of droplets' evaporation: Application to human whole blood. . *Ultrasonics Sonochemistry 32*, 132-136. doi:https://doi.org/10.1016/j.ultsonch.2016.03.003.

Patrick Laturnus., e. a. (2014). International Association of Bloodstain Pattern Analysis (IABPA). *Journal of Bloodstain Pattern Analysis (IABPA), Volume 30*

Wonder, A. Y. (2001). Blood dynamics. *Academic press*.

Yu lui, Daniel Attinger, Kris De Brabanter. (2020). Automatic Classification of Bloodstain Patterns Caused by Gunshot and Blunt Impact at Various Distances Wiley Online Library.

https://doi.org/10.1111/1556-4029.14262

Appendix A: Impact Angle 10-Degree Individual Bloodstain Samples

10-DEGREE – SAMPLE 1 (10_1_1 TO 10_1_10)

10-DEGREE-SAMPLE 2 (10_2_1_2 TO 10_2_10)

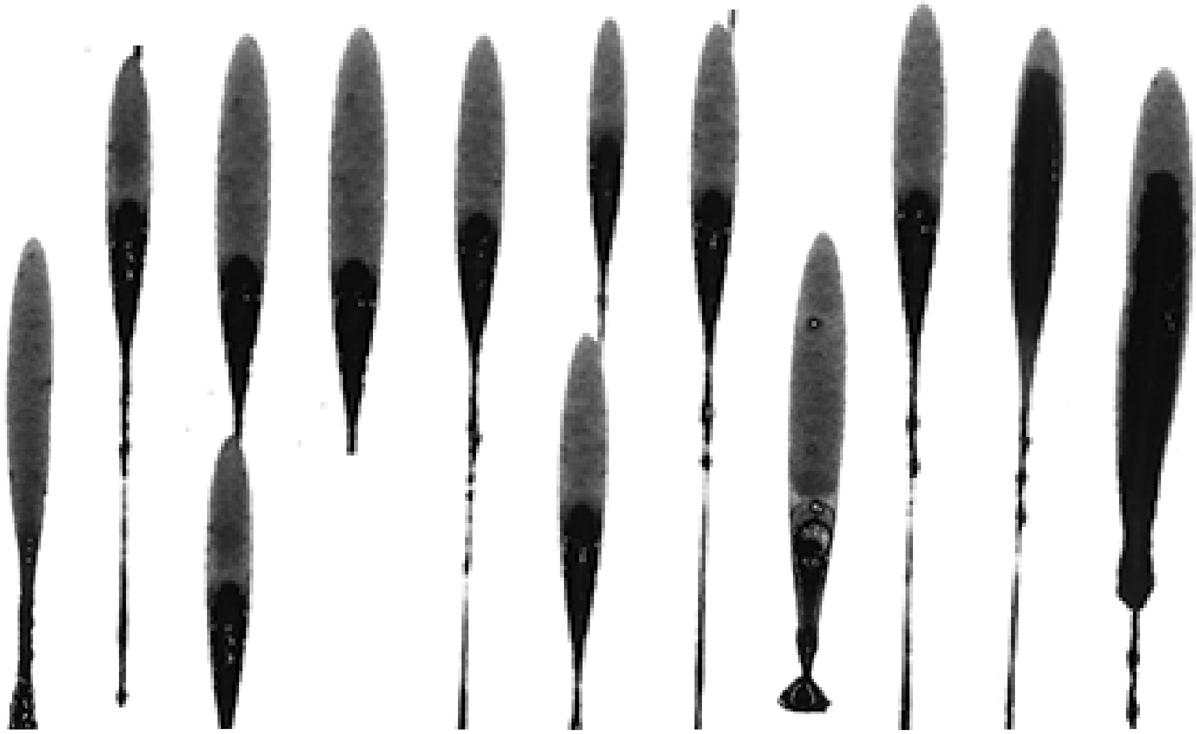

10-DEGREE- SAMPEL2 (10_2_11 TO 10_2_19)

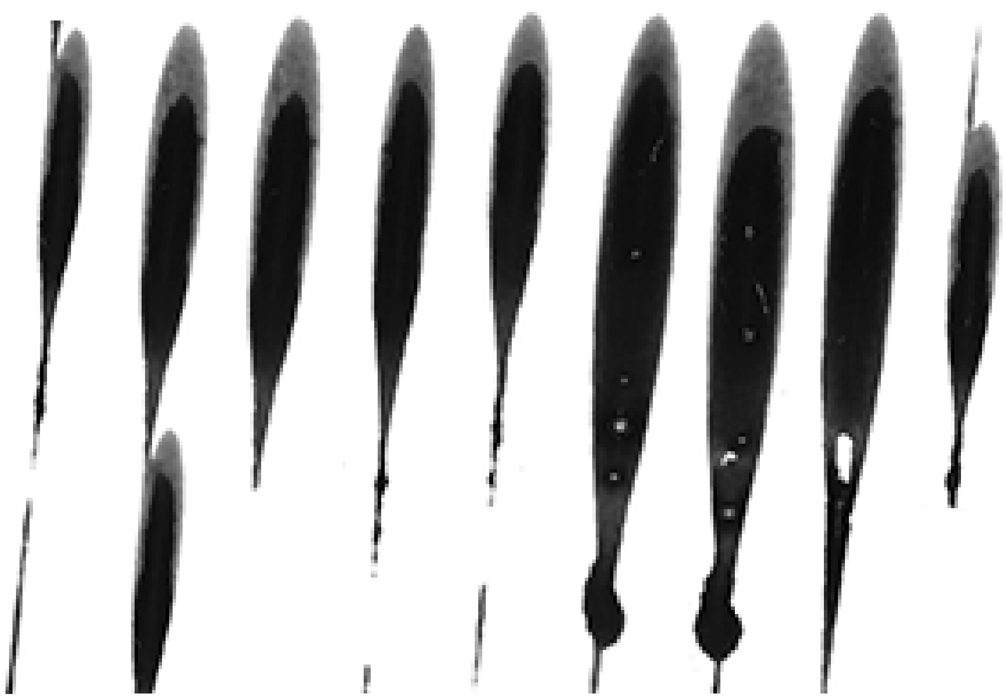

10 DEGREE- SAMPLE 3 (10_3_1 TO 10_3_8)

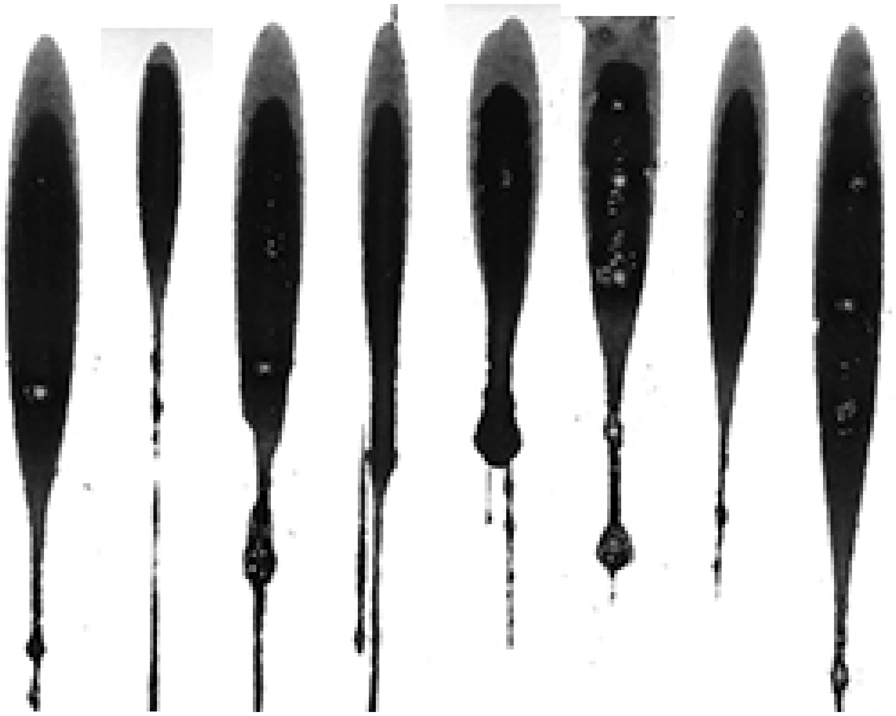

10 DEGREE- SAMPLE 3 (10_3_9 TO 10_3_16)

Appendix B: Impact Angle 20-Degree Individual Bloodstain Samples

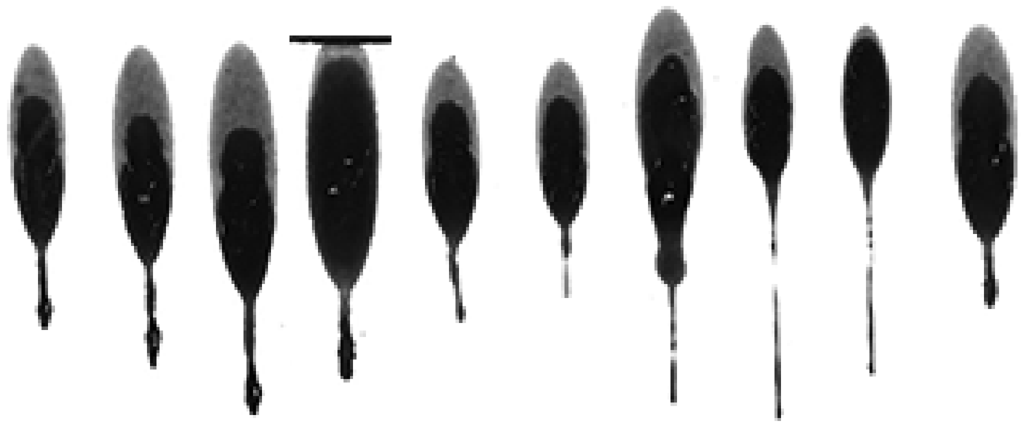

20 DEGREE – SAMPLE 1 (20_1 TO 20_10)

20 DEGREE – SAMPLE 1 (20_11 TO 20_15, 20_25 TO 20_29)

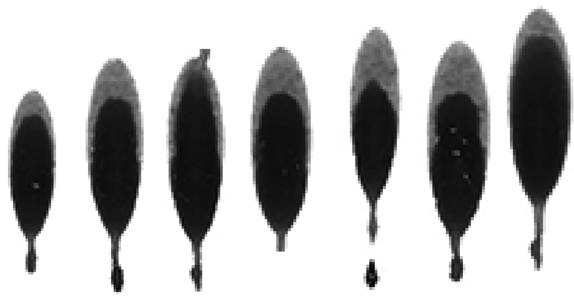

20 -DEGREE – SAMPLE 1 (20_30 TO 20_37)

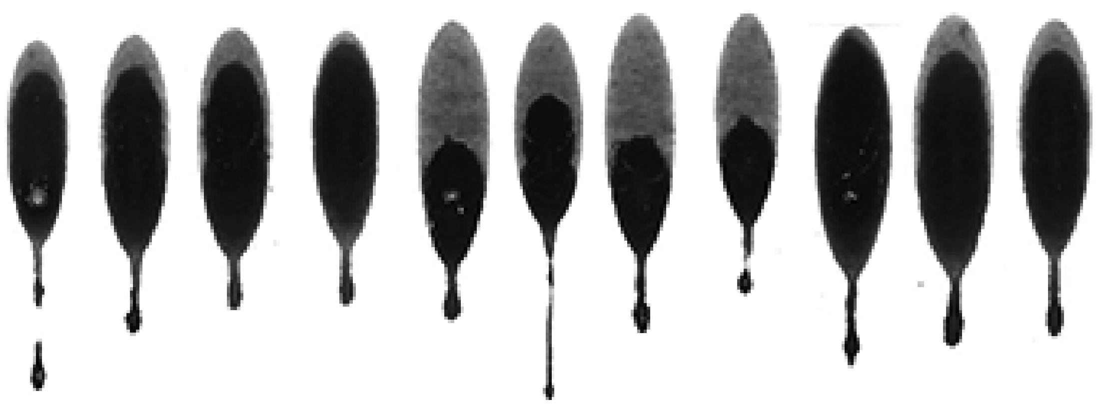

20 DEGREE – SAMPLE 1 (20_44 TO 20_54)

Appendix C: Impact Angle 30-Degree Individual Bloodstain Samples

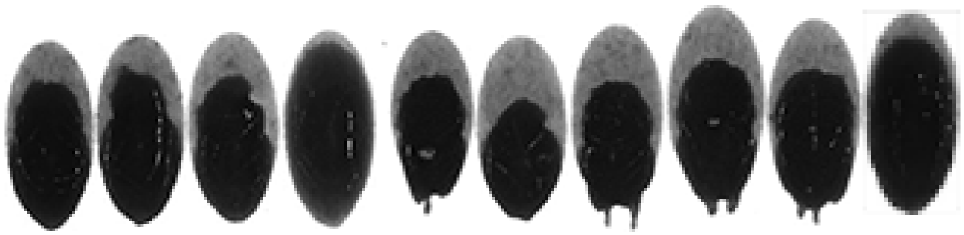

30 DEGREE- SAMPLE 1 (30_1 TO 10)

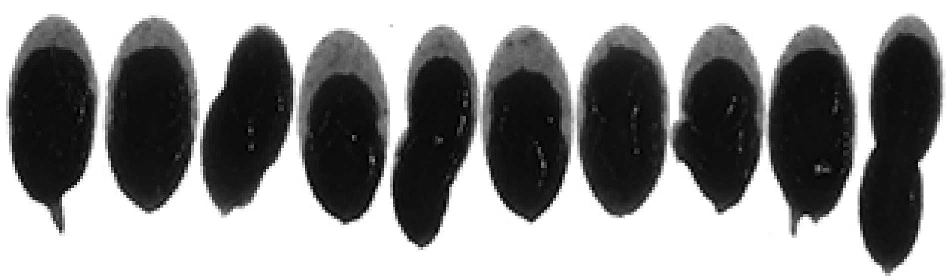

30-DEGREE- SAMPLE 1 (30_11 TO 30_20)

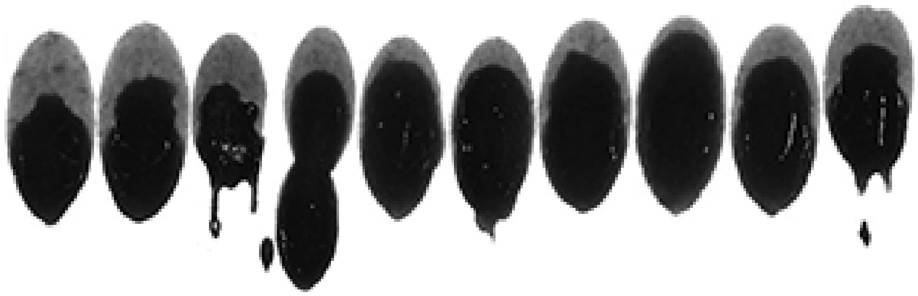

30-DEGREE- SAMPLE 1 (30_21 TO 30_30)

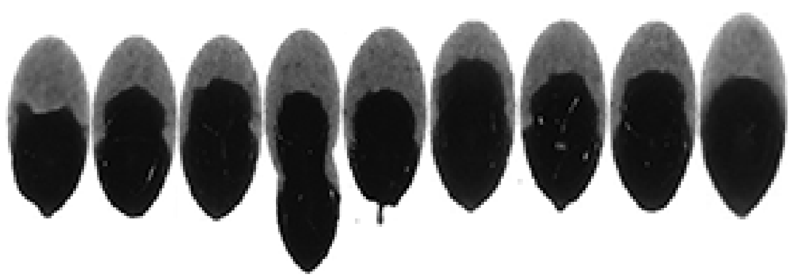

30-DEGREE- SAMPLE 1 (30_31 TO 30_40)

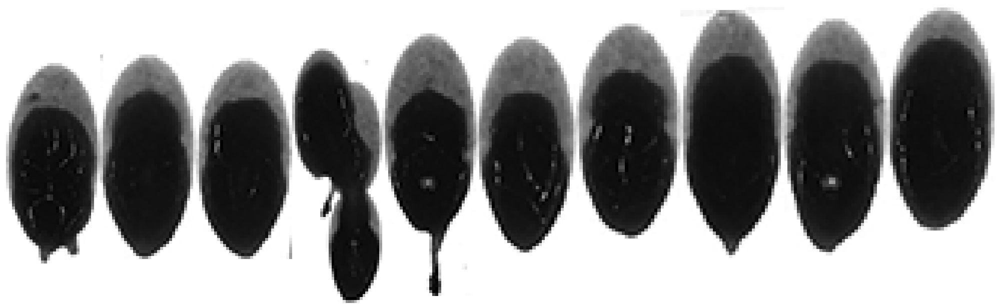

30-DEGREE- SAMPLE 1 (30_41 TO 30_50)

30-DEGREE- SAMPLE 1 (30_51 TO 30_60)

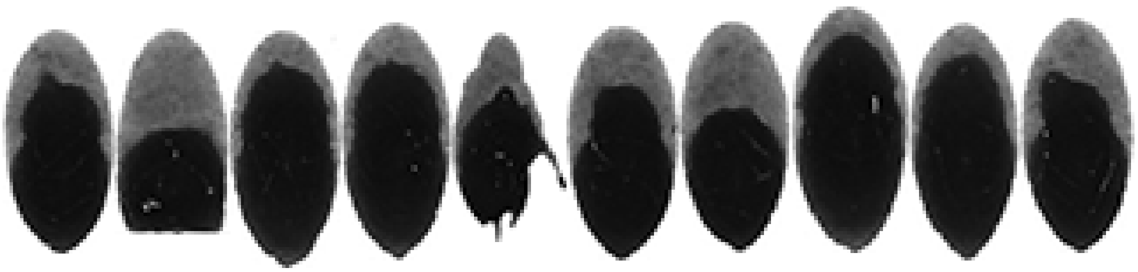

30-DEGREE- SAMPLE 1 (30_61 TO 30_70)

30-DEGREE- SAMPLE 1 (30_71 TO 30_80)

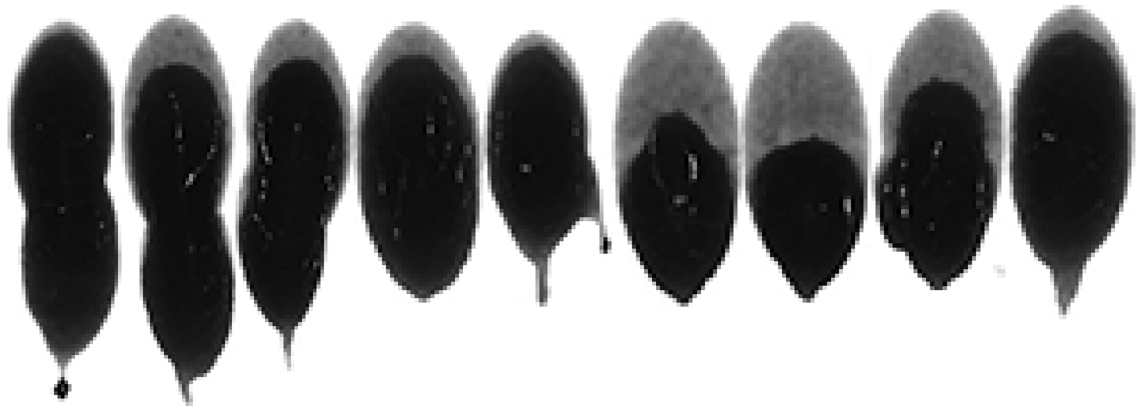

30-DEGREE- SAMPLE 1 (30_81 TO 30_90)

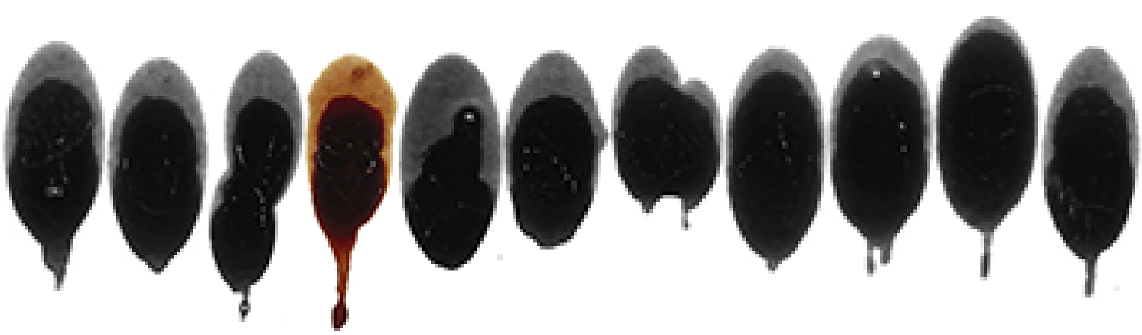

30-DEGREE- SAMPLE 1 (30_91 TO 30_101)

Appendix D: Impact Angle 40-Degree Individual Bloodstain Samples

40-DEGREE- SAMPLE 1 (40_1 TO 40_10)

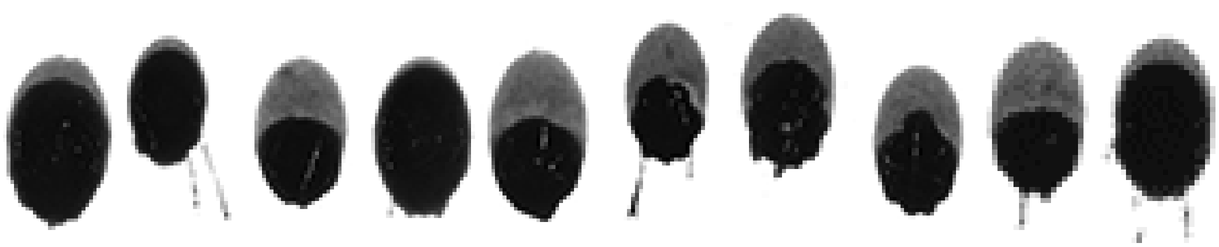

40-DEGREE- SAMPLE 1 (40_11 TO 40_20)

Appendix E: Impact Angle 50-Degree Individual Bloodstain Samples

50-DEGREE- SAMPLE 1 (50_1 TO 50_10)

50-DEGREE- SAMPLE 1 (50_11 TO 50_20)

50-DEGREE- SAMPLE 1 (50_21 TO 50_30)

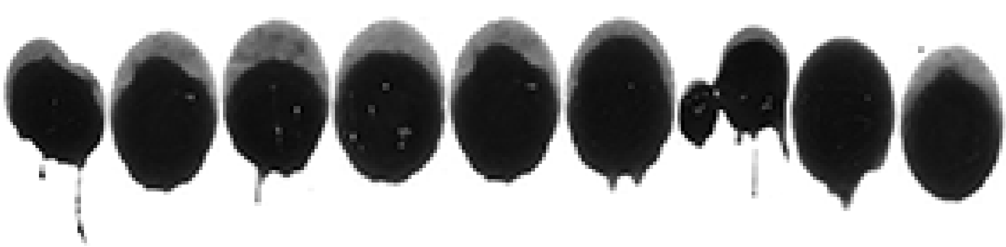

50-DEGREE- SAMPLE 1 (50_31 TO 50_39, AND 50_41)

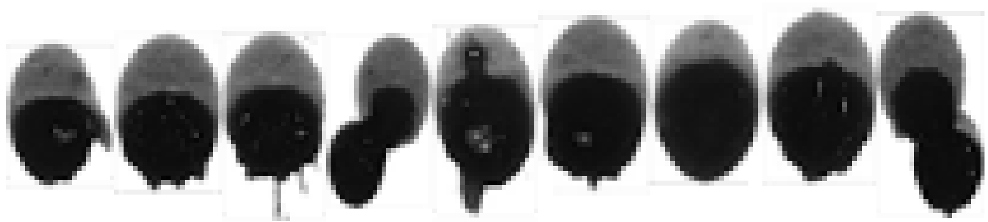

50-DEGREE- SAMPLE 1 (50_42 TO 50_50)

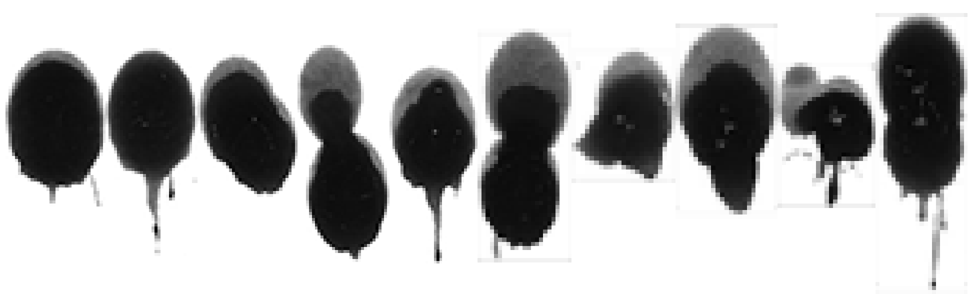

50-DEGREE- SAMPLE 1 (50_51 TO 50_60)

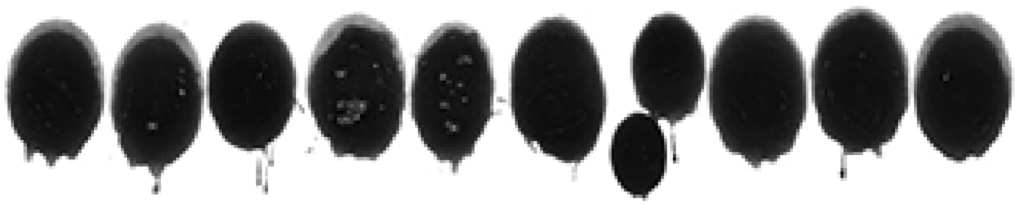

50-DEGREE- SAMPLE 1 (50_61 TO 50_70)

50-DEGREE- SAMPLE 1 (50_71 TO 50_79)

Appendix F: Impact Angle 60-Degree Individual Bloodstain Samples

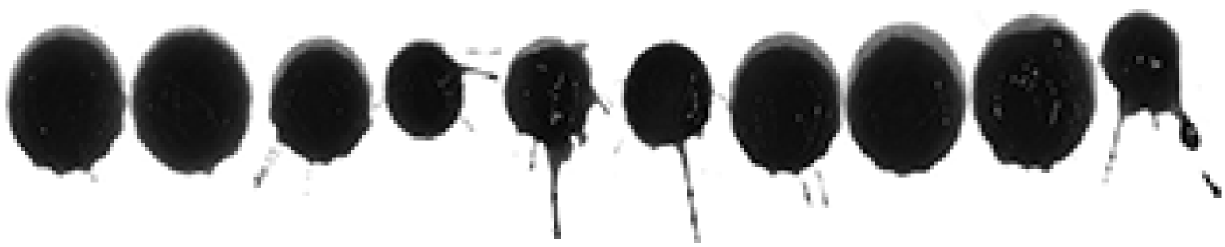

60-DEGREE- SAMPLE 1 (60_1 TO 60_10)

60-DEGREE- SAMPLE 1 (60_11 TO 60_15, AND 60_39 TO 60_43)

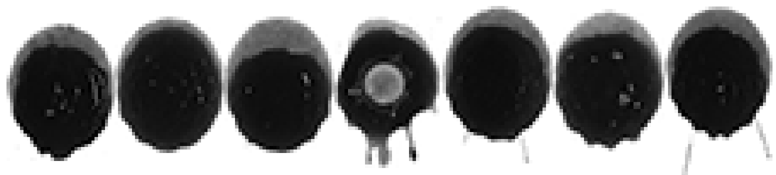

60-DEGREE- SAMPLE 1 (60_44, 60_45, 60_58, 60_59, 60_60, 60_61, AND 60_62)

Appendix G: Impact Angle 70-Degree Individual Bloodstain Samples

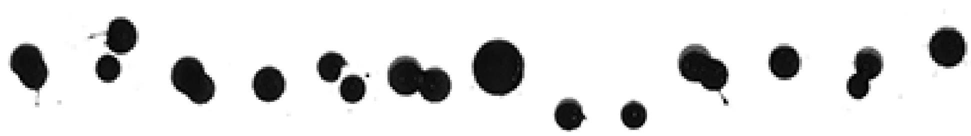

70-DEGREE- SAMPLE 1 (70_1_1 TO 70_1_10)

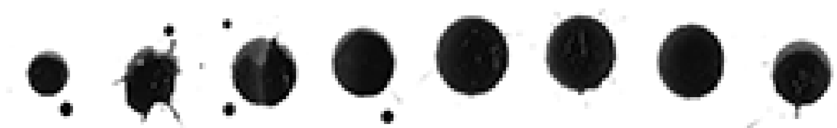

70-DEGREE- SAMPLE 2 (70_2_1 TO 70_2_8)

70-DEGREE- SAMPLE 2 (70_2_9 TO 70_2_16)

Appendix H: Impact Angle 80-Degree Individual Bloodstain Samples

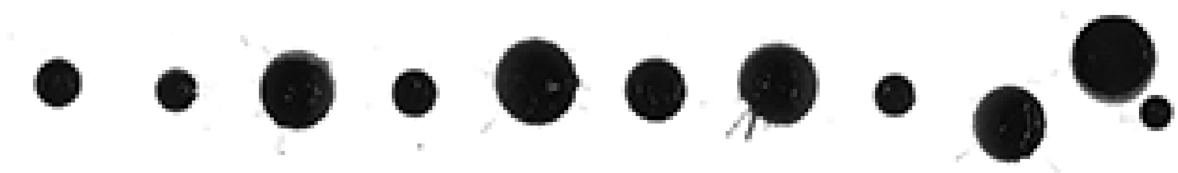

80- DEGREE- SAMPLE 1 (80_1_1 TO 80_1_10)

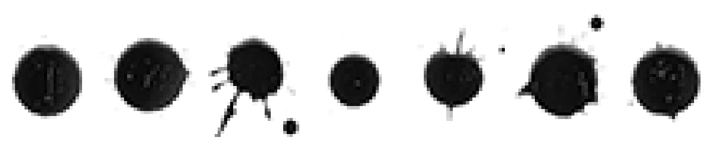

80- DEGREE- SAMPLE 1 (80_1_11 TO 80_1_18)

Appendix I: Impact Angle 90-Degree Individual Bloodstain Samples

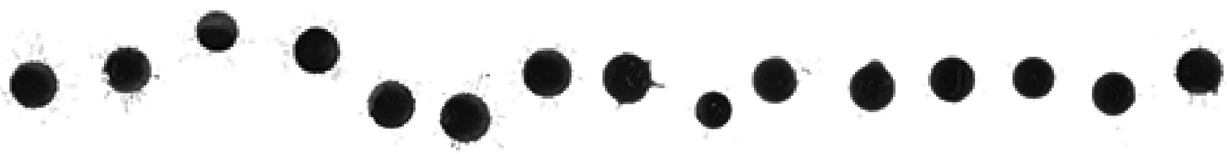

90-DEGREE- SAMPLE 1 (90_1_1 TO 90_1_15)

<u>Appendix J: Impact Energy 10-Degree Spatter Samples</u>

10 DEGREE

Appendix K: Impact Energy 20-Degree Spatter Samples

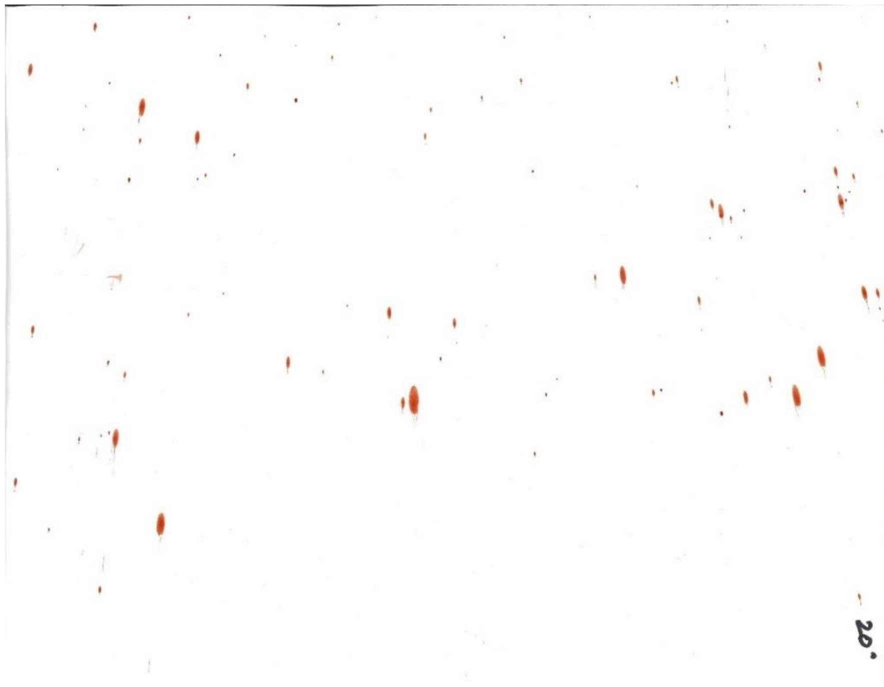

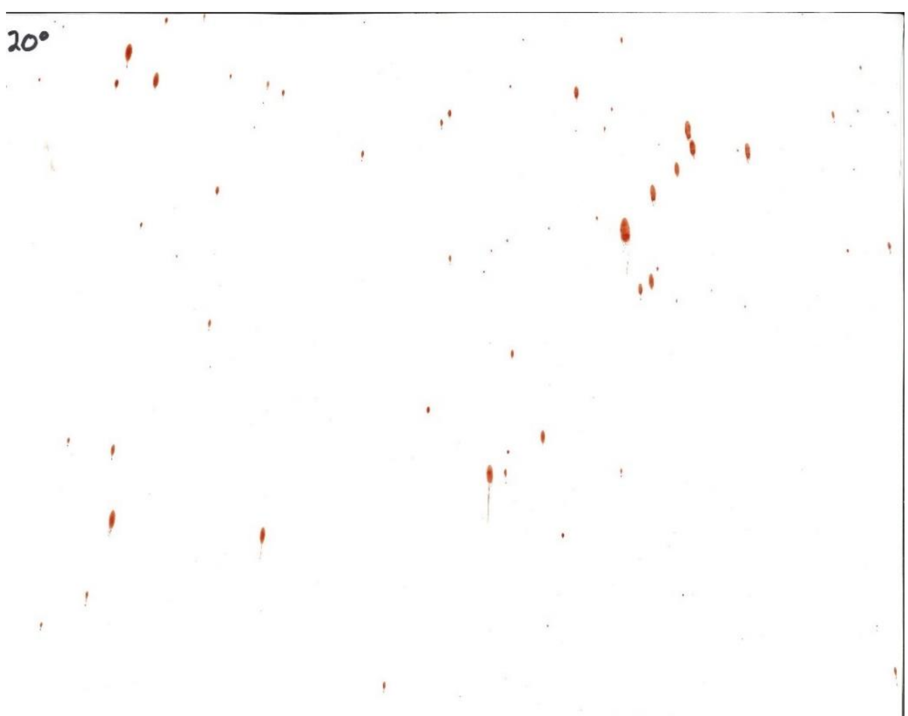

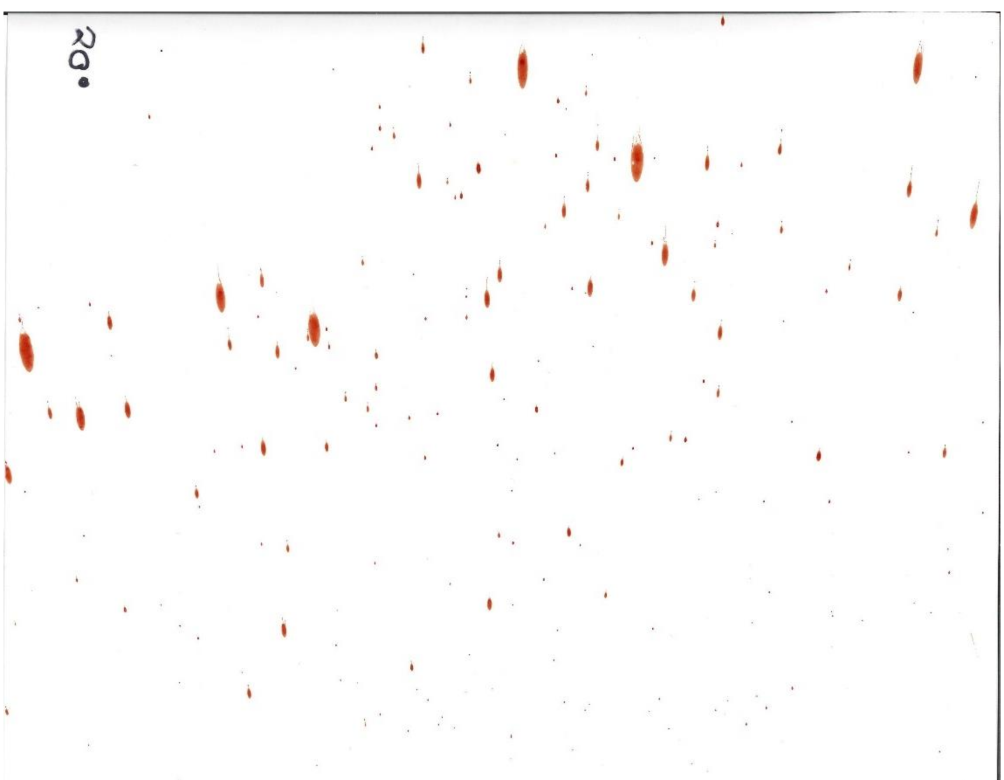

20 DEGREE

Appendix L: Impact Energy 30-Degree Spatter Samples

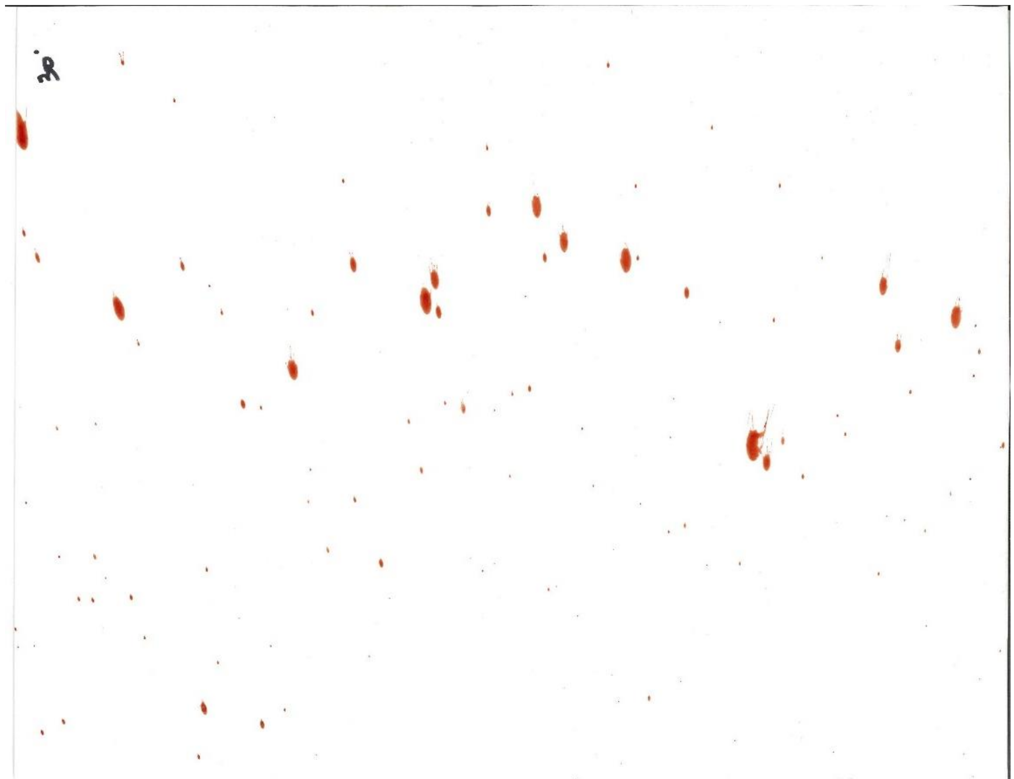

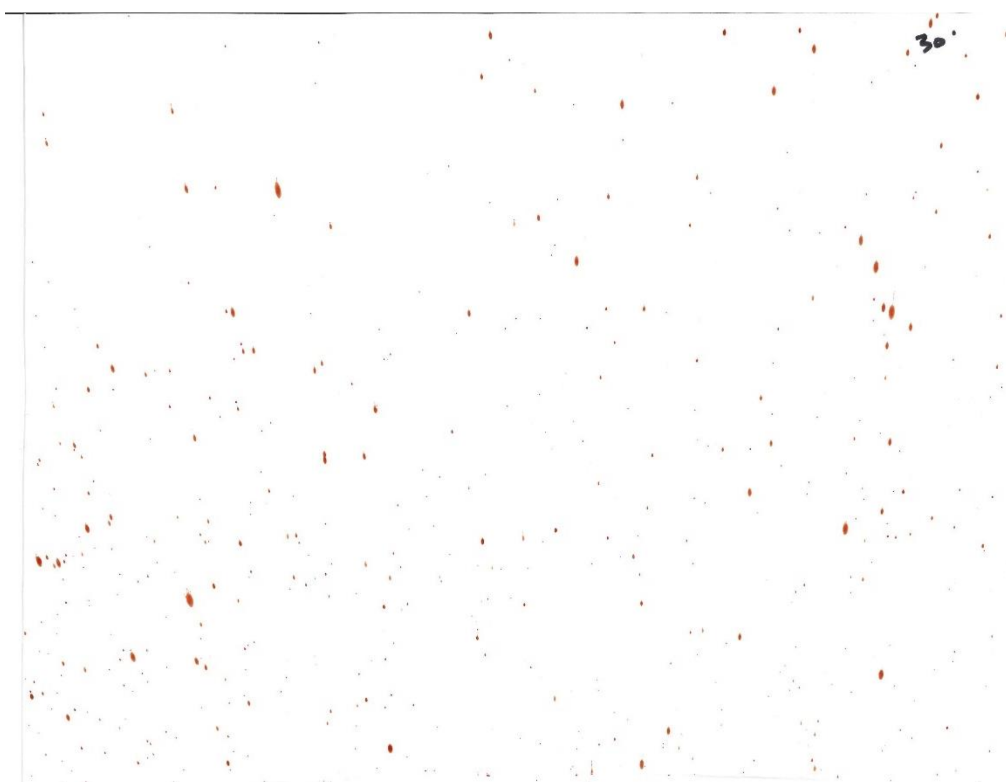

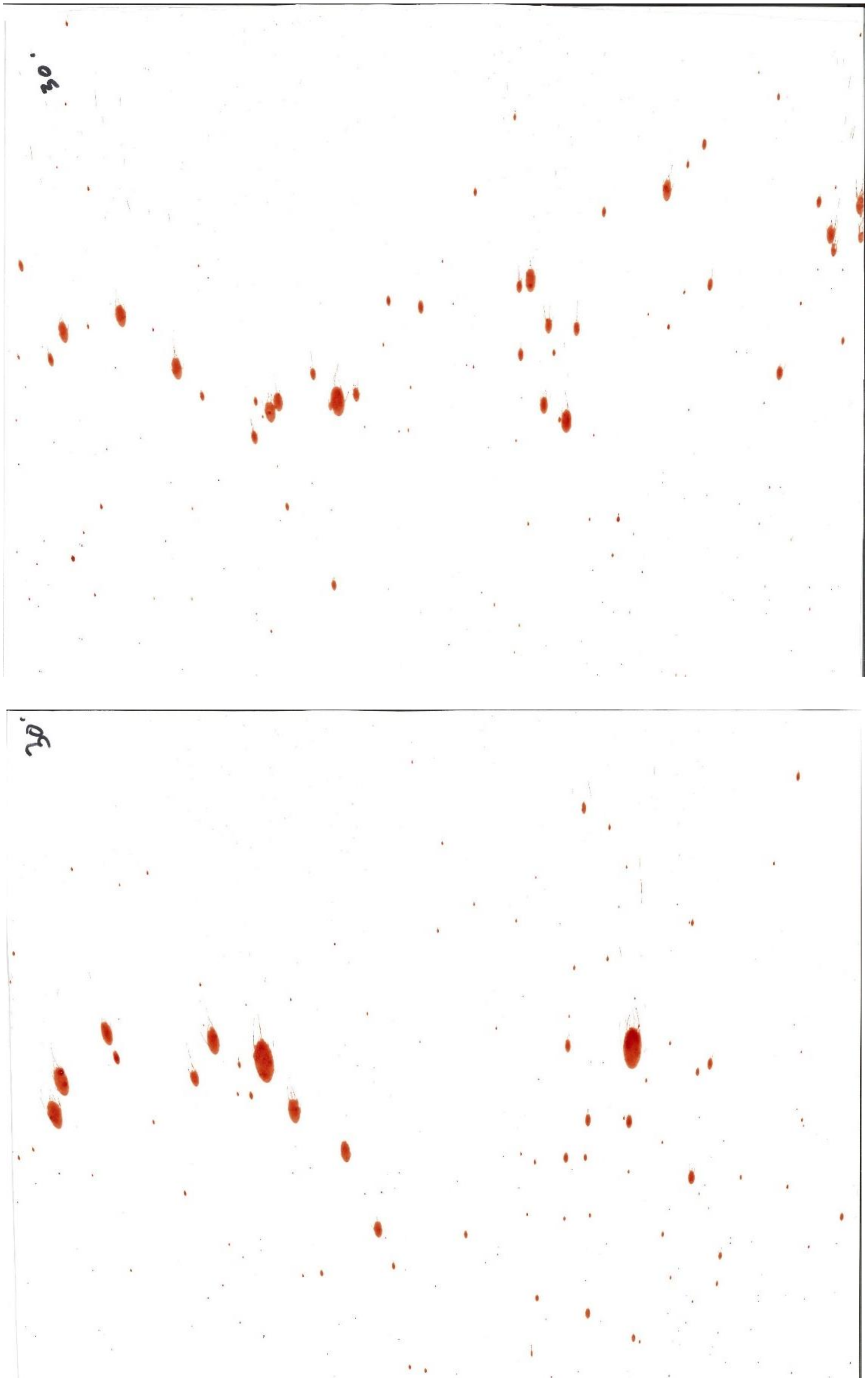

30- DEGREE

Appendix M: Impact Energy 40-Degree Spatter Samples

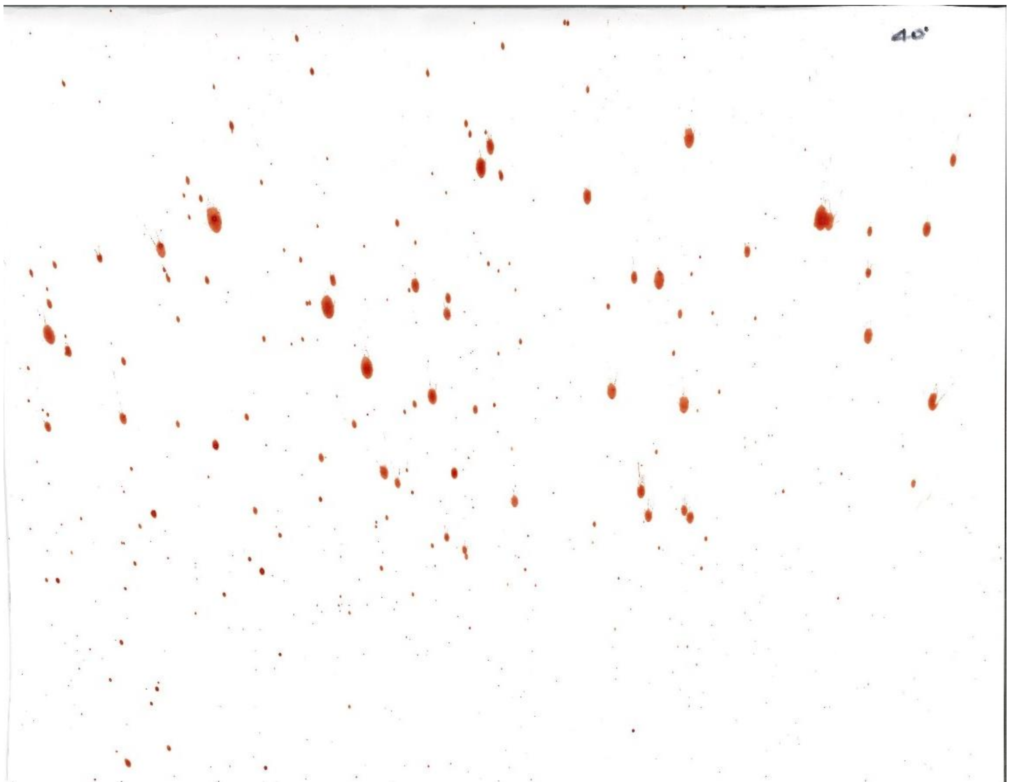

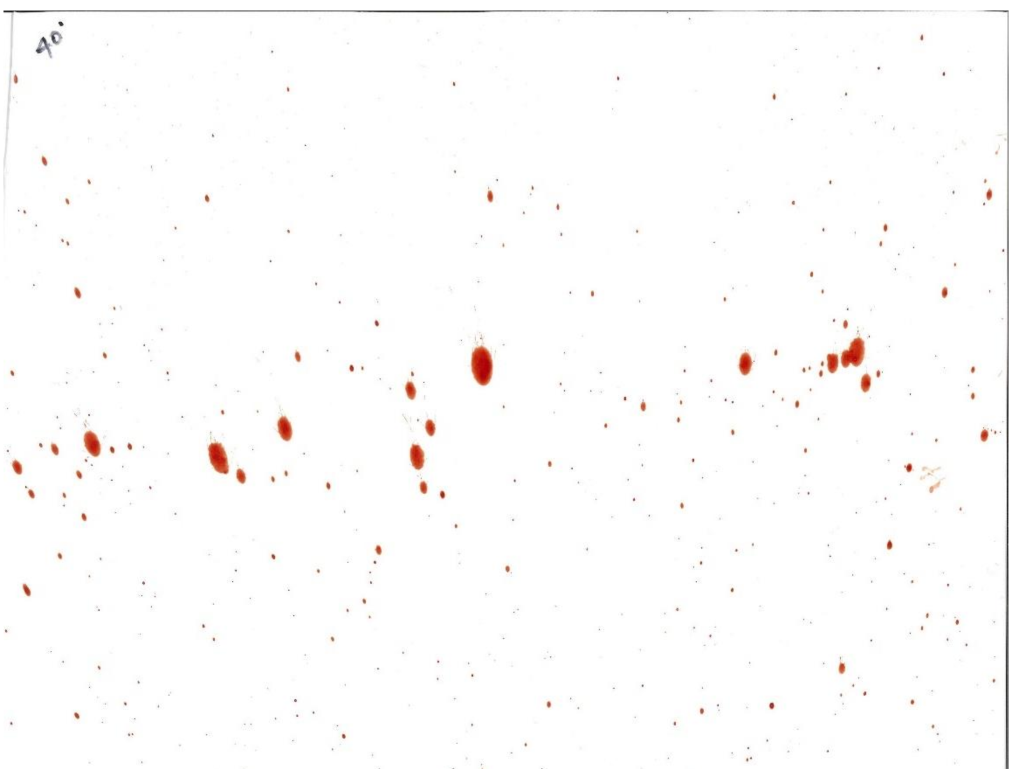

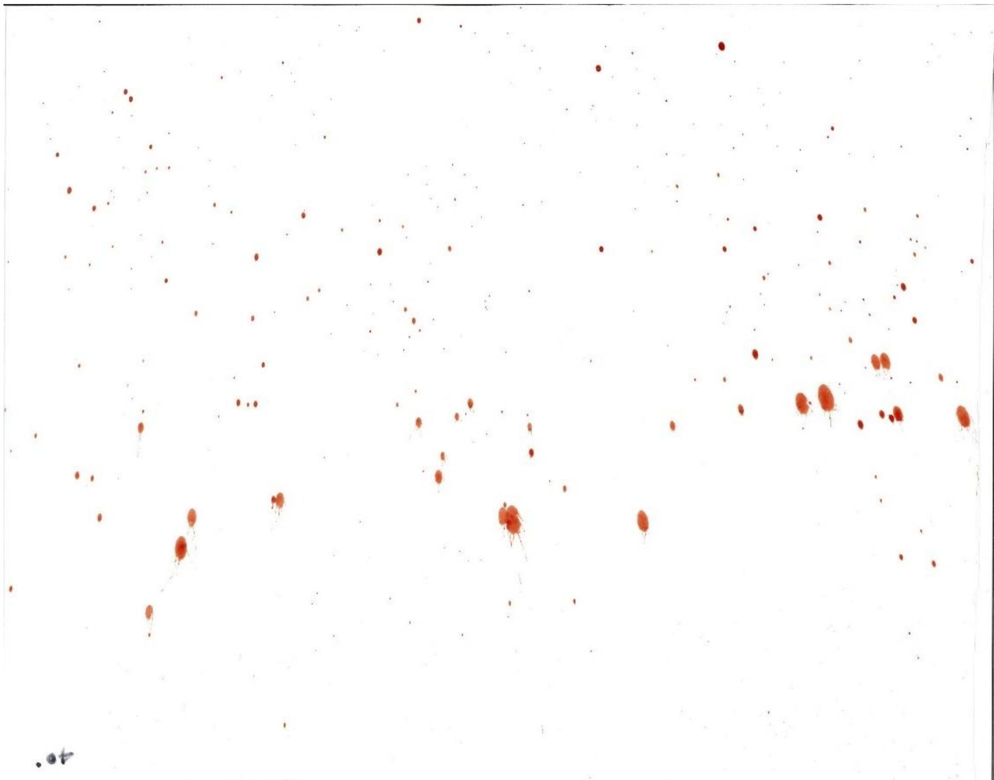

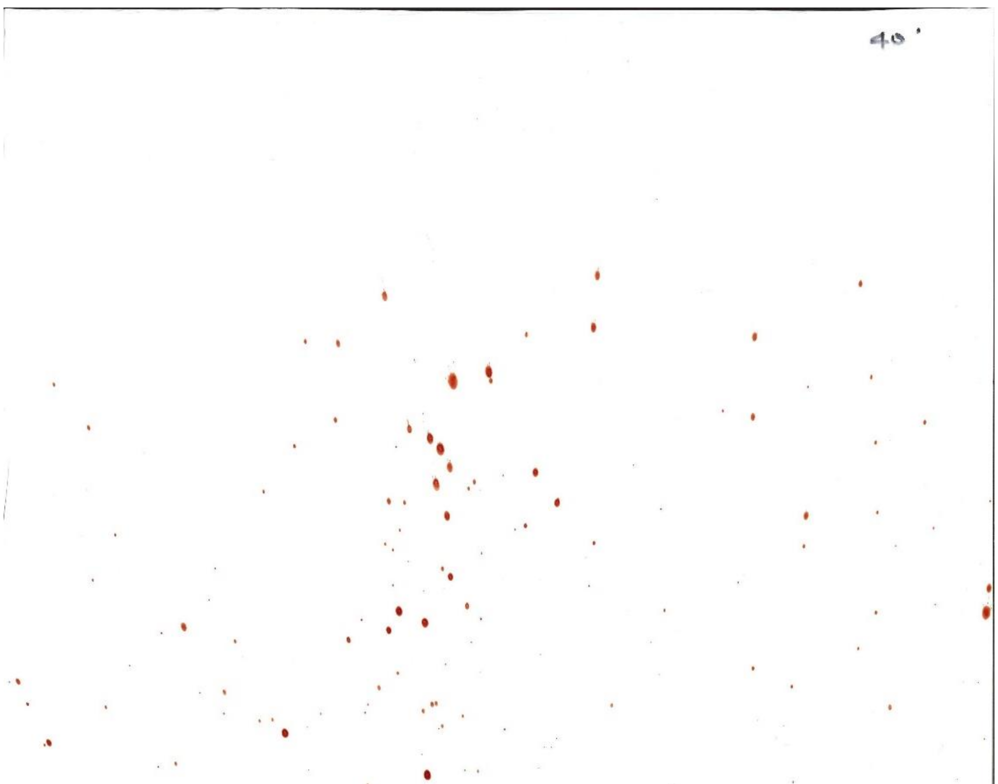

40-DEGREE

Appendix N: Impact Energy 50-Degree Spatter Samples

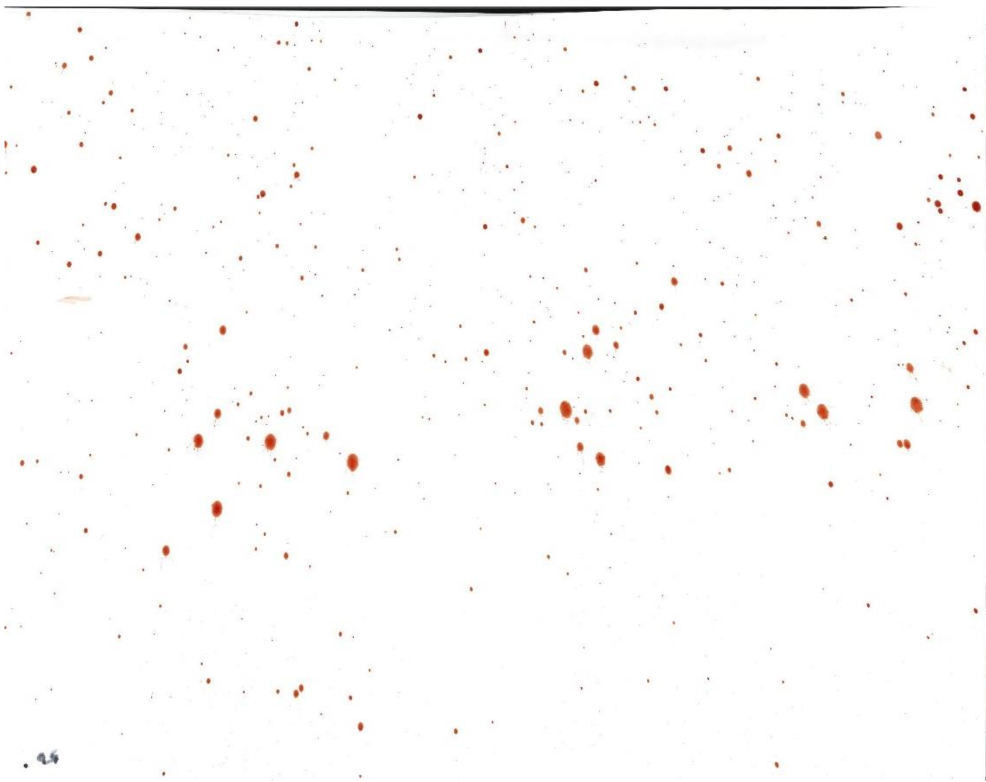

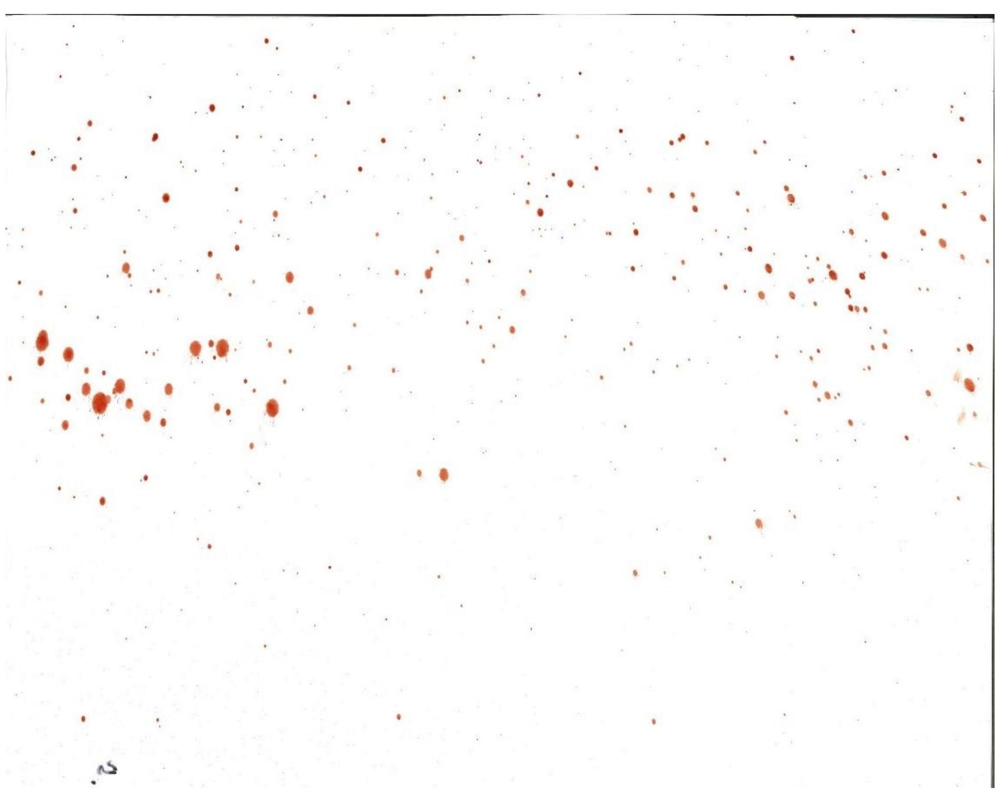

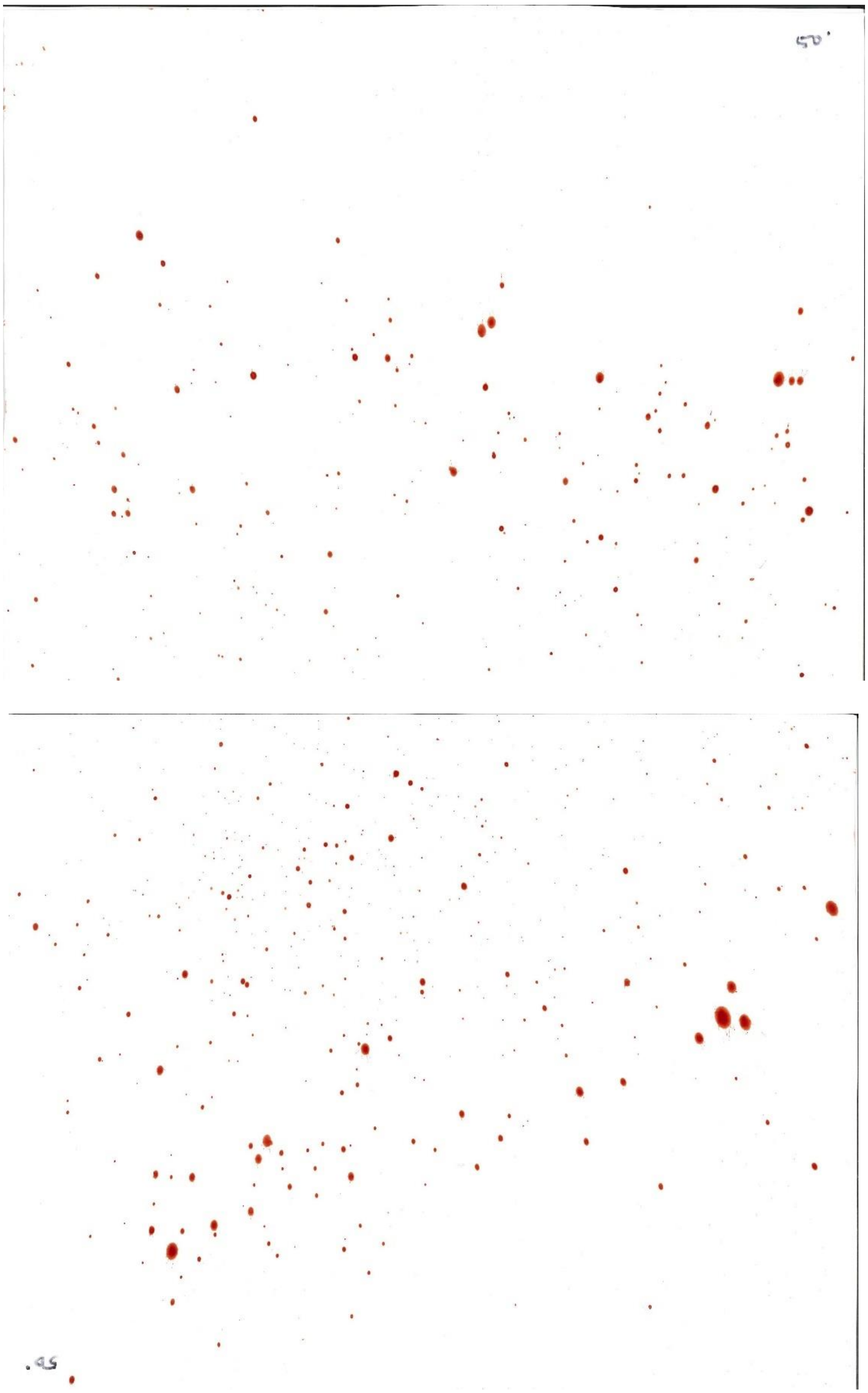

50-DEGREE

Appendix O: Impact Energy 60-Degree Spatter Samples

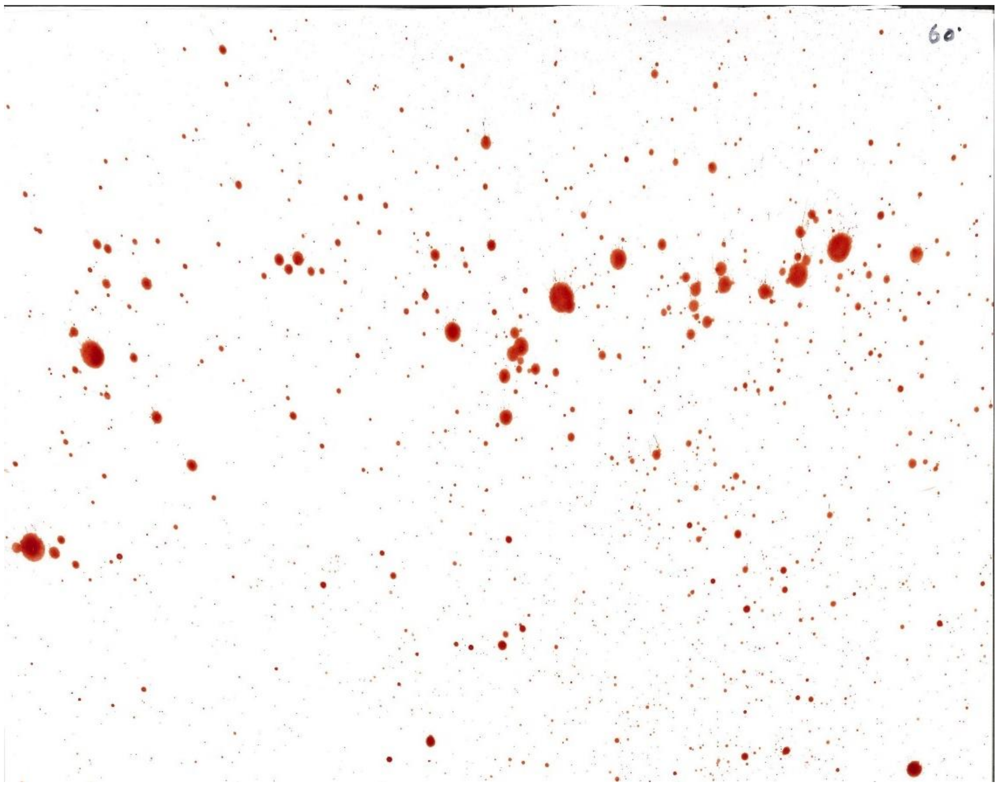

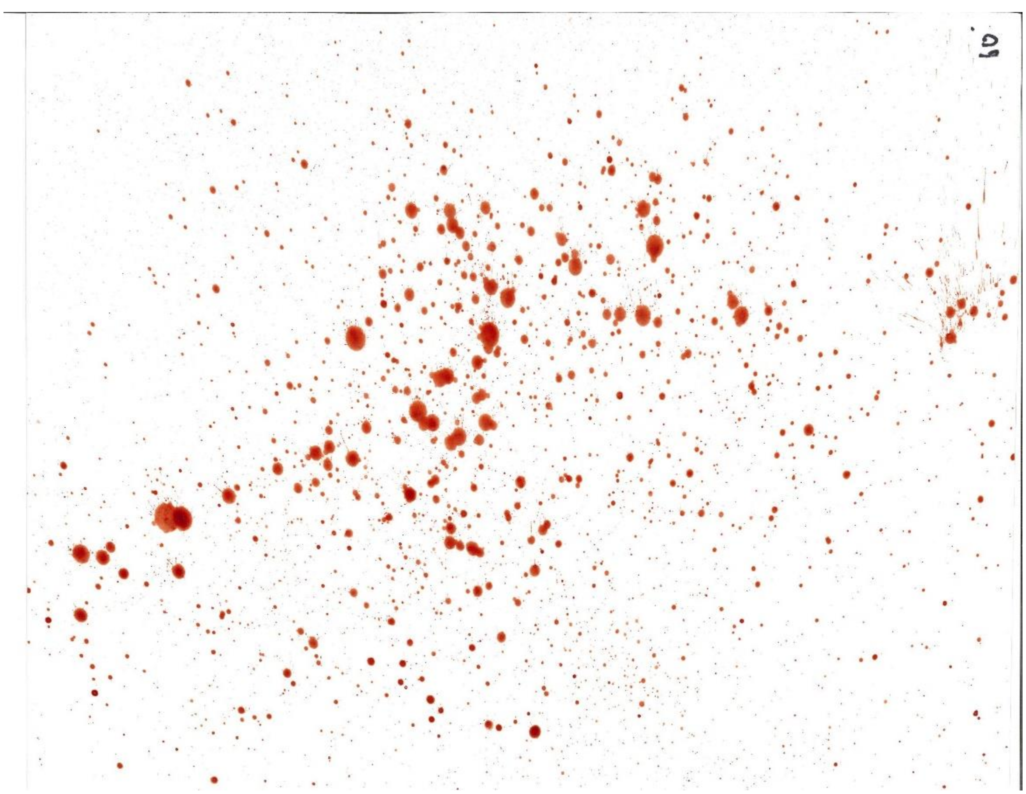

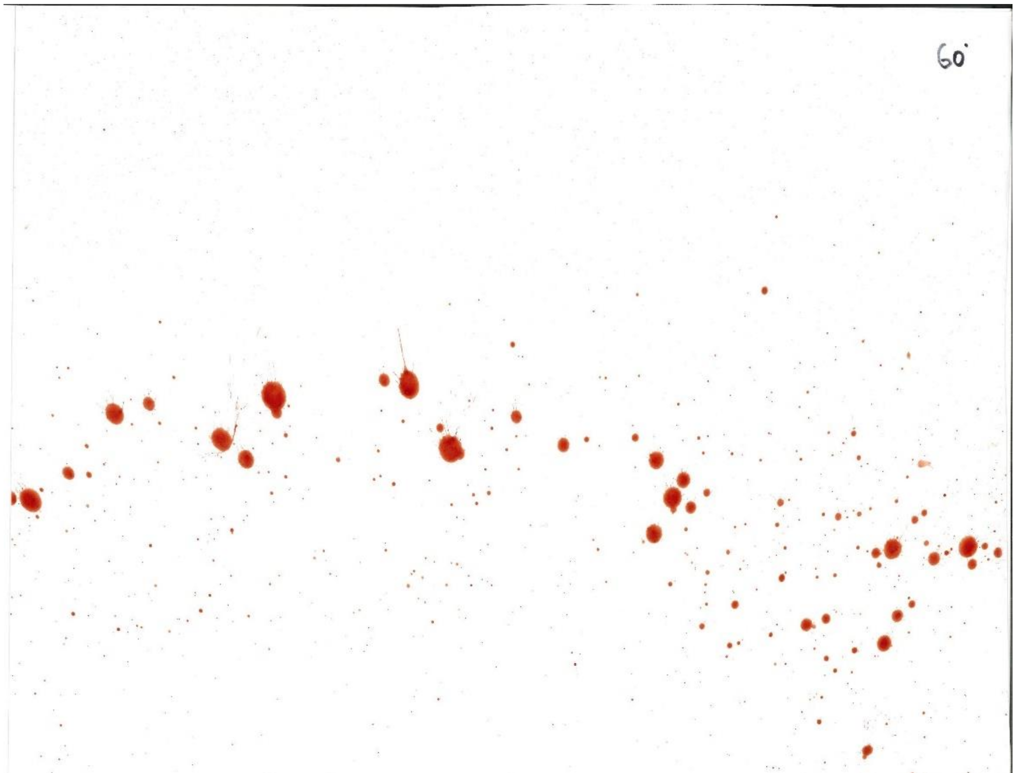

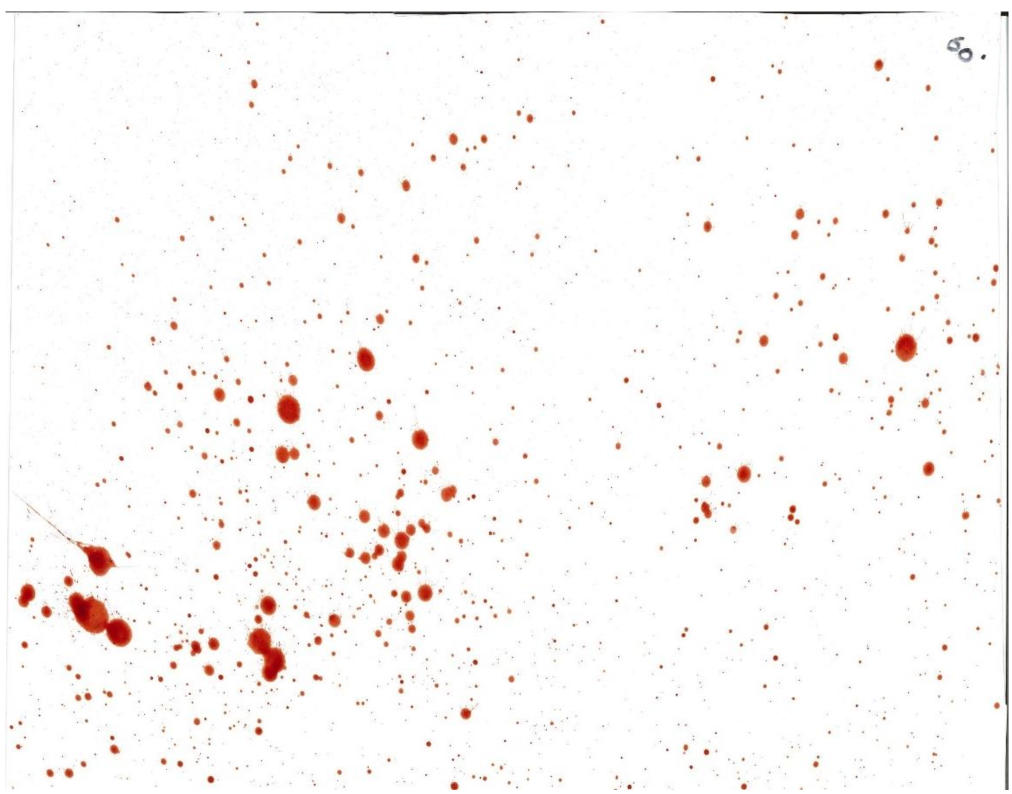

60-DEGREE

Appendix P: Impact Energy 70-Degree Spatter Samples

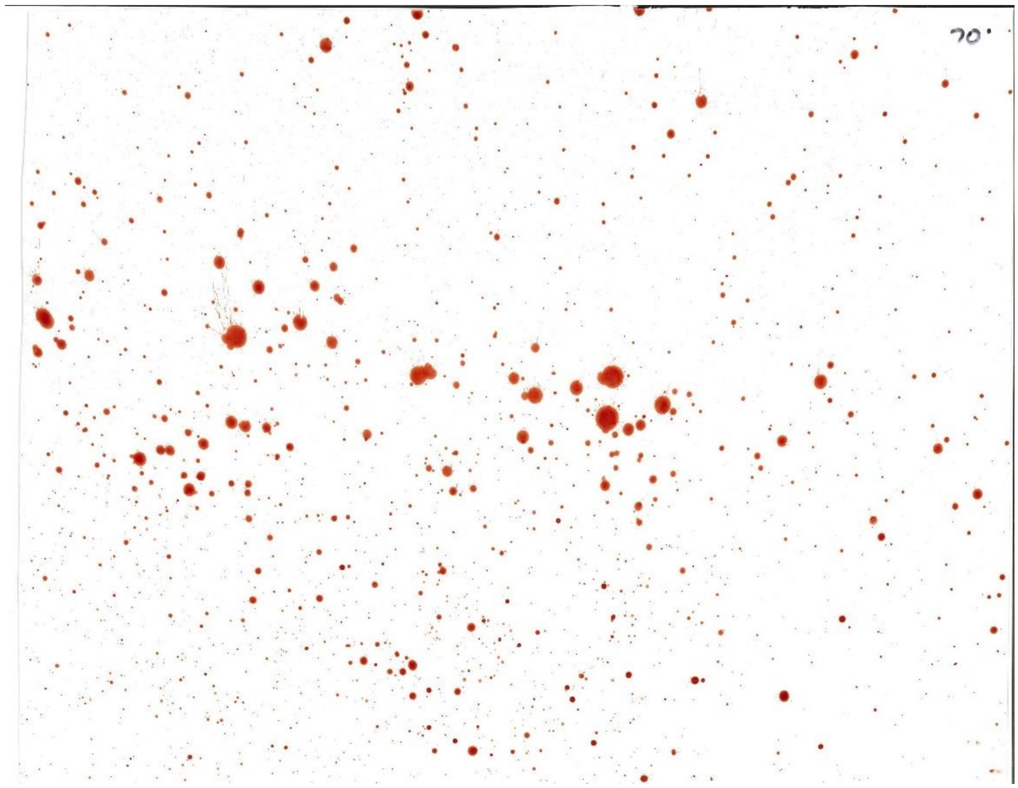

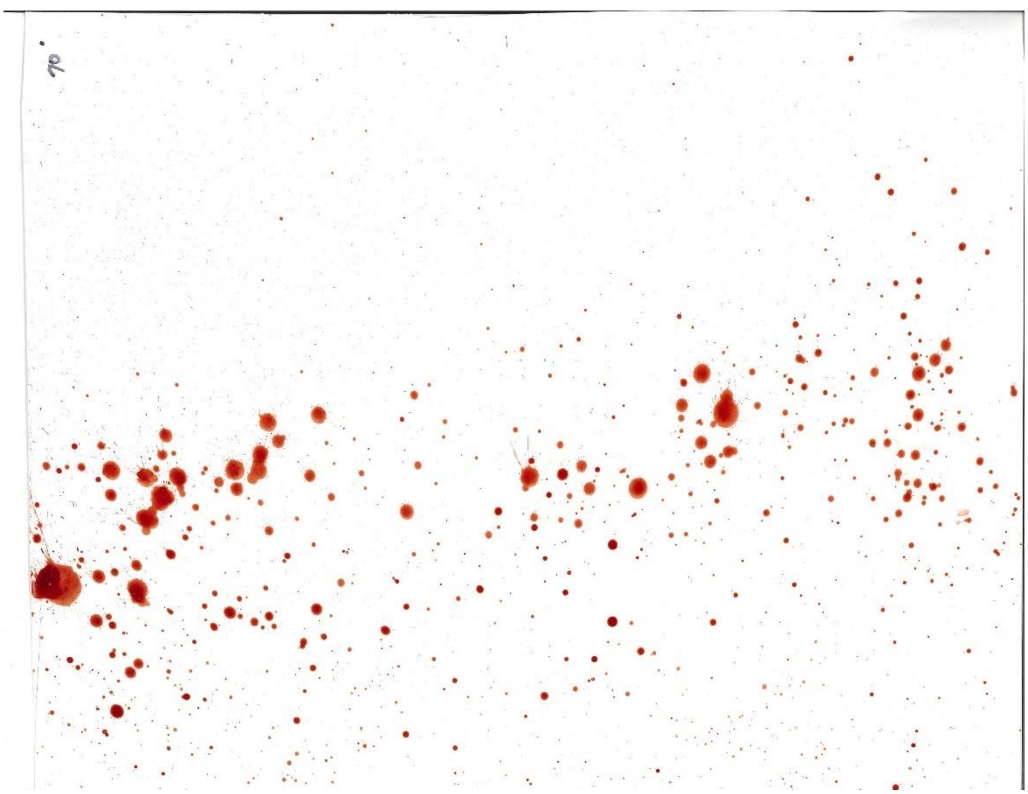

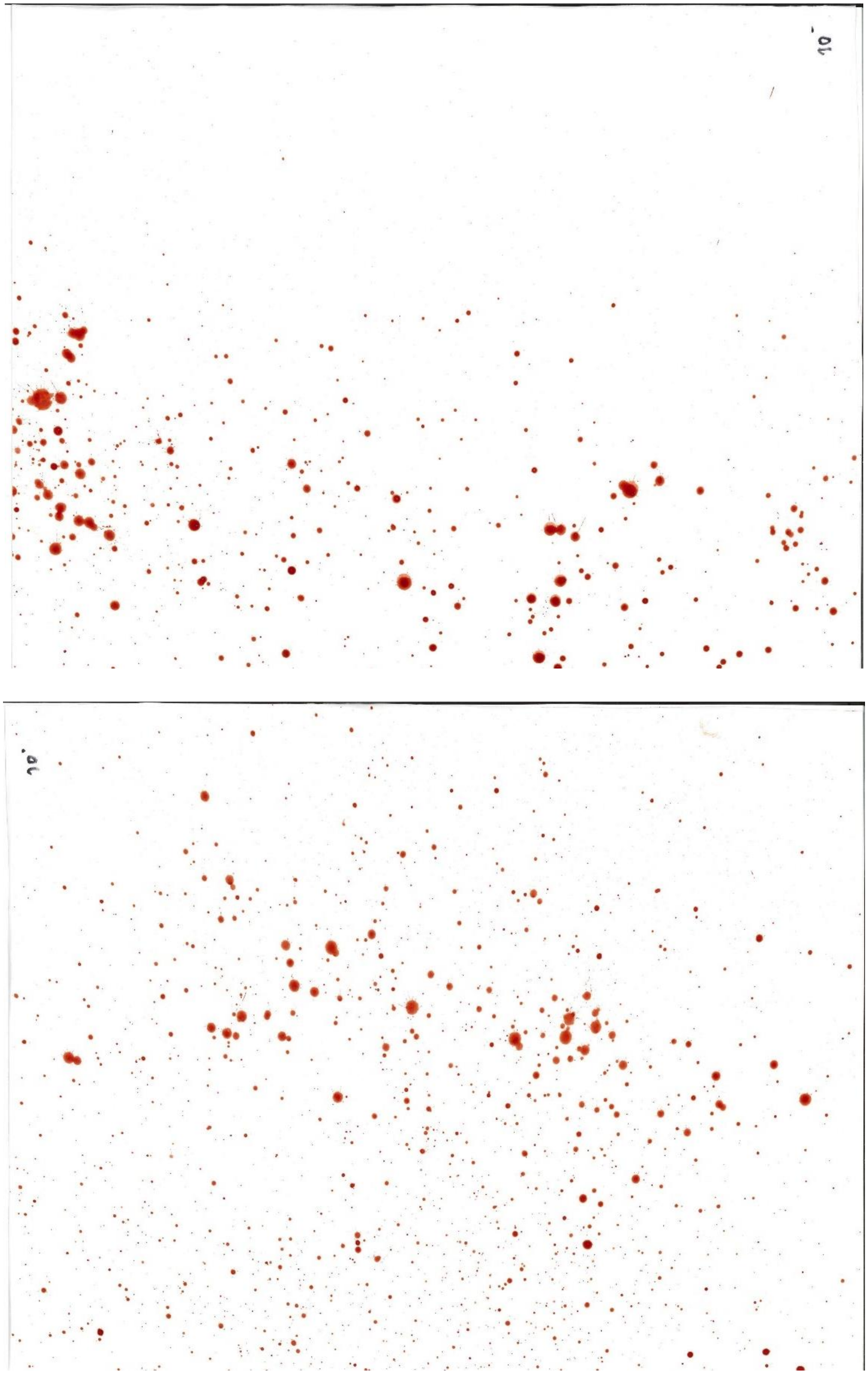

70-DEGREE

Appendix Q: Impact Energy 80-Degree Spatter Samples

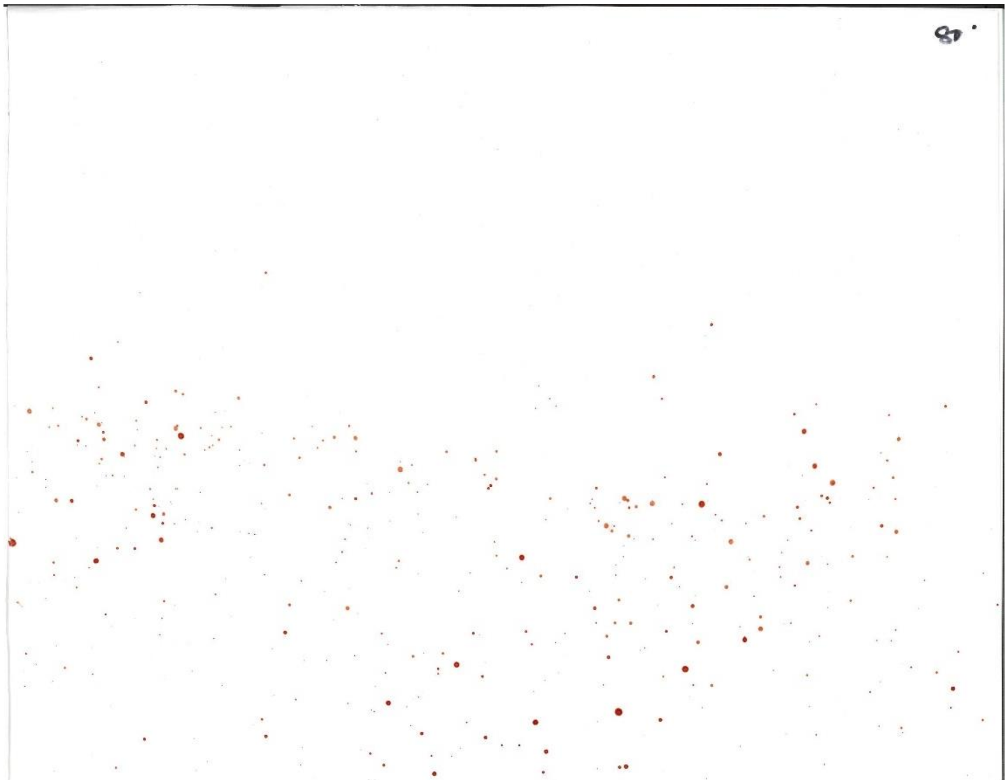

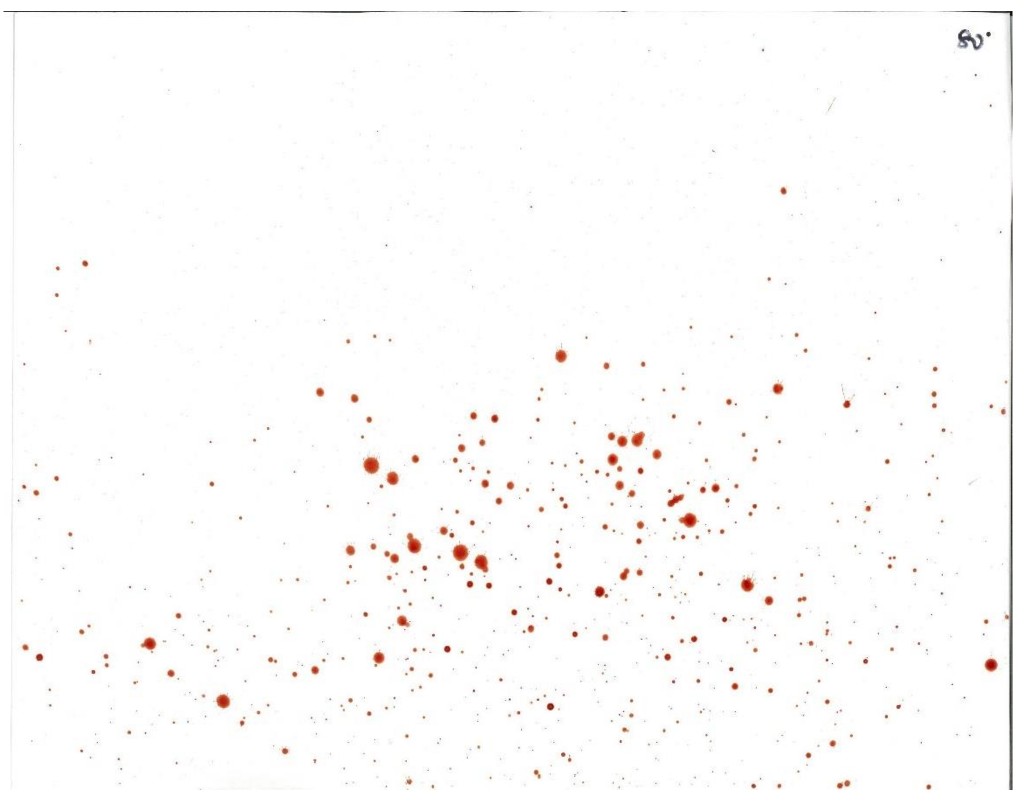

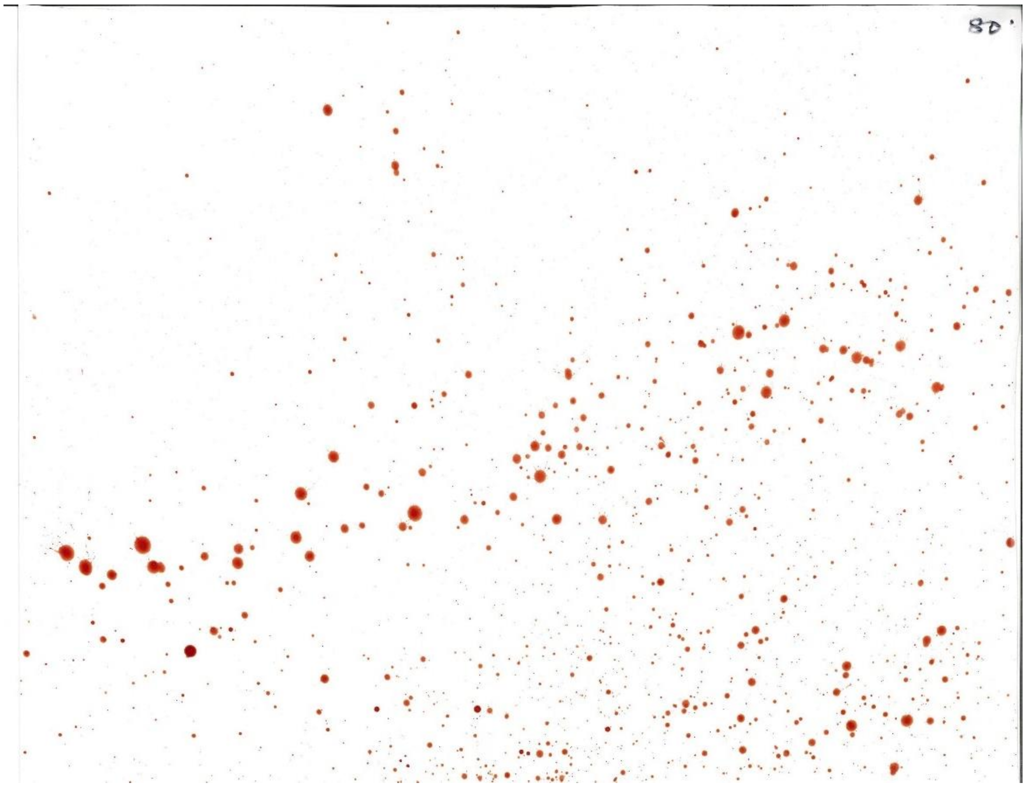

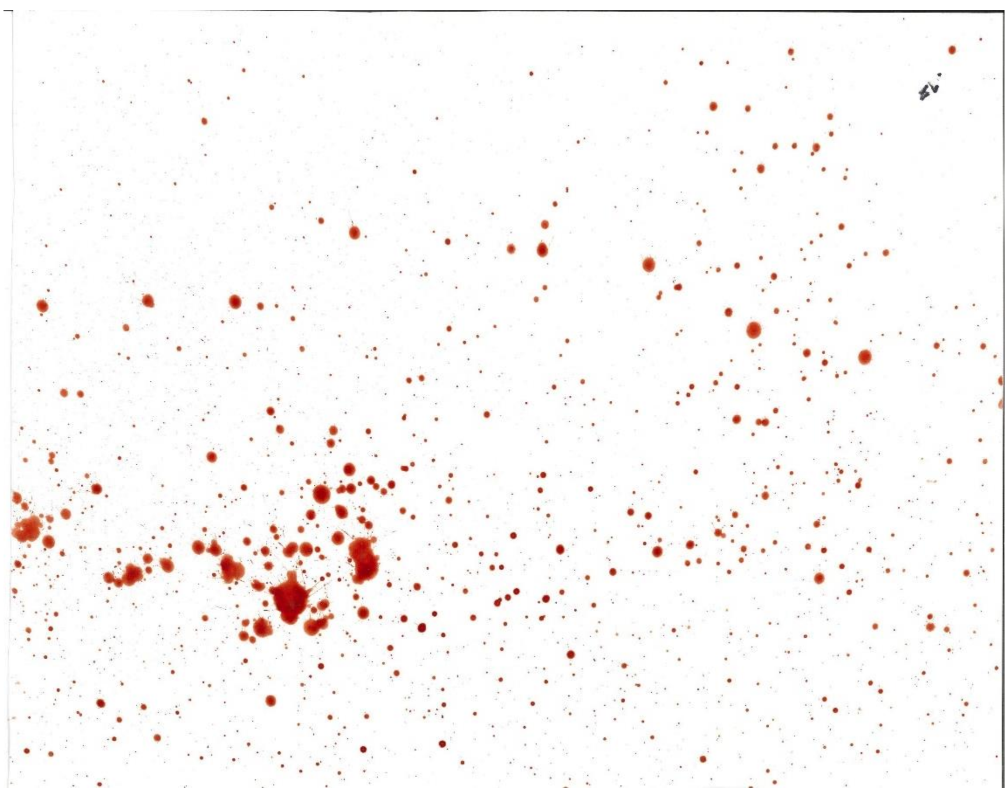

80-DEGREE

Appendix R: Impact Energy 90-Degree Spatter Samples

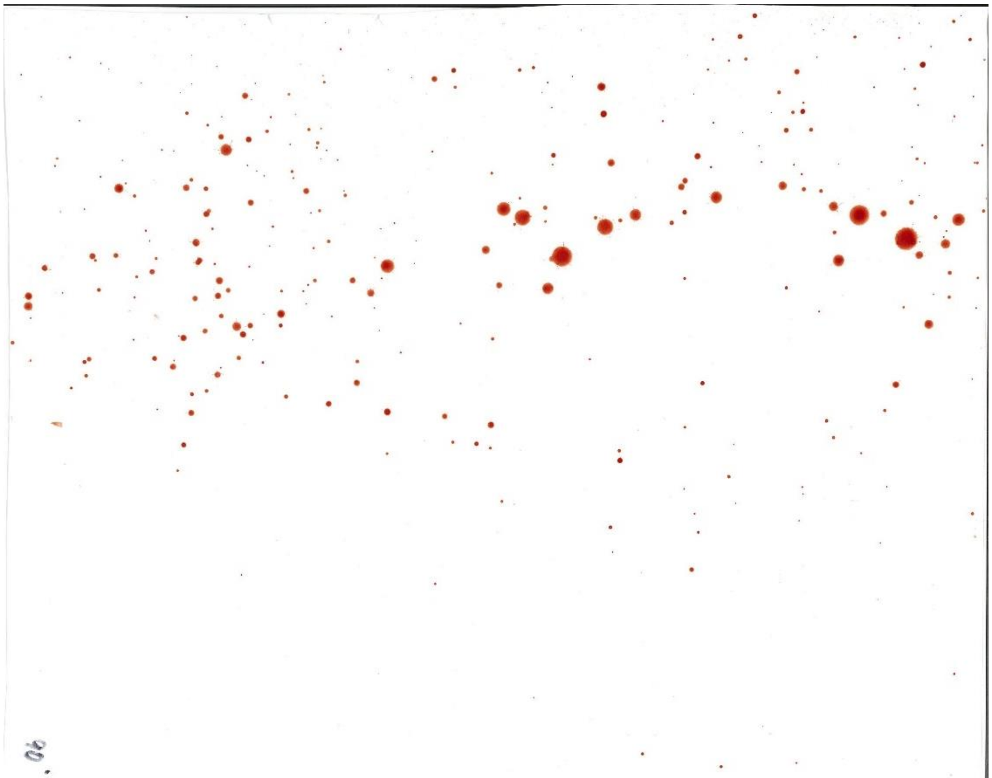

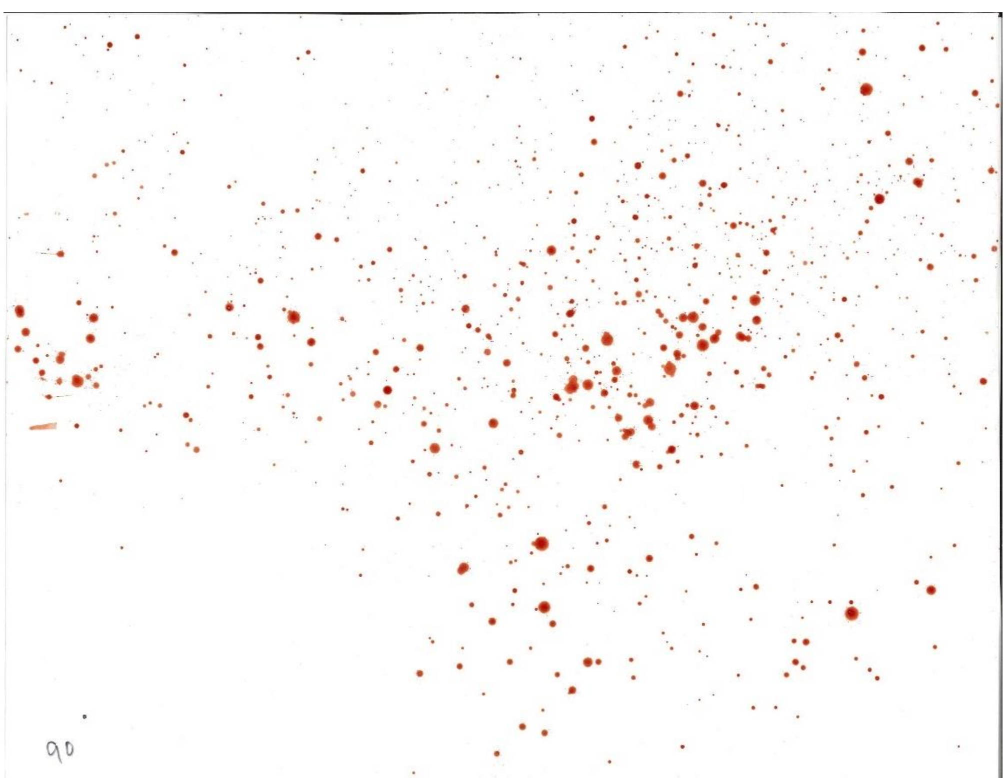

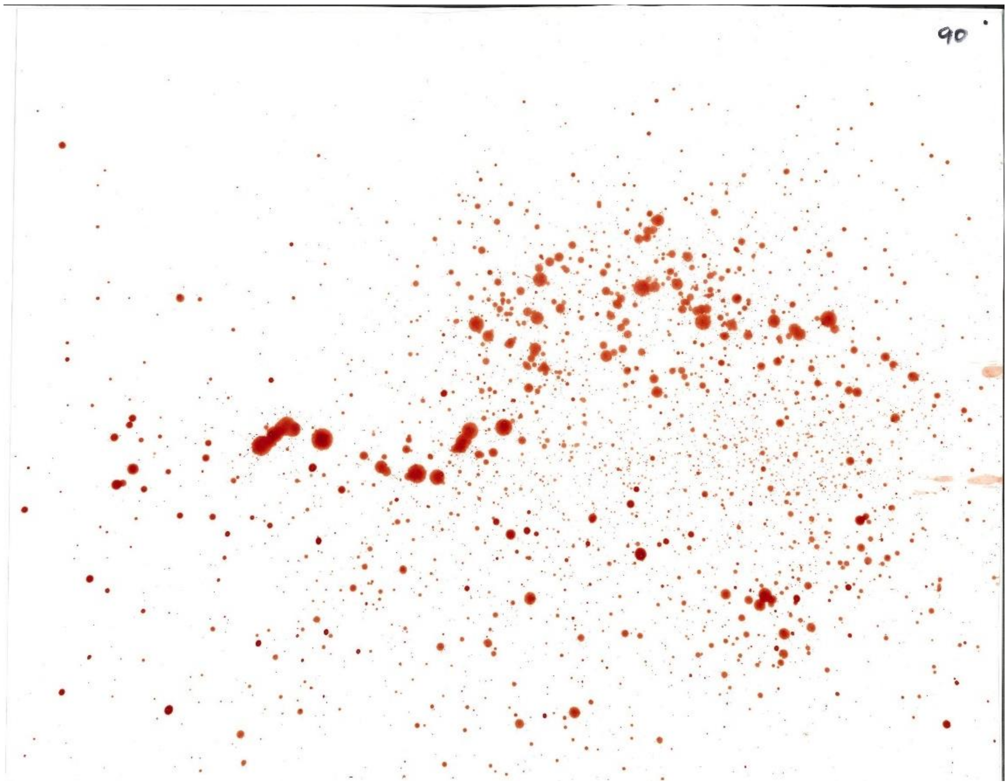

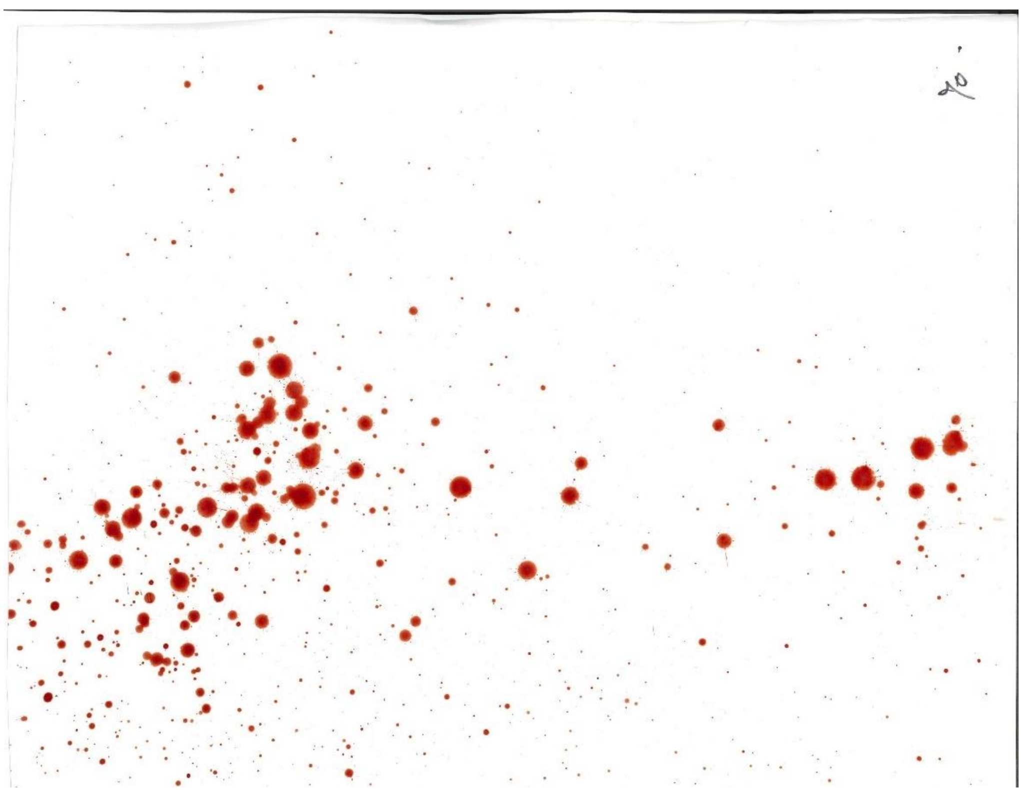

90-DEGREE

Appendix S: Impact Energy 30-Degree Spatter Samples - Questioned sample

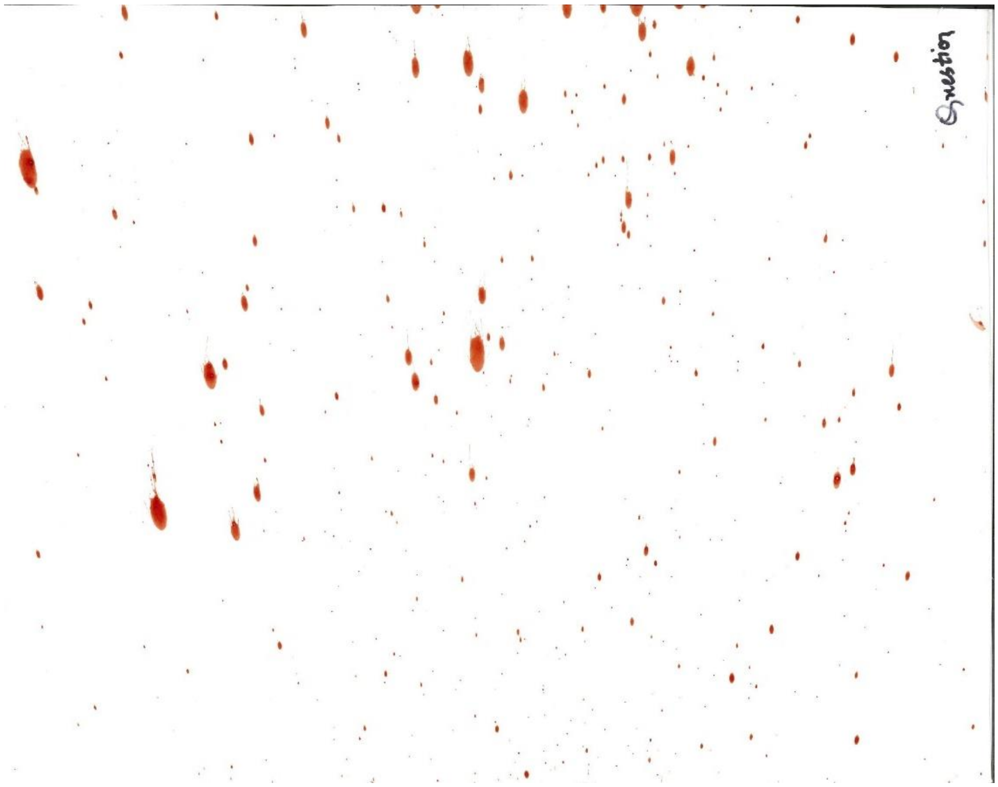

QUESTION- 30 DEGREE